Volume 12, Number 2, 2021 ISSN 1847-6996

FERIT
FACULTY OF ELECTRICAL ENGINEERING, COMPUTER SCIENCE AND INFORMATION TECHNOLOGY **OSIJEK**

IJECES International Journal of Electrical and Computer Engineering Systems

International Journal of Electrical and Computer Engineering Systems

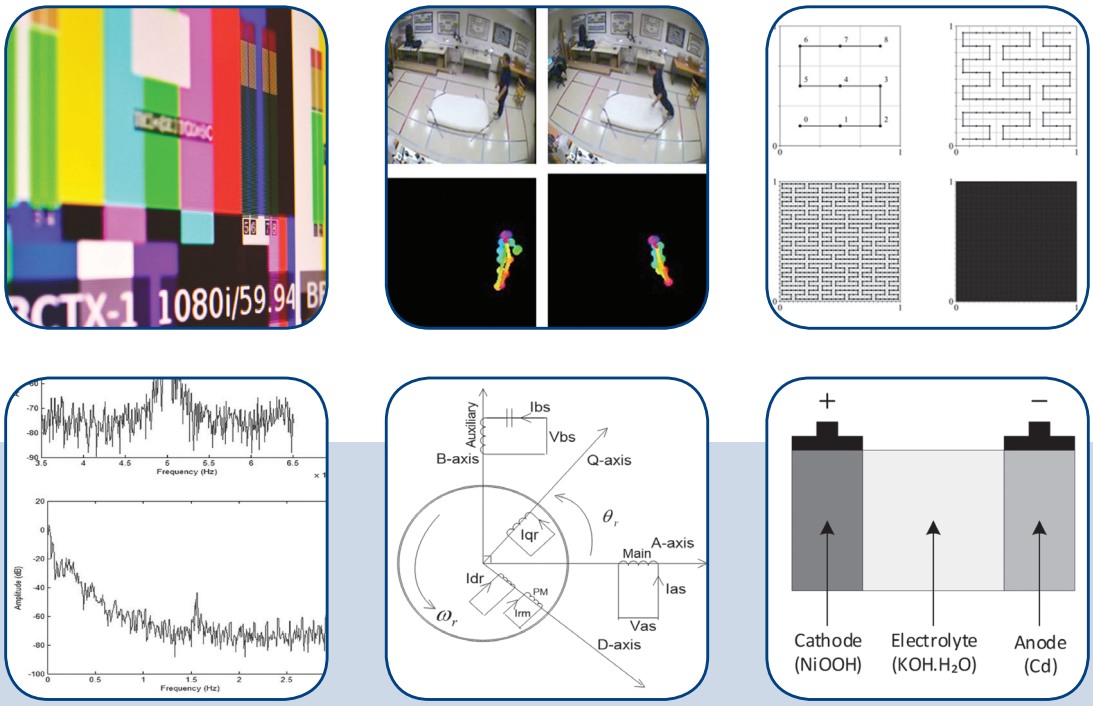

ISSN: 1847-6996

INTERNATIONAL JOURNAL OF ELECTRICAL AND COMPUTER ENGINEERING SYSTEMS

Published by Faculty of Electrical Engineering, Computer Science and Information Technology Osijek, Josip Juraj Strossmayer University of Osijek, Croatia

Osijek, Croatia | Volume 12, Number 2, 2021 | Pages 67-121

CONTACT

International Journal of Electrical and Computer Engineering Systems (IJECES)

Faculty of Electrical Engineering, Computer Science and Information Technology Osijek,
Josip Juraj Strossmayer University of Osijek, Croatia
Kneza Trpimira 2b, 31000 Osijek, Croatia
Phone: +38531224600, Fax: +38531224605
e-mail: ijeces@ferit.hr

Subscription Information

The annual subscription rate is 50€ for individuals, 25€ for students and 150€ for libraries.
Giro account: 2390001 - 1100016777,
Croatian Postal Bank

Journal is referred in:

- Scopus
- Web of Science Core Collection (Emerging Sources Citation Index - ESCI)
- Google Scholar
- CiteFactor
- Genamics
- Hrčak
- Ulrichweb
- Reaxys
- Embase
- Engineering Village

Bibliographic Information

Commenced in 2010.
ISSN: 1847-6996
e-ISSN: 1847-7003
Published: quarterly
Circulation: 300

IJECES online

https://ijeces.ferit.hr

TABLE OF CONTENTS

Performance Enhancement of a Hybrid AC-DC Microgrid Operating with Alternative Energy Sources Using Supercapacitor 67
Original Scientific Paper
Jayalakshmi N. S. | Pramod Bhat Nempu

The Influence of Open Source Software on Creativity, Communication and Students' Social Life 77
Original Scientific Paper
Dejan Viduka | Biljana Viduka | Davor Vrandečić

Performance comparison between virtual MPLS IP network and real IP network without MPLS 83
Case Study
Ivan Nedyalkov

Analyzing the Resilience of Convolutional Neural Networks Implemented on GPUs: Alexnet as a Case Study 91
Case Study
Khalid Adam | Izzeldin I. Mohd | Younis Ibrahim

Performance Investigation of Digital Lowpass IIR Filter Based on Different Platforms 105
Case Study
Raaed Faleh Hassan

A Proposed Model for Predicting Employee Turnover of Information Technology Specialists Using Data Mining Techniques 113
Review paper
Ahmed Hosny Ghazi | Samir Ismail Elsayed | Ayman Elsayed Khedr

About this Journal

IJECES Copyright Transfer Form

Performance Enhancement of a Hybrid AC-DC Microgrid Operating with Alternative Energy Sources Using Supercapacitor

Original Scientific Paper

Jayalakshmi N. S.
Department of Electrical and Electronics Engineering
Manipal Institute of Technology, Manipal Academy of Higher Education
Manipal, India – 576104
jayalakshmi.ns@manipal.edu

Pramod Bhat Nempu
Department of Electrical and Electronics Engineering
St Joseph Engineering College
Vamanjoor, Mangalore, India - 575028
pramodb@sjec.ac.in

Abstract *– Microgrids with non-conventional energy sources have become popular recently. Hybrid AC-DC microgrid (HMG) architecture is effectual as it avoids several power conversions for the consumers. Therefore, this article presents a comprehensive study on grid-tied HMG with PV array and wind energy conversion system (WECS) as principal sources. Fuel cell (FC) acts as the auxiliary source in the DC subgrid and the supercapacitor (SC) is used for instantaneous energy management. The hydrogen storage system is used to store surplus power produced by the PV array. The power flow between the subgrids is regulated using the interlinking converter (ILC) by a PQ controller. The main contribution of this article is the comparative investigation of system operation in the HMG configuration in the presence and absence of a supercapacitor bank on the DC bus. The maximum DC bus voltage fluctuation during load variations in the absence and presence of SC bank is found to be 6.6 V and 3.9 V respectively. Similarly, the maximum transient fluctuation in the power supplied to the DC load is found to be 830 W in the absence of SC bank and 340 W in the presence of SC bank.*

Keywords *– fuel cell, fuzzy logic controller, hybrid AC-DC microgrid, power management, supercapacitor*

1. INTRODUCTION

Due to increasing pollution, depleting fossil fuel resources and rising energy demand, the need for utilizing non-conventional sources of energy in power systems has increased. Sunlight and wind are available abundantly in nature and can be conveniently used to extract electrical power. The energy sources and storage devices supplying load operating either off-grid or on-grid together constitute a microgrid (MG). The MGs are dynamic systems characterized by continuous variations in load and generation. Many researchers are working on microgrids powered by renewable sources. MGs can work in DC MG, AC MG and HMG configurations. The energy sources and storage devices are integrated into a DC bus in DC MG architecture and to an AC bus in an AC MG structure. HMG consists of DC and AC subgrids. This configuration is reliable and efficient.

An autonomous PV-FC-SC system is investigated in [1]. The SC bank is used to facilitate power balance during abrupt power changes. In [2], a study on a grid-coupled PV-wind hybrid system is presented. The modelling and control techniques are discussed in detail. Paper [3] presents a survey of various maximum power point tracking (MPPT) controllers for WECS.

In [4], the control techniques for the DC MG comprising of a grid-independent PV-WECS-FC-SC hybrid system with electrolyzer (EL) are presented. The SC system is controlled to supply/absorb power during a sudden mismatch in generation and demand.

In [5], the grid-tied hybrid system involving WECS and FC is described in the presence and absence of a storage system. The MG system showed improved power and voltage regulation in the presence of storage systems. The grid integration of the WECS-PV-FC system is described in [6]. The system exhibited satisfactory performance by the control techniques employed for MPPT and power management. In [7], a detailed analysis of the AC MG is presented with PV and FC systems. However, the authors did not consider storage devices for the analysis.

In [8], an autonomous MG with PV, WECS and FC is analyzed for single-phase systems with a new MPPT control strategy. The application of artificial intelligence for computing the optimal controller gains in a MG is detailed in [9]. The control techniques of PV and WECS based HMG are described in [10]. In [11], a normalized droop control strategy is explained with an experimental study for stand-alone operation of the HMG. In [12], the control strategies and control requirements of different MG architectures are provided and different control techniques for MGs are reviewed.

Paper [13] discusses a model predictive control algorithm for regulating the DC-AC bidirectional converter. In [14], the control schemes are proposed for regulating the HMGs under pulsed load conditions. The benefits of D-FACTS in a HMG are evaluated in [15]. In [16], the authors proposed a decentralized control strategy for the power management of a HMG with PV array, WECS and FC and its success is assessed for unbalanced and non-linear loads. A robust control technique for a HMG with the PV array, WECS, diesel generator and battery is developed in [17]. Since diesel generator is known to cause harmful emissions, it can be excluded in MGs.

The output of the ILC or inverter contains higher-order harmonics. Generally, an L filter is used for filtering the harmonics. The price of L filter for bulk power applications is high and dynamic response of the system might be slow. LCL filter is proved to be effective in suppressing the harmonics created due to switching, but it creates a problem of resonance. Therefore, the design of the LCL filter must be carefully carried out to ensure stability, taking into account the correct resonance frequency to obtain a smooth sinusoidal supply for grid-tied MGs. The filter design is described in [18-20]. The usefulness of fuzzy logic controllers (FLC) in regulating the MGs is proved in [21, 22]. Thus in this work, to control the SC system, FLC is employed.

The application of metaheuristics in optimizing the control parameters in HMGs is described in [23]. The system is verified in the hardware in loop platform. A robust control scheme for the better dynamic performance of a HMG is proposed in [24]. Passivity based approach is found to be effective. The automatic centralized MG controllers for the energy management of the HMG are experimentally demonstrated in [25]. A coordinated frequency control system for HMGs is described in [26]. 98.2% efficiency was achieved with that control scheme.

This research paper [27], explores the control techniques for the HMG with same energy sources in autonomous mode, while this article analyses the HMG in grid-tied mode. In [28], the DC MG architecture is considered and the FLC is used in voltage and frequency control scheme.

There is sufficient study on improving the dynamic performance of control schemes in the HMGs in literature. However, the existing literature doesn't provide a detailed study on the operation and control of HMG functioning with several renewable sources of different characteristics. The impact of SC bank on individual subgrids in HMGs has not been explored thoroughly. SC is characterized by high power density and can be used for effective handling of power fluctuations if appropriately regulated with suitable control scheme. The significant contributions of this research are:

- The extensive analysis of a grid-tied HMG in the presence and absence of the storage system when the renewable sources with unpredictable output such as PV array and WECS are situated on both buses.
- Investigation of the significance of SC bank in improving the dynamic performance of the HMG under intermittent system conditions considered in both DC and AC buses.

This paper analyses the power flow within and between the subgrids of the grid-tied HMG in detail. In addition, the role of SC bank regulated by FLC based controller in minimizing the transient fluctuations is highlighted.

2. CONFIGURATION OF THE HMG

The schematic outline of the HMG considered for the study is presented in Fig. 1. The PV array that can produce up to 21.7 kW under standard conditions is one of the main energy sources. The single diode model of PV cell is used. The PV array is modelled as described in [1, 2]. The current output of the PV array (I_{PV}) is given by

$$I_{PV} = N_p \times I_{ph} - N_p \times I_r \left[\exp\left\{ \frac{q \times (N_p V_o + N_s I_o R_s)}{N_s N_p k T_c n} \right\} - 1 \right] \quad (1)$$

Where *Tc* is the absolute temperature of a solar cell, I^r is the reverse saturation current, *q* is the charge of a single electron, *k* is the Boltzmann's constant, N_p and N_s are respectively, the number of cells in parallel and series, R_p and R_s represent the shunt and series resistance of a PV cell, respectively, V_o represents the voltage output of a PV cell and I_o is the current output of the cell, I_{ph} is the photovoltaic current and *n* is the cell idealizing factor.

A 20 kW WECS with permanent magnet synchronous generator [2] is another main energy source employed in this work. The power obtainable in the turbine (P) is calculated as

$$P = \frac{1}{2} \rho A C_P v_w^{\ 3} \quad (2)$$

Where *A* is the swept area of the rotor, v_w is wind speed, ρ represents the density of air and C_p is the coefficient of performance.

A 10 kW FC system is the ancillary source for the DC bus. Modelling of the FC stack and EL system is detailed in [1, 4]. The output power of a FC stack is given as a

function of partial pressure (p) of H_2, O_2 and water and flow rate (q). The output voltage of the FC is obtained by adding the Nernst instantaneous voltage (E) and losses. E is given by

$$E = N_O \times \left[E_O + \frac{RT}{2F} \times \log\left(\frac{{}^{p}H_2 \times \sqrt{{}^{p}O_2}}{{}^{p}H_2O} \right) \right] \quad (3)$$

N_o is the number of cells in series, E_o is the no-load voltage (V), F is Faraday's constant, R is the universal gas constant and T is the absolute temperature. A 10 kW EL system is used to generate hydrogen when the PV system's output power exceeds the DC load demand.

The SC bank of 4 F, 400 V, assists in managing power fluctuation created by variations on both subgrids. The PV system operates in MPPT mode. The WECS is regulated by a MPPT controller [2]. Power converters are designed based on the procedure given in [29]. Then the output of the boost converter of WECS is delivered to the AC bus that is integrated into the grid (100 MVA, 3.3 kV, and 50 Hz) through the transformer. The DC and AC buses are coupled through an interlinking converter controlled using the PQ control scheme. The dynamic simulation of the HMG is carried out in MATLAB/Simulink software.

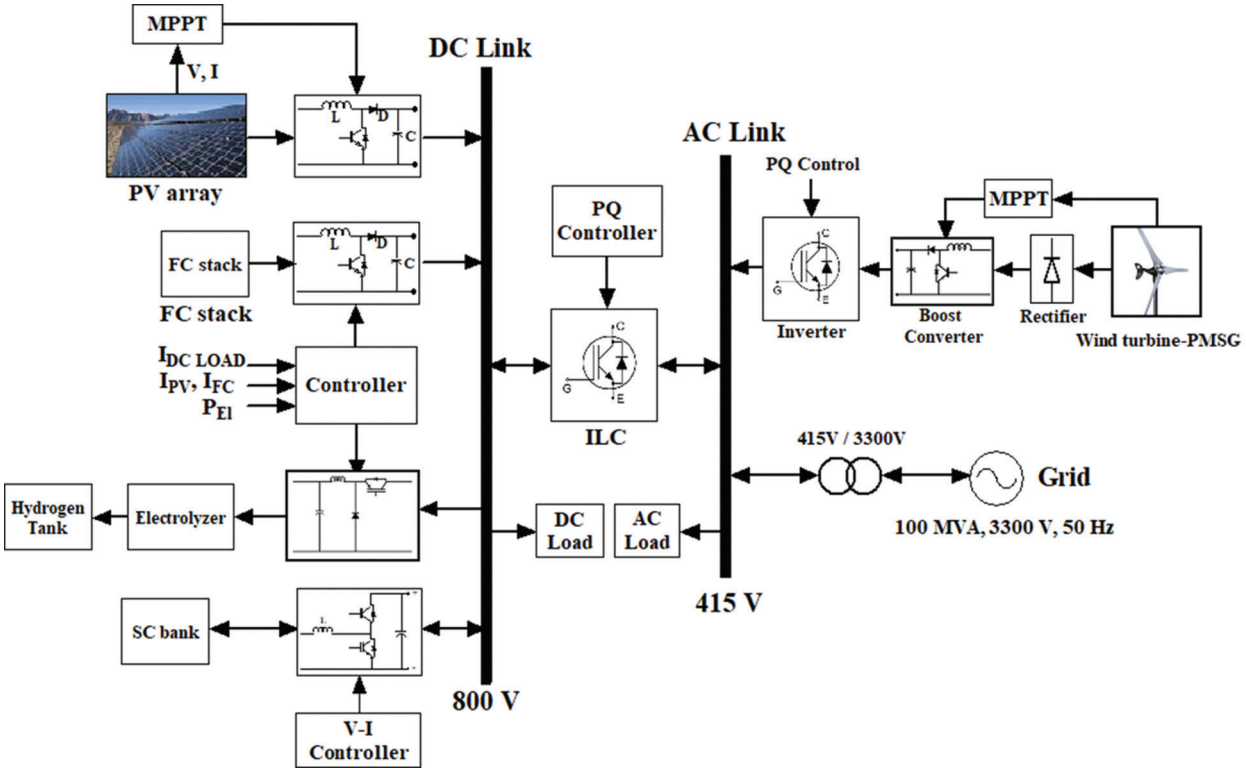

Fig. 1. Schematic representation of the HMG

3. CONTROL STRATEGIES AND DESIGN OF THE FILTER

In this section, control techniques used for regulating the HMG and the design methodology of the LCL filter are depicted in detail.

3.1. CONTROL STRATEGY OF FC SYSTEM

The control method of the FC system is depicted in Fig. 2. It is realized using a PI controller. When the DC load goes above the PV power, the FC supplies the additional power required to meet the demand. The current corresponding to the power deficit ($I_{DCLOAD} - I_{PV}$) is the reference and the feedback is the current from the output of the boost converter of the FC system (I_{FC}). The controller makes the error zero by computing the appropriate duty ratio for the boost converter making the FC stack produce the power required to meet the DC load demand.

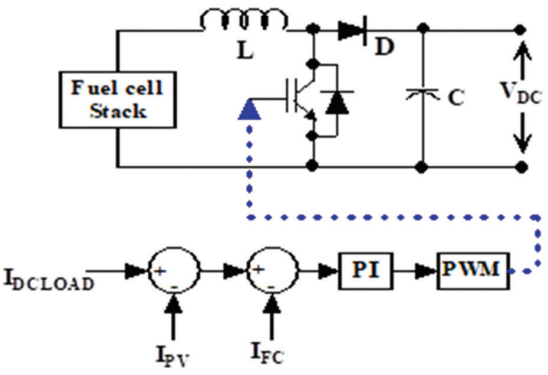

Fig. 2. FC system controller

3.2. CONTROLLER OF THE ELECTROLYZER

The power controller used to control the EL is shown in Fig. 3. A PI regulator is employed to realize it. When the DC load (P_{DCLOAD}) is smaller than PV power (P_{PV}), the excess power generated is given as the reference to the electrolyzer. The electrolyzer power (P_{EL}) is taken as feedback. Based on the duty ratio of the buck converter computed by the controller, the power sent to the EL varies. The hydrogen is produced by the EL based on the current through it. The produced hydrogen is then stored.

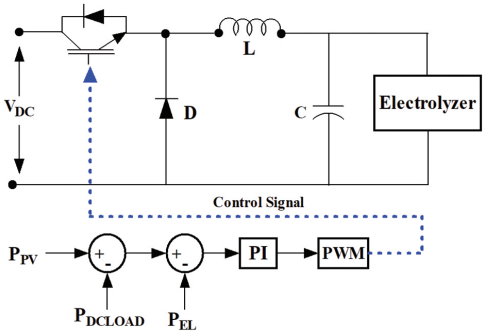

Fig. 3. The power controller of the electrolyzer

The FC and EL systems are responsible for the energy management of the DC subgrid. In this work, FC and EL systems are treated as separate systems for designing the controllers.

3.3 CONTROLLER OF SC BANK

Fig. 4 illustrates the V-I controller [30] of the SC bank. It has two loops. Depending on the DC bus voltage (V_{DC}), the external loop determines the current requirement of SC Bank, and the internal loop controls the SC bank's output current. The outer loop is realized with the FLC. The inputs to the FLC are error (E) and change in error (CE). The current reference of SC bank is the output. The triangular membership functions (MFs) used in FLC are shown in Fig. 5. The centroid method of de-fuzzification is incorporated. To design the rule base, FLCs developed in [21, 22] are taken as reference. This control scheme regulates the DC bus voltage and also facilitates immediate energy management based on the rise or fall of DC bus voltage.

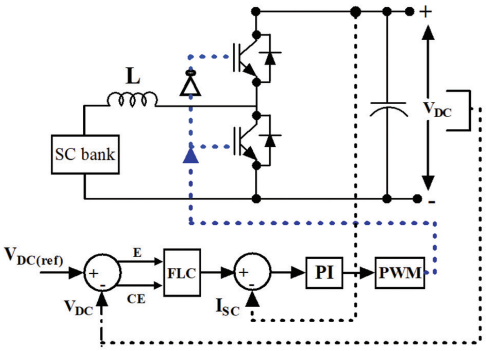

Fig. 4. V-I controller of SC bank

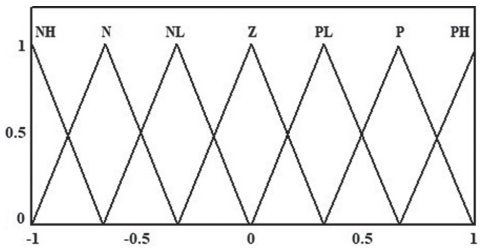

Fig. 5. MF used in FLC

Table 1 presents the rule base of FLC. The MFs are expressed in linguistic variables as Positive High (PH), Negative High (NH), Positive Low (PL), Negative Low (NL), Positive (P), Negative (N) and Zero (Z).

Table 1. The fuzzy logic rule base

E/CE	*NH*	*N*	*NL*	*Z*	*PL*	*P*	*PH*
NH	NH	NH	NH	NH	N	NL	Z
N	NH	NH	NH	N	NL	Z	PL
NL	NH	NH	N	NL	Z	PL	P
Z	NH	N	NL	Z	PL	P	PH
PL	N	NL	Z	PL	P	PH	PH
P	NL	Z	PL	P	PH	PH	PH
PH	Z	PL	P	PH	PH	PH	PH

3.4. THE PQ CONTROLLER

The interlinking converter is controlled by the PQ controller [2, 31]. This controller manages the power exchange between the buses and regulates V_{DC}. The PQ controller is shown in Fig. 6.

The power in a 3 phase system is expressed as

$$P(t) = v_a i_a + v_b i_b + v_c i_c \tag{4}$$

The active and reactive power (P and Q) in terms of the direct and quadrature axis voltages (V_d and V_q) and current (I_d and I_q) are given by,

$$P = 1.5(V_d I_d) \text{ and } Q = 1.5(V_d I_q) \tag{5}$$

The controller's outer loop regulates the V_{DC} and the inner loop controls the currents. The outer control loop computes the d-axis current reference for regulating P. In this work, the reference value of I_q is zero to ensure the power exchange at unity power factor. The inverter of WECS is also regulated by a similar PQ control scheme. The energy balance across the filter is given by

$$\begin{bmatrix} V_d^1 \\ V_q^1 \end{bmatrix} = R_f \begin{bmatrix} I_d \\ I_q \end{bmatrix} + L_f \frac{d}{dt} \begin{bmatrix} I_d \\ I_q \end{bmatrix} + L_f \begin{bmatrix} 0 & -\omega \\ \omega & 0 \end{bmatrix} \begin{bmatrix} I_d \\ I_q \end{bmatrix} + \begin{bmatrix} V_d \\ V_q \end{bmatrix} \tag{6}$$

Where ω is the angular frequency, L_f and R_f are the total inductance and resistance of the filter, respectively. The transfer function of the PQ controller (ignoring the disturbances and feed-forward) is presented in Fig. 7 [31].

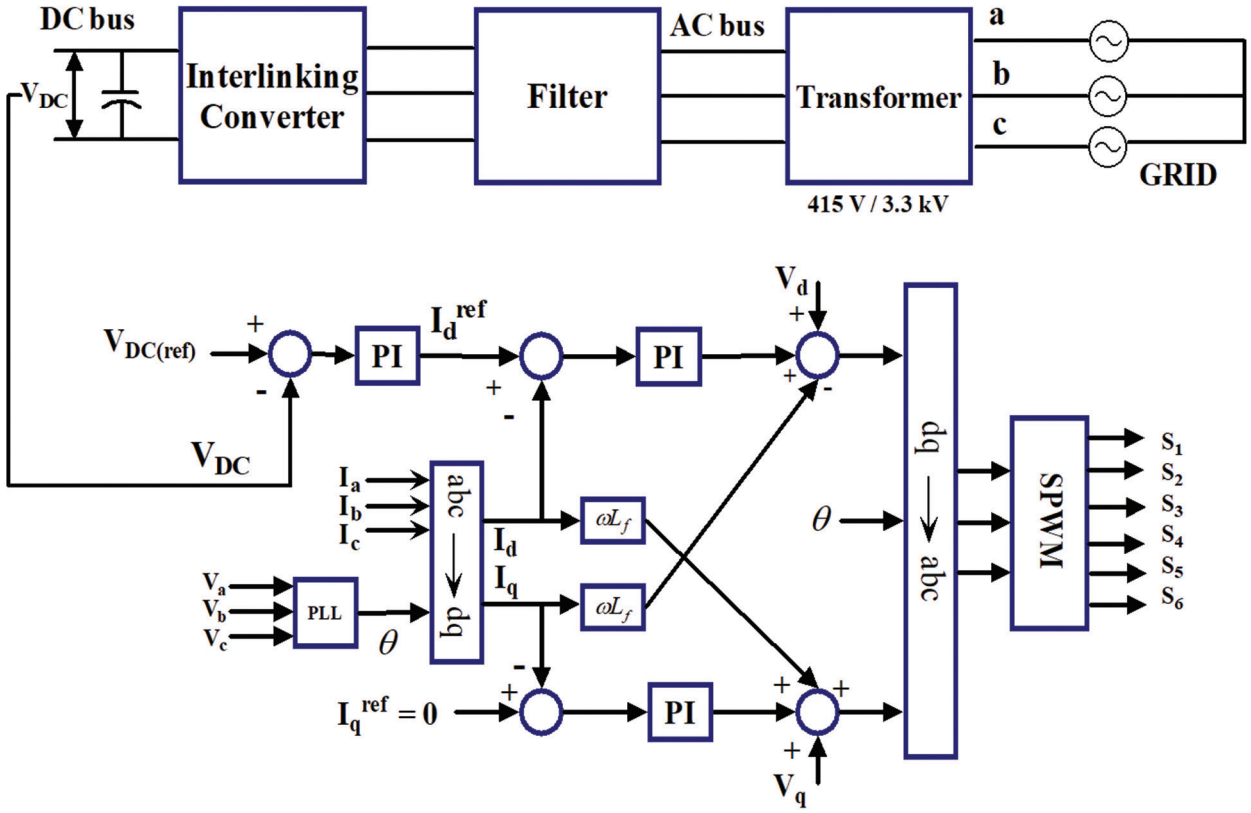

Fig. 6 PQ controller

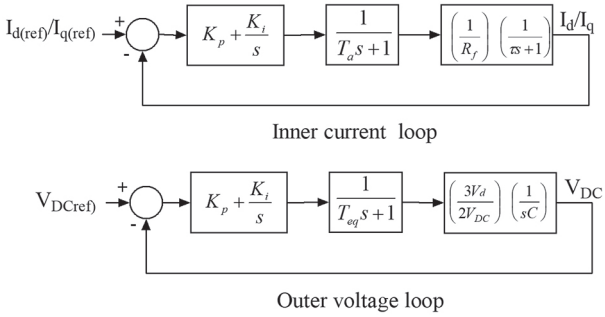

Fig. 7. The transfer function of the PQ controller

Where *Kp* and *Ki* represent controller gain values and C represents DC-link capacitance (5mF). The time constants in the transfer function (*Ta*, *Teq* and τ) are expressed as follows.

$$T_a = \frac{1}{2 f_{sw}} \tag{7}$$

$$T_{eq} = 2T_a \tag{8}$$

$$\tau = \frac{L_f}{R_f} \tag{9}$$

3.5. DESIGN OF THE FILTER

If *V* represents the voltage, *P* is power, *f* is the grid frequency, f_{sw} is the switching frequency (10 kHz), f_r is the resonance frequency, L_1 and L_2 are the ILC/inverter side and grid side inductors respectively, C_f is the filter capacitor, R_d is the damping resistance and $\Delta I_{L(max)}$ is the maximum ripple current allowed, then equations for designing the filter [18-20] are as follows.

$$Z_b = \frac{V^2}{P} \tag{10}$$

$$C_b = \frac{1}{2\pi f \times Z_b} \tag{11}$$

$$L_1 = \frac{V_{DC}}{6 f_{sw} \Delta I_{L(\max)}} \tag{12}$$

$$\Delta I_{L(\max)} = 0.1 \times \frac{P\sqrt{2}}{3V} \tag{13}$$

The C_f is calculated as 5% of its base value [18].

$$C_f = 0.05 C_b \tag{14}$$

Based on the attenuation required (k_a), L_2 can be computed as

$$L_2 = \frac{\sqrt{\frac{1}{k_a^2}} + 1}{C_f (\omega_{sw})^2} \tag{15}$$

The resonance frequency is computed as

$$f_{res} = \frac{1}{2\pi}\sqrt{\frac{L_1 + L_2}{L_1 L_2 C_f}} \tag{16}$$

The f_r should satisfy the equation

$$10f < f_r < 0.5 f_{sw} \tag{17}$$

A damping resistor R_d is included in series with the C_f.

$$R_d = \frac{1}{6\pi f_r C_f} \tag{18}$$

The design values are: L_1 = 5.86 mH, L_2 = 0.246 mH, C_f = 6.16 μF and R_d = 2.06 Ω.

The transfer functions of the filter [20] are given in equations (19) and (20). $G_1(s)$ and $G_2(s)$ represent the transfer functions without and with R_d respectively.

$$G_1(s) = \frac{1}{L_1 C_f L_2 s^3 + (L_1 + L_2)s} \tag{19}$$

$$G_2(s) = \frac{C_f R_d s + 1}{L_1 C_f L_2 s^3 + C_f (L_1 + L_2) R_d s^2 + (L_1 + L_2)s} \tag{20}$$

4. RESULTS AND DISCUSSION

The results of the analysis are presented in two subsections. In the first subsection, the results corresponding to the power management are presented. In the second subsection, the benefits of integrating the SC system on the HMG are analyzed.

4.1. OPERATION OF THE HMG

The step inputs are given to the PV array and WECS to investigate the operation of the HMG under intermittent conditions. The DC load demand and the power output of sources and storage devices in the DC subgrid are presented in Fig. 8. The FC system produces additional power needed (P_{FC}) to meet the demand and SC bank operates quickly under sudden variations in the system conditions. The surplus PV power generated is consumed by the EL (P_{EL}). Based on the EL current, hydrogen is produced. The hydrogen production and pressure variation in the storage tank are shown in Fig. 9.

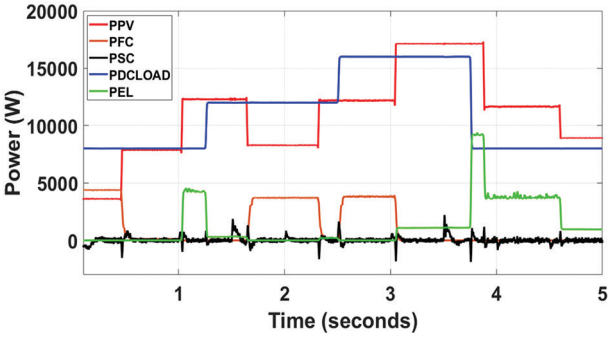

Fig. 8. The power output of PV, FC, EL, SC and DC load

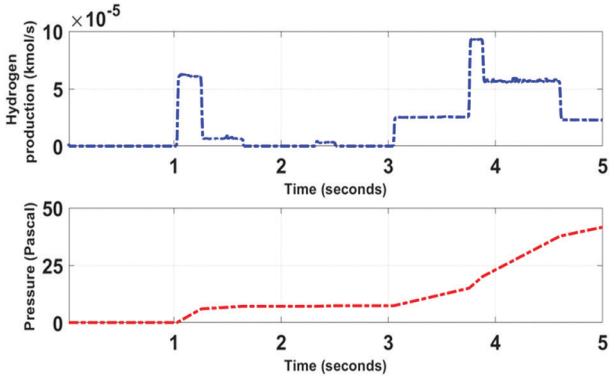

Fig. 9. Hydrogen production and pressure in the tank

In Fig. 10, the variation in AC load, power produced by WECS and the real power balance between MG and the grid are illustrated. The difference in the output power of WECS and the AC load is absorbed/delivered by the utility grid. SC bank provides or absorbs the energy to help the immediate power balance of the AC subgrid by providing and absorbing power from the DC bus as observable in Fig. 10.

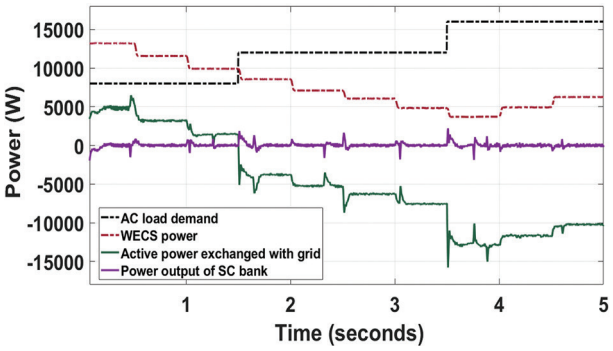

Fig. 10. AC load, power of WECS, power exchanged with grid and SC power

The power shared through the ILC with and without the EL system is shown in Fig. 11. When the EL is absent, the additional produced power in the PV power is transferred to the AC subgrid through ILC. As evident from Fig. 12, the extra power produced by the PV array is sent to the AC subgrid in the absence of the EL system. Thus the amount of power taken from the grid is reduced.

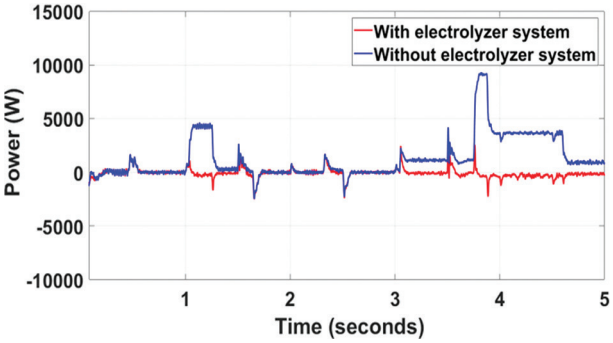

Fig. 11. The power exchanged between AC and DC subgrids

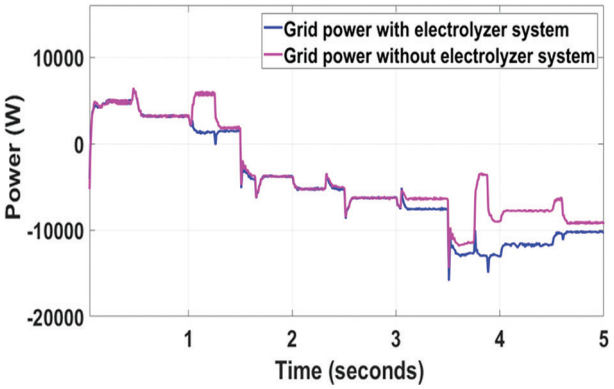

Fig. 12. Grid active power with and without EL system

Reactive power exchange is made zero by keeping q-axis current reference at zero which is presented in Fig. 13.

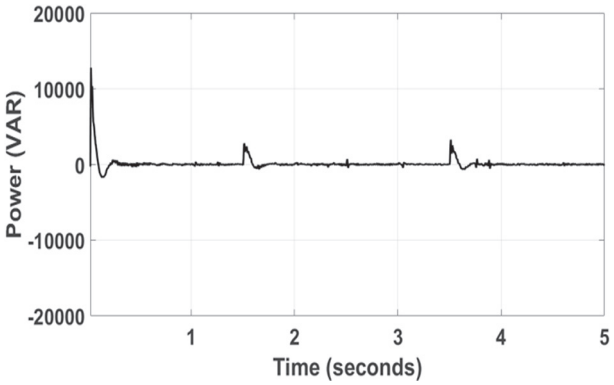

Fig. 13. Reactive power

The V_{DC} is regulated at 800 V by the PQ controller as shown in Fig. 14. Overshoot is found to be 7.5 percent. It is maintained at the reference value even under fluctuating conditions of source and load.

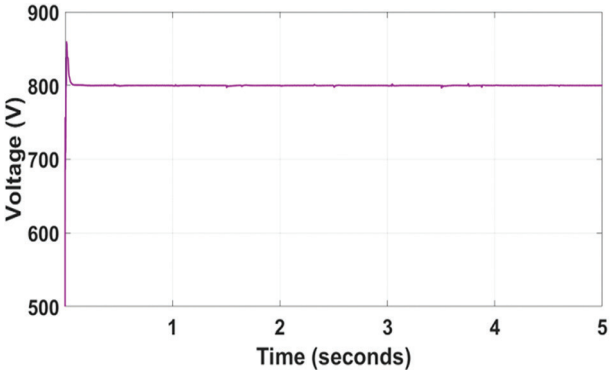

Fig. 14. DC bus voltage

The Bode plots of the filter in the absence and presence of the damping resistor are presented in Fig. 15 and Fig. 16 respectively. It is obvious from the figures that the filter may go unstable without a damping resistor. The filter performs stably with damping as phase margin and gain margin are positive.

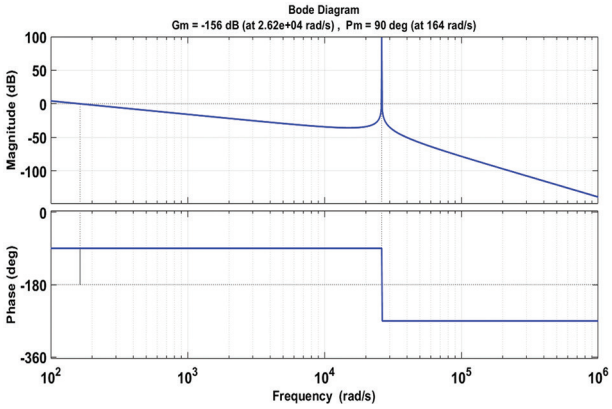

Fig. 15. Bode plot of the filter (in the absence of R_d)

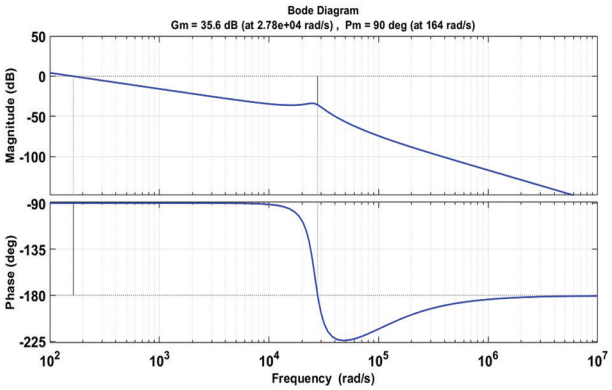

Fig. 16. Bode plot of the filter (in the presence of R_d)

Fig. 17 illustrates the harmonic spectrum of the grid current. Total Harmonic Distortion (THD) is lesser than the limit indicated in IEEE standards [32] since an appropriately designed filter is used.

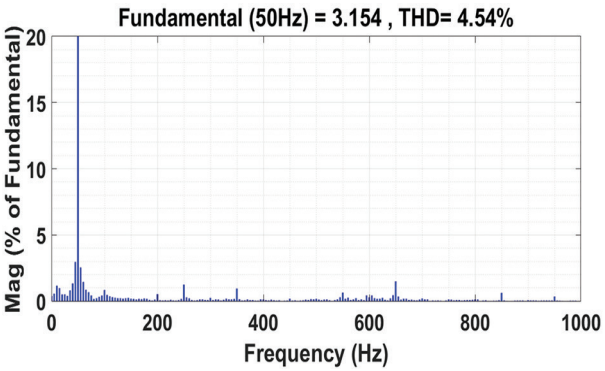

Fig. 17. Harmonic spectrum of grid current

4.2. BENEFITS OF INCORPORATING SC ON THE HMG

The HMG can operate even in the absence of SC bank. In Fig. 18 and Fig. 19, the load on the DC bus and power delivered to the load are shown in the absence and presence of the SC bank respectively. Smooth power is supplied to the DC load with very low fluctuations due to dynamic variations in the AC subgrid when the SC system is incorporated into the DC bus as it works quickly to allow immediate power balance.

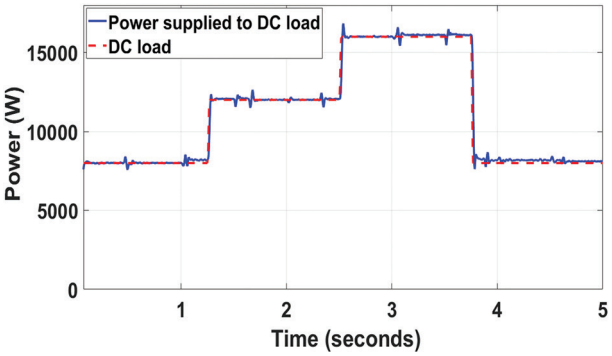

Fig. 18. Power supplied to DC load (in the absence of SC bank)

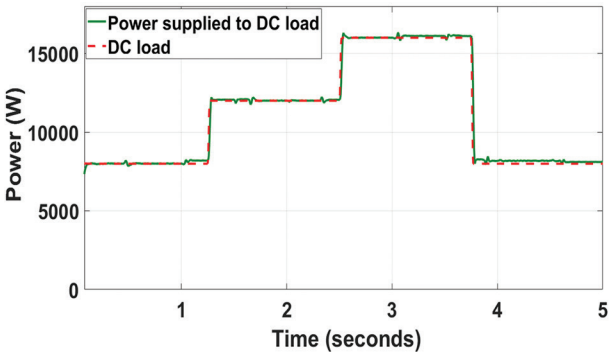

Fig. 19. Power supplied to DC load (in the presence of SC bank)

In Fig. 20, active power exchanged with the grid is shown in the presence and absence of SC bank. It is clear from the picture that the grid experiences fewer transients or stress when SC bank is used in the DC bus.

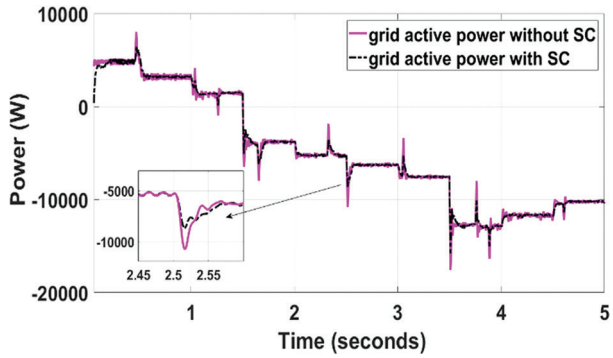

Fig. 20. Active power (in the presence and absence of SC bank)

Fig. 21 depicts the impact of using the V-I controlled SC bank in the system on the DC bus voltage profile. Fewer fluctuations are observed in the voltage when the SC bank is incorporated. The DC bus voltage variation during the change of load in the presence and absence of SC bank is found to be 3.9 V and 6.6 V respectively. Similarly, the maximum transient in the power supplied to the DC load is found to be 830 W without the incorporation of a controlled SC bank and 340 W in the presence of the V–I controlled SC bank. Hence it is always preferable to use the SC bank with the control scheme considered in this work in dynamic systems like HMGs involving PV array, WECS and FC characterized by continuously changing load.

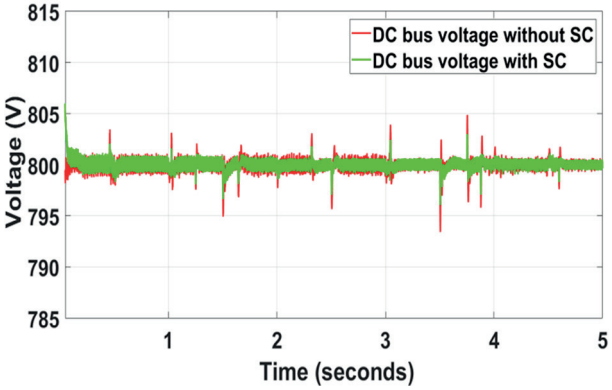

Fig. 21. DC bus voltage with and without SC bank

5. CONCLUSIONS

The performance study of a HMG with PV array, WECS and FC under intermittent load demand and power production is detailed in this article. The power-sharing in the HMG is analyzed with and without SC bank. The power flow among the DC and AC subgrids in the absence of the EL system is analyzed. By using the properly designed filter, the harmonics in load voltage and grid current are maintained within limits. Coordinated power management in the HMG is accomplished. The major research findings of this work are as follows.

- The SC bank facilitates immediate power balance and reduces the fluctuations in the power supplied to loads in the DC bus which are created by dynamic variations in the AC subgrid.
- By incorporating the SC system on the DC bus, the transient fluctuations in the real power exchanged with the grid are also considerably minimized.

The power smoothing techniques to enhance the performance of the same HMG are under investigation by the authors.

REFERENCES

[1] M. Uzunoglu, O. C. Onar, M. S. Alam, "Modeling, control and simulation of a PV/FC/UC based hybrid power generation system for stand-alone applications", Renewable energy, Vol. 34, No. 3, 2009, pp. 509-520.

[2] N. S. Jayalakshmi, D. N. Gaonkar, "Operation of grid integrated wind/PV hybrid system with grid perturbations", International Journal of Renewable Energy Research, Vol. 5, No. 4, 2015, pp. 1106-1111.

[3] M. A. Abdullah, A. H. Yatim, C. W. Tan, R. Saidur, "A review of maximum power point tracking algorithms for wind energy systems", Renewable and Sustainable Energy Reviews, Vol. 16, No. 5, 2012, pp. 3220-3227.

[4] O. C. Onar, M. Uzunoglu, M. S. Alam, "Modeling, control and simulation of an autonomous wind turbine/photovoltaic/fuel cell/ultra-capacitor hybrid power system", Journal of Power Sources, Vol. 185, No. 2, 2008, pp. 1273-1283.

[5] S. K. Ayyappa, D. N. Gaonkar, "Performance analysis of a variable-speed wind and fuel cell-based hybrid distributed generation system in grid-connected mode of operation", Electric Power Components and Systems, Vol. 44, No. 2, 2016, pp. 142-151.

[6] A. Eid, "Utility integration of PV-wind-fuel cell hybrid distributed generation systems under variable load demands", International Journal of Electrical Power & Energy Systems, Vol. 62, 2014, pp. 689-699.

[7] W. Bai, M. R. Abedi, K. Y. Lee, "Distributed generation system control strategies with PV and fuel cell in microgrid operation", Control Engineering Practice, Vol. 53, 2016, pp. 184-193.

[8] H. Fathabadi, "Novel standalone hybrid solar/wind/fuel cell power generation system for remote areas", Solar Energy, Vol. 146, 2017, pp. 30-43.

[9] A. F. Bendary, M. M. Ismail, "Battery Charge Management for Hybrid PV/Wind/Fuel Cell with Storage Battery", Energy Procedia, Vol. 162, 2019, pp. 107-116.

[10] X. Liu, P. Wang, P. C. Loh, "A hybrid AC/DC microgrid and its coordination control", IEEE Transactions on Smart Grid, Vol. 2, No. 2, 2011. pp. 278-286.

[11] P. C. Loh, D. Li, Y. K. Chai, F. Blaabjerg "Autonomous operation of hybrid microgrid with AC and DC subgrids", IEEE Transactions on Power Electronics, Vol. 28, No. 5, 2013, pp. 2214-2223.

[12] F. Nejabatkhah, Y. W. Li, "Overview of power management strategies of hybrid AC/DC microgrid", IEEE Transactions on Power Electronics, Vol. 30, No. 12, 2015, pp. 7072-7089.

[13] M. P. Akter, S. Mekhilef, N. M. Tan, H. Akagi, "Model predictive control of bidirectional AC-DC converter for energy storage system", Journal of Electrical Engineering & Technology, Vol. 10, No. 1, 2015, pp. 165-175.

[14] T. Ma, M. H. Cintuglu, O. A. Mohammed, "Control of a hybrid AC/DC microgrid involving energy storage and pulsed loads", IEEE Transactions on Industry Applications, Vol. 53, No. 1, 2017, pp. 567-575.

[15] A. A. Abdelsalam, H. A. Gabbar, A. M. Sharaf, "Performance enhancement of hybrid AC/DC microgrid based D-FACTS", International Journal of Electrical Power & Energy Systems, Vol. 63, 2014, pp. 382-393.

[16] H. R. Baghaee, M. Mirsalim, G. B. Gharehpetian, H. A. Talebi, "A decentralized power management and sliding mode control strategy for hybrid AC/DC microgrids including renewable energy resources", IEEE Transactions on Industrial Informatics, 2017. (in Press)

[17] M. Hosseinzadeh F. R. Salmasi, "Robust optimal power management system for a hybrid AC/DC micro-grid", IEEE Transactions on Sustainable Energy, Vol. 6, No. 3, 2015, pp. 675-687.

[18] S. Lim, J. Choi, "LCL filter design for grid connected NPC type three-level inverter", International Journal of Renewable Energy Research, Vol. 5, No. 1, 2015, pp. 45-53.

[19] M. Liserre, F. Blaabjerg, S. Hansen, "Design and control of an LCL-filter-based three-phase active rectifier", IEEE Transactions on Industry Applications, Vol. 41, No. 5, 2005, pp. 1281-1291.

[20] A. Reznik, M. G. Simões, A. Al-Durra, S. M. Muyeen, "LCL filter design and performance analysis for grid-interconnected systems", IEEE Transactions on Industry Applications, Vol. 50, No. 2, 2014, pp. 1225-1232.

[21] S. Mikkili, A. K. Panda, "Real-time implementation of PI and fuzzy logic controllers based shunt active filter control strategies for power quality improvement", International Journal of Electrical Power & Energy Systems, Vol. 43, No. 1, 2012, pp. 1114-1126.

[22] P. Bhat Nempu, N. Sabhahit Jayalakshmi, "A new power management strategy for PV-FC-based autonomous DC microgrid", Archives of Electrical Engineering, Vol. 67, No. 4, 2018, pp. 815-828.

[23] T. M. Aljohani, A. F. Ebrahim, O. Mohammed, "Hybrid Microgrid Energy Management and Control Based on Metaheuristic-Driven Vector-Decoupled Algorithm Considering Intermittent Renewable Sources and Electric Vehicles Charging Lot", Energies, Vol. 13, No. 13, 2020, p. 3423.

[24] S. Amirkhan, M. Radmehr, M. Rezanejad, S. Khormali, "A robust control technique for stable operation of a DC/AC hybrid microgrid under parameters and loads variations", International Journal of Electrical Power & Energy Systems, Vol. 117, 2020, p. 105659.

[25] S. Gangatharan, M. Rengasamy, R. M. Elavarasan, N. Das, E. Hossain, V. M. Sundaram, "A Novel Battery supported Energy Management System for the effective handling of feeble power in Hybrid Microgrid Environment", IEEE Access, Vol. 8, 2020, pp. 217391-217415.

[26] J. Huang, X. Zhang, A. Zhang, P. Wang, "Comprehensive coordinated frequency control of symmetrical CLLC-DC transformer in hybrid AC/DC microgrids", IEEE Transactions on Power Electronics, Vol. 35, No. 10, 2020, pp. 10374-10384.

[27] P. B. Nempu, N. S. Jayalakshmi, "Coordinated Power Management of the Subgrids in a Hybrid AC–DC Microgrid with Multiple Renewable Sources", IETE Journal of Research, 2020, pp.1-11.

[28] P. B. Nempu, N. S. Jayalakshmi, K. Shaji, M. Singh, "Fuzzy-PI Controllers for Voltage and Frequency Regulation of a PV-FC Based Autonomous Microgrid", Proceedings of the IEEE International Conference on Distributed Computing, VLSI, Electrical Circuits and Robotics, Manipal, India, 11-12 August 2019, pp. 1-6.

[29] D. W. Hart, "Power electronics", Tata McGraw-Hill Education, 2011.

[30] X. Liu, P. Wang, P. C. Loh, F. Gao, F. H. Choo "Control of hybrid battery/ultra-capacitor energy storage for stand-alone photovoltaic system", Proceedings of the IEEE Energy Conversion Congress and Exposition, Atlanta, GA, USA, 12-16 September 2010, pp. 336-341.

[31] K. Tatjana, "Control of voltage source converters for power system applications", Norwegian University of Science and Technology, Master's thesis, 2011.

[32] ISC Committee, "IEEE standard for interconnecting distributed resources with electric power systems", New York, NY: Institute of Electrical and Electronics Engineers, 2003.

The Influence of Open Source Software on Creativity, Communication and Students' Social Life

Original Scientific Paper

Dejan Viduka
University Business Academy - Novi Sad,
Faculty of Applied Management,
Economics and Finance
Belgrade, Serbia
dejan@viduka.info

Biljana Viduka
University Business Academy - Novi Sad,
Faculty of Applied Management,
Economics and Finance
Belgrade, Serbia
biljana@viduka.info

Davor Vrandečić
J. J. Strossmayer University of Osijek,
Faculty of Electrical Engineering, Computer Science
and Information Technology Osijek,
Kneza Trpimira 2b, Osijek, Croatia
davor.vrandecic@ferit.hr

Abstract *– Today's global, knowledge-based society and economy need creative thinkers in all fields: engineering, medicine, arts, entrepreneurship and education. Educational institutions are tasked with finding new ways of encouraging students to become creative both as individuals and groups. Still, motivation and creativity are only a few of the primary educational goals. They are ambiguous by nature, theoretical, and hard to implement in the real world. Nevertheless, it is a common belief that creativity is an important trait that students should possess in order to face the quickly evolving world. The purpose of this study is to examine the related published works on games, software, imagination, education and creativity. We seek to gather useful information that would both draw attention to this problem and how Open-Source Software (OSS), as a model, can drive students' creativity.*

Keywords *– creativity, education, open source software, digital gap, innovation*

1. INTRODUCTION

Information and communication technology is a force that has changed many aspects of our lives. In the beginning of the twenty-first century informational technology became an inevitable element in education. The vast possibilities that such technology provides are insufficiently leveraged in many developing countries. This situation is due not only to deficient school equipment but also to poor teachers' training for the usage of such equipment. This situation has been changing over the past few years mostly due to the increasing number of schools that are equipped with IT infrastructure. At the same time, the internet connection in developing countries is improving as well [1].

Generally speaking, our culture, along with our lives at home, at work, and in school are becoming extremely integrated with technology [2]. Unlike the traditional teacher-based teaching that rests on on one-way communication, the use of IT and OSS as teaching tools is possible in all stages of primary, secondary and college education. Even though there are disagreements in terms of how much computers actually generate creativity, there is a general consensus that they can transform and inspire human creativity [3]. The contribution of such means to the learning process consists of encouraging students in the classroom as well as during independent studies to be as efficient as possible. Such processes include solving problems, divergent thinking, different combinations, metaphorical thinking, and analogy [4].

According to the futurist, Alvin Toffler, the illiterate people of the twenty-first century "will not be the ones who do not know how to read, but those who are incapable of learning"[5] The use of IT and OSS will trigger interest in children to recognize, research and solve the problem in question throughout the whole learning process. Many countries and schools mostly use commercial software that is very expensive and therefore inaccessible for many other schools. The high price is one of the major problems that prevents schools with poor financial means from integrating technology into their curriculum. Fortunately, there is an alternative software that can offer some assistance to schools. Alternative software refers to Open Source Software that is very useful in the field of mathematics, numerical analysis, data processing, graphics, text processing and other similar products. The use of OSS in computer science education is in expansion in the last several years. Open code software refers to all the software whose source code is available under the "Open Source" license [6]. Source code is accessible in some programming languages. Unlike commercial tools, OSS can be changed and rearranged according to one's personal needs. Technical training was introduced in formal programs which resulted in influencing the cultural and pedagogical paradigm in education [7].

Aside from the technical aspect, it is important to mention that the author of OSS may use his or her experience as a starting point for discussion on social aspects of software engineering such as ethics and licensing laws for software. Some of the research showed the existence of different learning styles that represent strategy or regular mental behavior that individuals habitually apply in the process of learning [8].

To have success with those changes in the field of science and technology we have to work on modernization in the field of education. Modern education is expected to shape students as flexible individuals who will easily accept current changes. Such needs imposed certain changes in the way how we organize classes. The organization of classes with the help from computers has certain advantages over the traditional organization. Some of them are the following:

(1) Teaching and learning process with the whole class can be simultaneously individualized. (2) Educational programs are of better quality. This guarantees better learning results, better approach and endless motivational possibilities. (3) Computer-based educational programs trigger more senses for learning. (4) Efficient learning is no longer explicitly linked to the educational institution, classroom, or a working day or hour. (5) Computers can simplify the grading process and lower the likelihood of a teacher making a mistake while grading a students work. (6) Computers in education can be used for a stream of different activities such as: efficient management of learning processes, governance of many administrative and personal projects, and many other types of work related to imminent organization and realization of broader work in education.

It is our obligation to provide students with opportunities to practice and raise their natural creative abilities. In order to make education more efficient, we have to create proper learning environments in our classrooms [9]. If teachers are reluctant to accept digital technology, it may open a gap between educators who are slow to go along with technology and the world that assimilated technology quickly [10]. One of the main duties of every educational reform is not only to equip schools with modern computer devices and other high-tech equipment but also to provide the basic tutoring for their application.

2. OPEN SOURCE SOFTWARE

Open Source programs are seen by average computer users as something that is free of charge but also as something that is not good enough and that lacks the quality for commercial use. OSS or free software is often defined as a free software. The basic philosophy of OSS is extremely simple. When software programmers are allowed to work freely on their source code, it is inevitable that it will improve because collaboration helps with fixing mistakes. Collaboration also enables adjustment to different needs and hardware platforms [11]. OSS is becoming more popular by the day. OSS distinguishes itself from other programming solutions in the way how it is made and how much it costs. OSS licenses enable a lot of freedom for the distribution of software, although they do not necessarily return large profits for their authors. Such licenses facilitate free use as well as modifications for personal needs [12].

In the world of computer science, there are software programs that are free of charge, but only in the sense of free use [13]. Users are forbidden from distributing and improving such programs. In such cases there are no guarantees that those programs will be available for use in the future. They are usually used for marketing and promotional purposes. Contrary to this programs that are free of charge, but not free to change, OSS can always be adapted by the end user and is very often free of charge. The free use of OSS is reflected in the fact that the licenses guarantee their use, but the author maintains the selling rights as well as the rights to change the license. This implies that everything that has been licensed as a free software once, remains under the license regardless of modifications and regardless of who introduces those changes. Free software can be modified under clearly defined rules.

2.1. OPEN SOURCE DEFINITION

Open Source is a category of methods and technologies that is used in developing computer software that is accessible to broad communities without major limitations. In order to better develop the software, communication between developers and users takes place. The source code of the program in such cases is the final product of the Open Source process. Evolution of such communities creates additional products and

services that often lead to developing independent projects. Programmers are not the only ones who participate in developing these projects. The majority of software users can contribute (through testing, asking questions, translations, directions, tracking of mistakes, promotion and support for the less experienced users) to a faster envelopment of projects [14].

2.2. OPEN SOURCE COMMUNITY

The main advantage of the open source software is its accessibility and possibility for modification and advancement. In fact, there are lot of studies that identify factors that can lead individuals to participate in OSS projects [15]. The prerogative of this concept is the possibility to attract free-lance programers to advance and further develop programs. Members of those communities regularly communicate with each other in order to exchange their knowledge and collaborate in the search for solutions to problems that may arise [16].

The development of the internet enabled users to communicate with each other and to work on such software. Previously, there was a communication problem caused by geographical and other limitations, which is why Open Source used to be more limited before widespread internet use. Today it is possible to write a program, publish it under one of the free licenses, and upload it to internet either for free use or in order to sell it. Today authors can simply search the internet looking for similar solutions to what they are programming. There are many free programs online that publish precisely what the author needs, but they also allow adjustments to individual needs [14].

There is a variety of completely functional operating systems, as well as many included apps, that are widely used and do not require the purchase of any commercial computer program.

The typical open source software author is a relatively young programmer. There are, of course, older users who, while applying their knowledge and effort, make a living with programming. In their spare time, as a hobby or as a matter of prestige, they may work on further development of an open source project. Such groups of developers, when compared to big software development companies that are stationed at a fixed place and led by their managers, have less chance of success and less chance of finding clients.

In spite of the common opinion that individuals cannot outsmart the software companies, OS is fighting its way through the mainstream software for massive use. The reasons for the success can be found in high quality technology that they use as well as in a very quick pace by which the OS spreads among users. All this enables the open code software to make a break through and fight the competition.

3. OPEN SOURCE SOFTWARE INFLUENCE

In the twenty-first century, creativity poses one of the essential projections of human existence, and it is very present in furthering education. Many institutions that deal with this field refer to creativity very often. Creativity is viewed differently in different disciplines. In education we call it "innovation", in business we call it "entrepreneurship" and in music it is called "performance" or "composition"[17]. Most researchers agree that creativity is a production of something that is original and worthy. "Something" can be a theory, a dance, a chemical product, a process, a dinner or anything else [18].

Since the beginning of this century, creativity has been perceived as a characteristic and a necessity of every human being. Through follow-up research and work with young people who are well disposed towards creativity, we are able to increase the development of creativity with adult individuals. It is precisely because of such needs in our modern society that we have to pay attention to all the possible ways of enabling the development of creativity with young people in the course of their education.

One of the reasons is the lack of knowledge and skills about creativity that should be taught in higher education [19]. Creativity is not represented in colleges and universities in an adequate way and it could be viewed as a consequence of their personal experience. It can be seen as an insight into the lack of creativity in college education. It can also be linked to critique that is characteristic for the younger generation [20].

Motivation and creativity are some of the primary educational goals. They are naturally unstable, hard to understand and are often speculated on [21]. Aside from savings and flexibility that are achieved by the usage of OSS, schools will be in the position to show their leadership in solving problems related to social and ethical issues. Creative individuals invent. They imagine different situations and things, solve problems in various fields, and make communication through innovative methods possible [22]. Creative thinking skills imply the search for innovation and difference. They imply independence, persistence and high aspirations and standards [23].

Globalization brings along the internationalization of knowledge and it exerts pressure on modern states and nations to be involved in those processes [24]. There are several reasons why the operational definition of creativity based on the product seems to be the most appropriate [25]. The scope and the nature of creativity of new products is key to managing innovation [26].

OSS helps to overcome the issue of digital gap because it removes the burden of expenses and limitations of software licenses for schools. It results in a more accessible IT in schools [14]. This way the schools would be able to create the ICT (Information - Communication and Technology) environment that would satisfy the needs of a larger number of students. In addition,

there is a possibility to help the students and their families who do not have a new computer at home which would enable them to set up the new software. One example would be for schools to define which GNU/Linux distribution they use in their classes.

Facilitating access to the same software packages for all students would be very helpful, and it would not require additional financial means for classes. Since the software requirements for setting up this operating system are quite modest, it can be installed even on older computer models. Purchasing them is also much cheaper.

There is a number of social issues that schools encounter while introducing ICT One of the most important responsibilities of the schools is making sure that all students have equal access to it [27]. The integration of ICT in schools demands a special attention to its influence on digital distribution. Digital distribution refers to the gap between those who can use new information and communication tools efficiently and those who cannot. Research on the digital gap is often focused on socioeconomic factors and their influence on family income, level of education and equality. When education is in question, the focus is often on the approach to modern technologies that are available both at school and at home. Any kind of modern technology is expensive once it first appears on the market and only a limited number of users can afford it. As a result, students with modest means do not have the opportunity to have access to technology outside the school.

When students can read, distribute, and modify software, they can get included into a large community of programmers who constantly work on exchange of ideas and removal of programming mistakes. Such communities (Figure 1.) gather a great number of activists who foster various OSS projects via the internet regardless of where they live. Such a unique type of virtual community provides an ideal learning environment that teaches how to communicate, cooperate, and eventually learn from other members of the community. Constant improvement, production and efficient reception of new services, products or processes poses a huge industrial challenge [28]. OSS has become more accessible and more successful in the last decade mainly because of the growing number of users who exchange ideas and work on improving OSS software. Different types of online behavior are positively correlated [33].

Fig. 1: Image of OSS organization and structure

This way students communicate with their peers with whom they share the same passion. This helps them to master their computer skills, their communication skills as well as their English skills (English being the language mainly used in communication) [29]. Creativity, and its essential role in the classroom, is often considered to be the answer to the background of quick social, technological, spiritual and ecological changes [30]. OSS is a resource for development of innovation and creativity of its users. When it comes to schools, it is a resource for furthering knowledge during the process of learning. Motives for involving with OSS can be defined in three categories:

- enjoyment based on inner motivation
- obligation towards the community
- outside motivation

4. EXAMPLES OF OSS USAGE IN EDUCATION

In most cases, teachers decide to teach their students with commercial software applications. The usage of OSS in computer education has expanded in the last several years. One of the exceptions is the subject called "programming" that is being researched in schools of higher education. The learning process basically comes down to learning how to program cell phone application for Android, being the operating system that dominates the world market.

It is estimated that Android takes up more than 80% of the cell phone market. In the same fashion the subject of internet technology or web programming in schools is taught in order to learn how to use of HTML, CSS, JavaScript and PHP programming languages, or some of the WCMS (Web Content Management System) solutions as for example Joomla, Wordpress or Drupal, which are also developed under the OS licenses.

There are other examples that can teach students how to use OSS and that can be an excellent choice depending on the needs of the user. OSS could be distributed in different ways for the needs of learning processes that take place in a classroom. Its anatomy, with an available source code, gives students a unique opportunity to freely experiment with the goal of achieving a better education. Much can be learned by using OSS that is based on practical examples as opposed to theoretical learning. That kind of learning has often been embraced by teachers who use books with their simple examples.

This system enables the users during their educational process to freely "peep below the hood" and see the complex systems in which they are written and how they are projected in practice on intricate software solutions. It is those examples that show very clearly that it is essential to introduce the OSS in higher education especially in schools that research software engineering and areas of study that would introduce students into OSS philosophy. By doing this their attention would be drawn to both advantages and disadvantages of the currently known software packages. This type of education enables students with greater opportunities for an independent choice of software that they

would use in their studies and work. At the same time it shortens the time that each individual might need in order to discover the possibilities this concept offers.

5. CONCLUSIONS

Nowadays, developed countries use educational systems more and more as open and flexible modules that are incorporated into digital contents. Educational technology applies them efficiently. In developed countries, educational software is a part of the learning process starting with the primary education. A new model of teaching that students are more interested in has been created so that students are more motivated compared to the model that was used previously. Specific software development skills are being researched outside the university systems, in trade schools, interim courses or short courses [31].

The tools for such processes are easily available, mostly free of charge and they are also enriched by multimedia contents. They are also accessible through the web so that both teachers and students can adjust to new technologies by using interesting methods. Using such tools teaches students to present their papers and thesis as well as to play didactically elaborated games and solve assignments while using computers.

Following this course, the new electronic, multimedia based and interactive model of learning is being introduced. This model increases the students' motivation for and efficiency at learning the material. Educational software, with a help of technological devices (internet connection, connected computers, projectors and smart boards, etc.) contribute to better learning. Implemented learning software enables all the classical types of approaches like pair work, individual work and group work.

The methods of learning and presenting while using electrical boards (interactive boards, smart boards) put students in an active role in the process of learning and acquiring knowledge (projected pedagogy). The possibilities that these new media offer (like for example, internet, multimedia-learning, projected educational contents, experience) will enable the building of new teaching models whose effects will be measurable. While using the internet, students will acquire technical skills and enter the virtual world. (Each one of these models has its advantages and disadvantages, which is why we have to strive towards optimal use.)

Bulgaria is a good example where the use of OSS was approved by a legal act. As a result, it was introduced in education as well as in other areas. OSS can help to facilitate work, and it is good to know that OSS is good enough to be considered as an alternative to other expensive software. Microsoft Office packages where the user learns how to use the tools (text editing, spread sheets, contents presentation etc.) can be replaced by a LibreOffice package that is free of charge. This tells us that it is essential to learn how to use the tools and how to create a document and insert graphics, pictures, tables, etc. It would be good to implement the example of Bulgaria to other countries. Then, new standardized books would be published that would teach teachers. Eventually those materials would be used for teaching purposes. As a matter of fact, it is the teachers themselves who enable the maximum learning potential of their students. They are also a channel for releasing of those potentials in the classroom [32]. Aside from basic convenience it is necessary to thoroughly look into the advantages of OSS. Some of the advantages that students have while applying this concept influence the developing of creativity, communication and social skills.

6. REFERENCES

[1] D. Viduka, B. Viduka, "Term and Implementation of Electronic Education in Serbia", Proceedings of the 4th International Conference on Technics and Informatics in Education, Čačak, Serbia, 1-3 June 2012, pp. 461-468. (in Serbian)

[2] T. Alexander, "TechKnowLogia", Proceedings of the International Conference on "Dissolving Boundaries: ICTs and Learning in the Information Age", Dublin, Ireland, 4-5 May, 1999.

[3] J. McCormack, M. D'Inverno, "Computers and Creativity: The Road Ahead", Computers and Creativity, Springer, Berlin, Heidelberg, 2012, pp. 421-424.

[4] T. Lewis, "Creativity in technology education: providing children with glimpses of their inventive potential", International Journal of Technology and Design Education, Vol. 19, 2009, pp. 255-268.

[5] V. L. Tinio, ICT in Education, Manila E-ASEAN Task Force, Kuala Lumpur, 2003.

[6] D. Viduka, "Possibilities of using Open Source software in modern business", Proceedings of the 12th International Conference on E-commerce, Palić, Serbia, 2012.

[7] K. Kazerounian, S. Foley, "Barriers to creativity in engineering education: A study of instructors and students perceptions", Journal of Mechanical Design, Vol. 129, No. 7, 2007, pp. 761-768.

[8] V. Ružić., R. Nikolić, N. Žižović, "Electronic materials for blended learning", YU INFO Conference, 2010.

[9] R. M. Felder, "Creativity in Engineering Education", Chemical Engineering Education, Vol. 22, No. 3, 1988, pp. 120-125.

[10] J. Blac, K. Browning, "Creativity in Digital Art Education Teaching Practices", Art Education, Vol. 64, No. 5, 2015, pp. 19-34.

[11] A. Bonaccorsi, C. Rossi, "Why Open Source software can succeed", Research Policy, Vol. 32, No. 7, 2003, pp. 1243-1258.

[12] C. A. Kenwood, "A Business Case Study of Open Source Software", Mitre Corporation, MP 01B0000048, 2001.

[13] H. Singh, D. Seehan, "Open Source vs. Proprietary Solutions: Case Study of Windows and Linux, A Consumer Perspective", International Journal of Advanced Technology & Engineering Research, Vol. 2, No. 4, 2012, pp. 28-37.

[14] D. Viduka, "Interoperability model of information system based on open source software in education", Singidunum University, Belgrade, Serbia, PhD Thesis, 2017. (in Serbian)

[15] W. Ke, P. Zhang, "The Effects of Extrinsic Motivations and Satisfaction in Open Source Software Development", Journal of the Association for Information Systems Vol. 11, No. 12, 2010, pp.784-808.

[16] Y. Ye, K. Kishida, "Toward an Understanding of the Motivation of Open Source Software Developers", Proceedings of the 25th International Conference on Software Engineering, Portland Oregon, USA, 3-10 May 2003, pp. 419-429.

[17] D. C. C. K. Kowaltowski, G. Bianchi, V. Teixeira de Paiva, "Methods that may stimulate creativity and their use in architectural design education", International Journal of Technology and Design Education, Vol. 20, 2010, pp. 453-476.

[18] Lj. Arar, Ž. Racki, "The nature of creativity", Psychological topics, No. 12, 2003, pp. 3-22.

[19] A. K. Palaniappan, "Web-based Creativity Assessment System", International Journal of Information and Education Technology, Vol. 2, No. 3, 2012, pp. 255-258.

[20] S. B. Maksić, V. Z. Spasenović, "Educational Science Students Implicit Theories of Creativity", Creativity Research Journal, Vol.30, No. 3, 2018, pp. 287-294.

[21] P. Chakalisa, D. Mapolelo, D. M. Totev, Ir. E. D. Totev, "Modern Methods for Stimulating Creativity in Education", Informatica, Vol. 30, 2006, pp. 421-425.

[22] A. Cocua, E. Pecheanua, I. Susnea, "Stimulating Creativity through Collaboration in an Innovation Laboratory", Procedia - Social and Behavioral Sciences, Vol. 182, 2015, pp. 173-178.

[23] L. G. Richards, "Stimulating creativity: teaching engineers to be innovators", Proceedings of the 28th Annual Frontiers in Education Conference. Moving from 'Teacher-Centered' to 'Learner-Centered' Education, Tempe, Arizona, USA, 4-7 November 1998, pp. 1034-1039.

[24] S. Maksic, "Encouraging creativity in school", Institute for Pedagogical Research, Belgrade, Serbia, ISBN 89-7447-068-8., 2007.

[25] T. M. Amabile, "The Social Psychology of Creativity: A Componential Conceptualization", Journal of Personality and Social Psychology, Vol. 45, No. 2, 1983, pp. 357-376.

[26] D. H. Cropley, J. C. Kaufman, A. J. Cropley, "Measuring Creativity for Innovation Management", Journal of Technology Management & Innovation, Vol. 6, No. 3, 2011, pp. 3-30.

[27] D. Viduka, A. Basic, B. Viduka, V. Varadjanin, "Open Source software as Alliterative and Effective Learning Environments", Journal SYLWAN, Vol. 161, No. 6, 2017.

[28] L. A. Zampetakis, L. Tsironis, V. Moustakis, "Creativity development in engineering education: the case of mind mapping", Journal of Management Development, Vol. 26, No. 4, 2007, pp. 370-380.

[29] D. Viduka, A. Bašić, V. Kraguljac, "Social Engineering of Open Source Software", Serbian Journal of Engineering Management, Vol. 3, No. 1, 2018, pp. 56-60.

[30] A. Craft, "Creativity in Schools: Tensions and Dilemmas", Abingdon, Routledge, 2005.

[31] M. Shaw, "Software Engineering Education: a Roadmap", Proceedings of the Conference on The Future of Software Engineering, Limerick, Ireland, June 2000, pp. 371-380.

[32] K. C. Tsai, "Play, Imagination, and Creativity: A Brief Literature Review", Journal of Education and Learning; Vol. 1, No. 2, 2012, pp. 15-20.

[33] I. Boric Letica, "Some Correlates of Risky User Behavior and ICT Security Awareness of Secondary School Students", International Journal of Electrical and Computer Engineering Systems, Vol. 10, No. 2, 2019, pp. 85-89.

Performance comparison between virtual MPLS IP network and real IP network without MPLS

Case Study

Ivan Nedyalkov
South – West University "Neofit Rilski"
Faculty of Engineering, Department of Communication and Computer Engineering,
Ivan Mihailov str. 66, Blagoevgrad, Bulgaria
i.nedqlkov@gmail.com

Abstract *– In this paper an IP based network consisting of two separate IP networks - a virtual one, running MPLS and an experimental IP network, connected to the virtual one, have been studied. VoIP traffic is exchanged between the two networks. Both networks are connected to the Internet and exchange traffic with it. The virtual network is created by using GNS3. The purpose of this paper is to show a comparison in the performance between the two IP networks. In addition, mathematical distributions and approximations have been made to be used to further evaluate the performance of the two networks. The used methodology in the present work can be applied in the study of different IP networks through which different types of real-time traffic passes.*

Keywords *– GNS 3, IP networks, Monitoring VoIP traffic, Wireshark*

1. INTRODUCTION

The IP networks are constantly expanding - becoming larger and more complex. Subscribers of these networks are also growing. As a result, these networks must continually provide new and new services to subscribers. In addition, more and more devices are gaining access to these networks. This leads to an increase in the number of network devices in such a network. All of this causes network congestion and slows down the network. Reducing the speed of the IP network leads to a deterioration in the quality of services offered, which in turn leads to consumer dissatisfaction [1]. In order to avoid delays in the network MPLS (Multiprotocol Label Switching) is introduced [2, 3, 4, 5, 6, 7]. In order to find out if the use of MPLS will lead to a significant improvement in the speed of data exchange in a particular network with a particular type of traffic, research needs to be done. Setting up such an experimental network is expensive and not every institution would allow such an experiment. It is therefore appropriate to use programming environments for modeling of IP networks [8, 9, 10, 11, 12, 13].

The purpose of the present work is to study and compare the performance between a virtual network using MPLS and a real IP network not using MPLS. The two IP networks are interconnected and exchange traffic between each other and the Internet. What the two networks have in common are the subscribers of the IP telephone exchange, which is located in the real network. The real network does not use the MPLS technology but the virtual IP network does. Therefore, it is possible to monitor the voice traffic that is exchanged between the two networks and make a comparison of the performance between the two networks (study of the time delay between the individual packets).

2. TOPOLOGY OF THE NETWORK

2.1. TOPOLOGY OF THE EXPERIMENTAL NETWORK

Figure 1 shows the topology of the experimental network, which is part of the bigger real network – the IP network of university campus building.

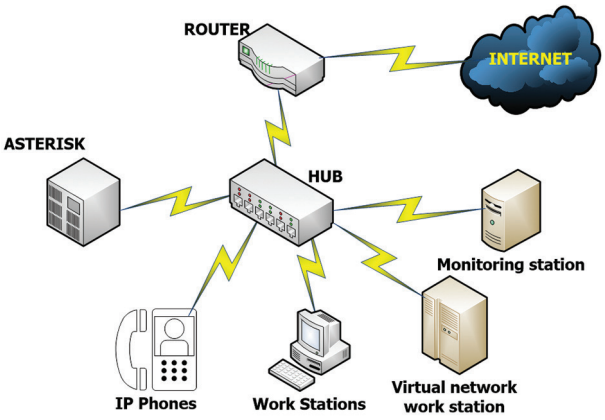

Fig. 1. Topology of the real network

Due to the lack of a layer 2 switch with a "mirror port", a hub is used to monitor the traffic in the experimental network. Figure 1 shows an idea of what the part of the

real network that will be studied looks like. Therefore, the topology has the shape of a star and the hub is at its center. The experimental real network is composed of several IP phones connected to the IP telephony exchange Asterisk, a router that provides Internet connectivity, several workstations, and a hub that forwards all the traffic in the experimental network to the monitoring station. At the monitoring station specialized software for traffic monitoring - Wireshark is installed. The workstation where the virtual network is running is also connected to the hub.

2.2 TOPOLOGY OF THE VIRTUAL NETWORK

Figure 2 shows the topology of the virtual network. The GNS 3 platform is used for the modeling [14, 15]. The platform enables integration with specialized network monitoring programs and connection to real IP networks and emulating real network devices. Device emulation is the imitation (emulation) of a device's hardware. This allows the users to start and work with real images of working network devices.

The network is configured to work with the dynamic routing protocol OSPF. The network uses MPLS. R1 to R4 are the routers. These are disk image emulations of real routers. S1 to S2 are switches, more precisely, these are simulations of switches. Router_Firewall is a module that connects the virtual network to real networks. Test_PC_1 and Test_PC_2 are virtual machines that are used to generate network traffic. Test_PC_1 has a software phone installed on it. It is used to generate VoIP calls to the IP phones on the real network. Additionally, an Internet browser is used to generate Internet traffic – the browser is used for opening Internet pages of any kind (forums, pages with multimedia content, news sites, etc.). Test_PC_2 is used only to generate traffic from the Internet. This will simulate the most common business network traffic - IP telephony and Internet access.

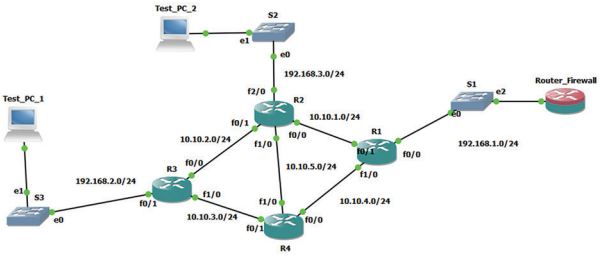

Fig. 2. Topology of the virtual network

3. METHODOLOGY FOR CONDUCTING THE MEASUREMENTS

As mentioned above, in the real network, a hub is used to forward all the generated traffic to the monitoring station [16, 17, 18]. The software used for monitoring is Wireshark [19, 20, 21]. In the virtual part of the network, due to the functionality of GNS 3, Wireshark will monitor the traffic in all the links between the routers.

One of the Wireshark functionalities for IP telephony analysis, in particular, RTP streams analysis, will be used to evaluate the two networks. The parameters to be monitored are:

- Delta: this is the difference in the receipt of one packet from the previous packet. As the devices in one RTP session are not synchronized, each device and the network itself cause additional delay. The receiving party must cope with this delay and synchronize with the transmitting party. To be able to do the synchronization, the receiving party uses the timestamp information of the RTP packet. The Delta parameter shows exactly this difference in the timestamps of the captured RTP packets. This parameter is characteristic of the network layer and reflects the arrival of the capture interface packet (where timestamp is placed);
- Jitter: this is the difference in packet delay. Also known as spurious phase modulation. In IP networks the jitter is used to measure the time difference between packet arrivals. It is expressed as the displacement of packets in time. This is not a particular problem with data transmission, but with voice transmission, jitter is important.

4. RESULTS

4.1 RESULTS OBTAINED IN THE VIRTUAL NETWORK

Based on the monitoring of the traffic in the virtual network, it was found out that the traffic generated by Test_PC_1 passes through R3, R4, R1, Router_Firewall and vice versa. The traffic from Test_PC_2 flows through R2, R4, R1, Router_Firewall and vice versa. No additional configurations for QoS or route prioritization have been made in the virtual network. Therefore, the traffic passes through these nodes. Based on the dynamic routing protocol used, OSPF, and the configured MPLS, the routers themselves chosen these routes to traverse the data flows. On the other links only service information is exchanged, such as: OSPF Hello packets, LDP packets, and other service packets.

During the study of the virtual network, all links between the routers are monitored, but the presented results are for only one of the monitored links, because the obtained results from this connection provide sufficient information to evaluate the performance of the virtual network. The monitored link in the virtual network is the link between R1 and R4. Firstly, this link is chosen because the whole traffic in the virtual network passes through it and so it is more deeply studied. Secondly, the obtained data from the measurement can be used as a representative sample for the whole network. From the analysis of the results obtained by Wireshark for all links between the routers of the virtual network, for the values of the jitter and the delta parameter in the various links, there is a con-

tinuous increase of their values, approaching the Router_Firewall. This is due to the fact that each subsequent router begins to process more and more data streams, and eventually Router_Firewall processes all the traffic from the virtual network to the real one. As a result, there is an increase in the delay after each subsequent router. For this reason, in the present work, it was decided to present the results only from the link between R1 and R4. Presenting the results of all links would be unnecessary because they will not provide any different information.

Figure 3 shows summary results for a single stream (forward – reverse direction) of a VoIP call. The device with the IP 192.168.2.2 is the software phone on the virtual machine - Test_PC_1 and the device with the address 192.168.31.50 is the Asterisk IP telephony exchange. According to Cisco [22], the average one-way jitter should be less than 30 ms. As it can be seen, the mean jitter value is well below the 30 ms limit for both directions. The summary results obtained by Wireshark also contain other data such as: packet loss. The results show that there are no losses in the forward stream – to the Asterisk, but in the reverse direction there are 146 lost packages or about 0.13%. Information is also given about the total number of RTP packets for each of the streams. Information about the duration of the call is also available - 2326 seconds. Figure 3 also shows the sampling frequency - 8000 Hz (as can be seen, there is a deviation from this frequency for both directions), as well as the deviation from the clock frequency. From this data, it is also possible to get an idea of the delay between the packets, by following the values of Delta and Skew. Delta shows the time difference between the receipt of the previous packet from the stream and the packet that is now received. Skew shows how long the current packet is ahead of or behind the entire call, relative to the nominal speed of the packet. In the presented case, it is noticed that the packet lags behind the whole conversation.

Forward		Reverse	
192.168.2.2:8000 → 192.168.31.50:15968		192.168.31.50:15968 → 192.168.2.2:8000	
SSRC	0x0d8caaea	**SSRC**	0x66531d9e
Max Delta	173.02 ms @ 583606	**Max Delta**	512.56 ms @ 597773
Max Jitter	17.91 ms	**Max Jitter**	51.93 ms
Mean Jitter	1.81 ms	**Mean Jitter**	3.42 ms
Max Skew	-1175.93 ms	**Max Skew**	-572.50 ms
RTP Packets	116227	**RTP Packets**	116191
Expected	116227	**Expected**	116337
Lost	0 (0.00 %)	**Lost**	146 (0.13 %)
Seq Errs	0	**Seq Errs**	141
Start at	2079.460558 s @ 313834	**Start at**	2079.489061 s @ 313840
Duration	2325.53 s	**Duration**	2326.81 s
Clock Drift	-1224 ms	**Clock Drift**	-398 ms
Freq Drift	7996 Hz (-0.05 %)	**Freq Drift**	7999 Hz (-0.02 %)

Fig. 3. Summary results from Wireshark

Figure 4 shows the jitter distribution throughout the whole session in the direction from the virtual machine to the Asterisk (forward direction), and figure 5 shows the jitter distribution in the opposite direction. X is for the whole duration of the conversation, and Y stands for the values of the jitter at each moment of the conversation. From figure 4 it is noticed that during the whole conversation the jitter in the forward direction, for every moment of the conversation, does not exceed the limit of 30 ms. As a result, there is a lack of packet loss.

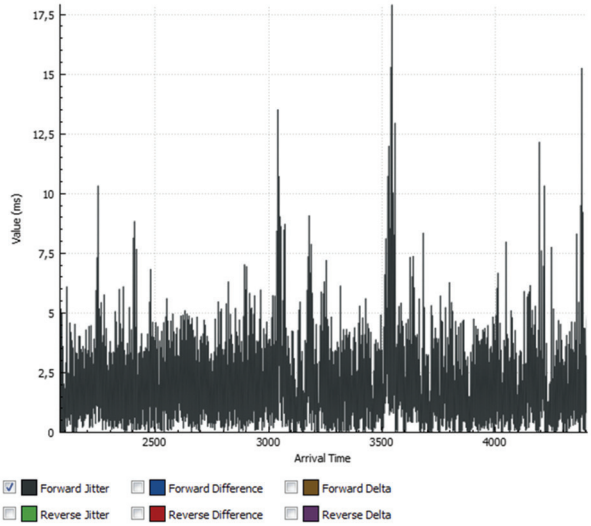

Fig. 4. Forward jitter for the whole stream

The results in figure 5 are quite different. It is noticed that the jitter repeatedly exceeds the limit of 30 ms. - reaches values of 50 ms, which is unacceptable. As a result, there is a loss of packets in the reversed direction, also evident from figure 3. This increase in the values in the reversed direction is due to the accumulation of delay in the real network.

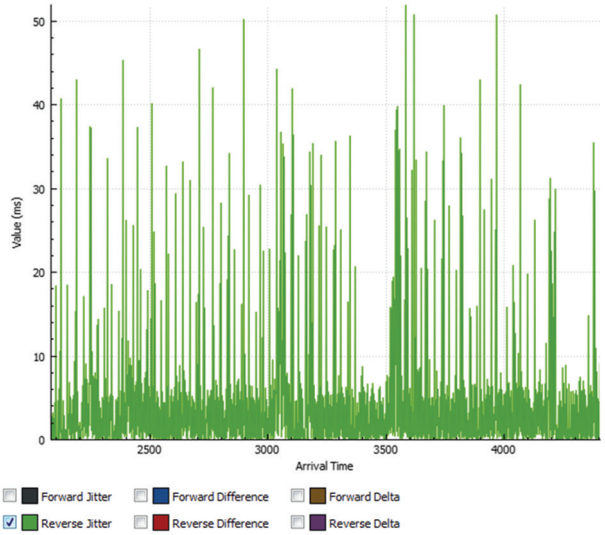

Fig. 5. Reversed jitter for the whole stream

Figures 6 and 7 show the delta values for each second of the call in both directions. Again X stands for the whole duration of the conversation, and Y stands for the values of the delta at each moment of the conversation. As explained above, this parameter indicates the arrival time between two packets or known as a

time delay. By default, it almost always coincides with packetization time - 20ms. Due to the presence of jitter on the network, its value can increase and lead to packet loss. The one-way transmit delay should not exceed 150 ms. (G.114 recommendation) [23] and the maximum round-trip delay should not exceed 300ms. As can be seen from figure 6, the delta in the forward direction exceeds the 150 ms limit only two times. The results in the reversed direction are getting worse because of the high value of the jitter.

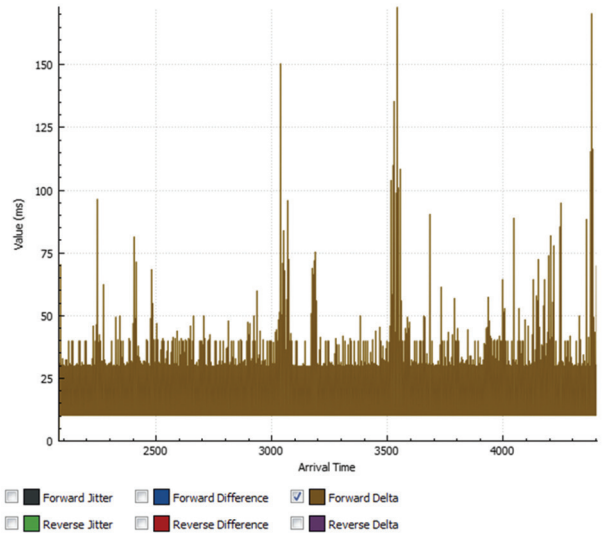

Fig. 6. Forward delta for the whole stream

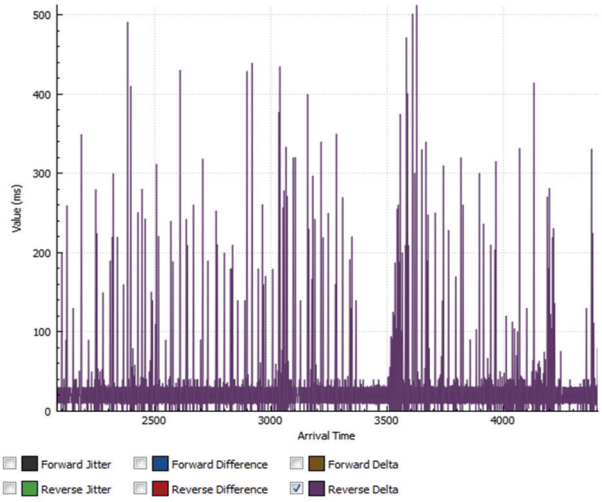

Fig. 7. Reversed delta for the whole stream

In the virtual network, the values of the delta in the reverse direction decrease after each node passed. This is due to the presence of the MPLS. Figures 8 and 9 and 10 show these dependences. As can be seen from the summarized results for the reverse flow for the link between R3 and R4 (Figure 8), the values of Delta and max jitter decreases. The graph for Delta for the whole conversation period (figure 9), for the link R3 - R4, compared to the result of figure 7 shows a significant improvement in the instantaneous values of the parameter.

Forward		Reverse	
192.168.2.2:8000 → 192.168.31.50:15968		192.168.31.50:15968 → 192.168.2.2:8000	
SSRC	0x0d8caaea	**SSRC**	0x66531d9e
Max Delta	271.03 ms @ 554197	**Max Delta**	501.56 ms @ 567725
Max Jitter	36.27 ms	**Max Jitter**	37.54 ms
Mean Jitter	0.83 ms	**Mean Jitter**	3.60 ms
Max Skew	-1161.29 ms	**Max Skew**	-1785.42 ms
RTP Packets	116227	**RTP Packets**	116175
Expected	116227	**Expected**	116337
Lost	0 (0.00 %)	**Lost**	162 (0.14 %)
Seq Errs	0	**Seq Errs**	148
Start at	2041.299212 s @ 301343	**Start at**	2041.396725 s @ 301361
Duration	2325.52 s	**Duration**	2327.04 s
Clock Drift	-925 ms	**Clock Drift**	31 ms
Freq Drift	7997 Hz (-0.04 %)	**Freq Drift**	8000 Hz (0.00 %)

Fig. 8. Summary results from Wireshark

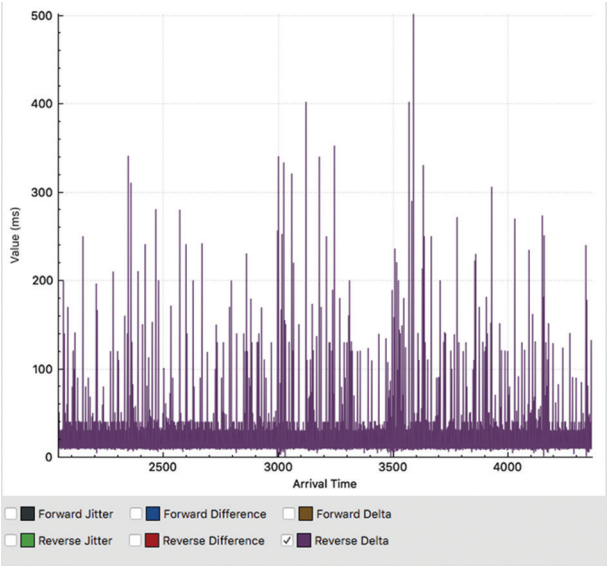

Fig. 9. Reversed delta for the whole stream

Figure 10 presents the graph for the reversed jitter for the whole conversation period for the link R3 - R4, compared to the result of figure 5 shows a significant improvement in the instantaneous values of the parameter.

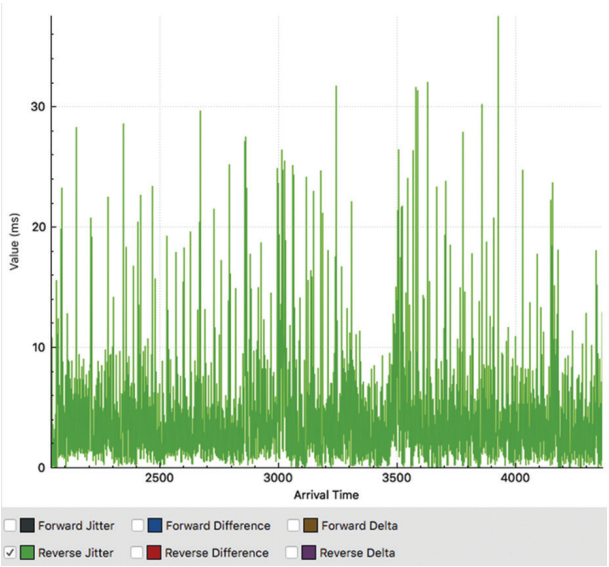

Fig. 10. Reversed jitter for the whole stream

Another method for assessing the performance of an IP network is by using mathematical distributions and approximations for distribution of the intervals between the arrival times of packets (time delays between individual packets) [24, 25, 26]. Such mathematical distribution is made for the link between R1 and R4. The distribution is made as the captured packets from Wireshark are further processed by a specialized program on the parameter intervals between the moments of arrival of the packets. Figure 11 shows the mathematical distribution of the captured packets from the link between R1 and R4. On "x" are the times of arrival of the individual packets – the whole conversation stream and "y" indicates the delay of the received packet compared to the previous packet. As it can be seen from the distribution, it can be argued that the time delay is almost constant after a short period of oscillation due to the network establishment time. The Wakeby approximation further confirms the constant time delay between the packets. The use of this approximation makes it easier to read the obtained results of the mathematical distribution. The constant time delay is due to the use of the MPLS technology in the virtual network.

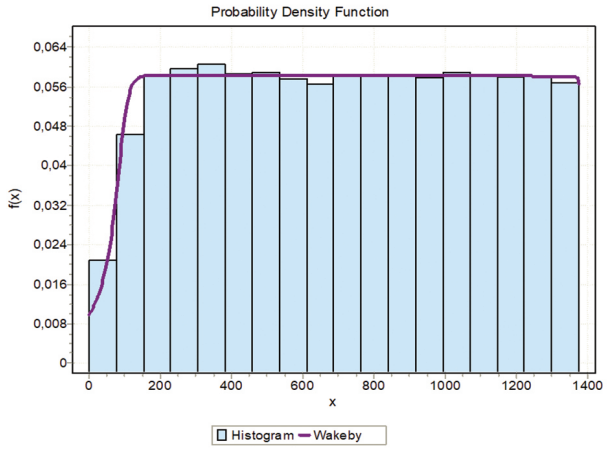

Fig. 11. Mathematical distribution for the R1–R4 link

4.2 RESULTS FROM THE EXPERIMENTAL NETWORK

Figure 12 shows the summarized results for the same VoIP call stream discussed in 4.1 (forward – reverse direction). As the results show, in the forward direction from the virtual network (192.168.31.67 exit/entry interface of the virtual network) to the Asterisk (192.168.31.50) the mean jitter value is much higher than that of the virtual network, but is still smaller than the limit of 30 ms. As the voice flow in the reverse direction (from Asterisk to Test_PC1) starts from this network, the first lost packets in this direction are noticed - 28 (0.02%).

Figure 13 shows the jitter distribution for every second of the call in the forward direction. The graph shows that the jitter significantly exceeds the 30 ms limit. As a result, a large percentage of lost packets is observed - 0.3%, compared to the same flow in the virtual network where there is no packet loss.

Figure 14 presents the jitter distribution for the entire duration of the call in reverse direction. From the graph, it can be argued that the results obtained are almost identical to those of figure 5, except that the lost packets are much smaller here.

Forward		Reverse	
192.168.31.67:33970 → 192.168.31.50:15968		192.168.31.50:15968 → 192.168.31.67:33970	
SSRC	0x0d8caaea	**SSRC**	0x66531d9e
Max Delta	394.95 ms @ 1088690	**Max Delta**	509.65 ms @ 1789675
Max Jitter	39.33 ms	**Max Jitter**	53.46 ms
Mean Jitter	5.76 ms	**Mean Jitter**	1.76 ms
Max Skew	-2744.92 ms	**Max Skew**	-567.46 ms
RTP Packets	115884	**RTP Packets**	116309
Expected	116227	**Expected**	116337
Lost	343 (0.30 %)	**Lost**	28 (0.02 %)
Seq Errs	228	**Seq Errs**	27
Start at	2168.778674 s @ 951198	**Start at**	2168.783591 s @ 951201
Duration	2325.52 s	**Duration**	2326.82 s
Clock Drift	-870 ms	**Clock Drift**	-420 ms
Freq Drift	7997 Hz (-0.04 %)	**Freq Drift**	7999 Hz (-0.02 %)

Fig. 12. Summary results from Wireshark

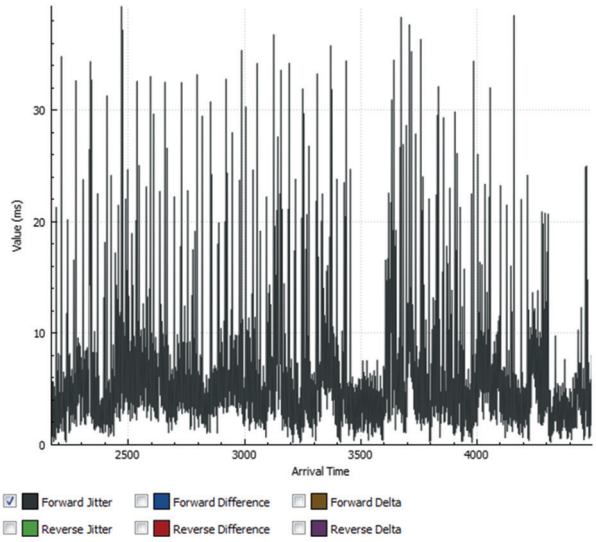

Fig. 13. Forward jitter for the whole stream

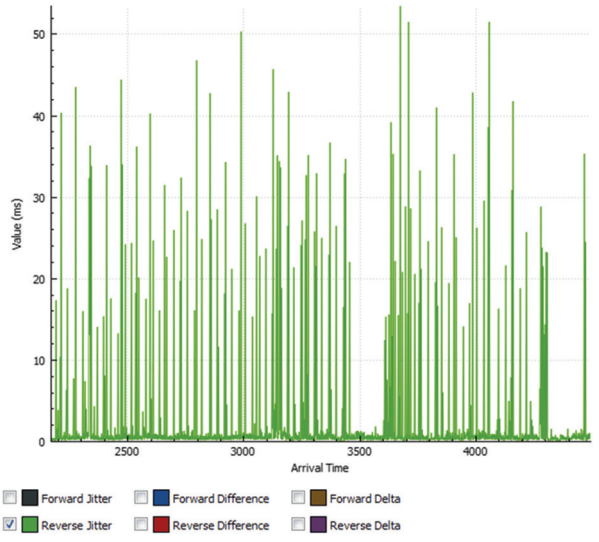

Fig. 14. Reversed jitter for the whole stream

The better jitter values in the forward direction on the virtual network are due to the fact that MPLS is used in the virtual network, which accelerates the network operation while it is not used in the real network. As it can be seen, the deterioration of the parameters of the stream in the reverse direction in the virtual network starts in the experimental network and in the virtual network they are getting worse.

Figure 15 shows the results for the delta in the forward direction. There is a significant deterioration in the values of this parameter - many times it is exceeding the 150 ms limit.

The results of figure 16 for the reverse delta are almost identical to those of Figure 7.

Again, to further evaluate the performance of the real network, a mathematical distribution of the intervals between the moments of packet arrival is made. Figure 17 shows the resulting distribution for the time delay between the packets.

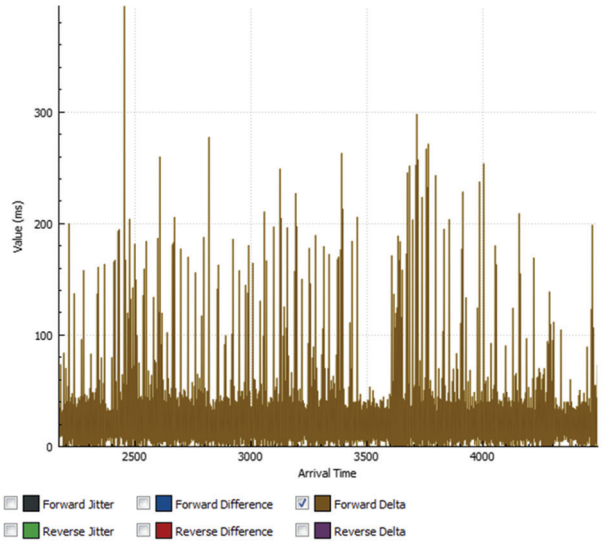

Fig. 15. Forward delta for the whole stream

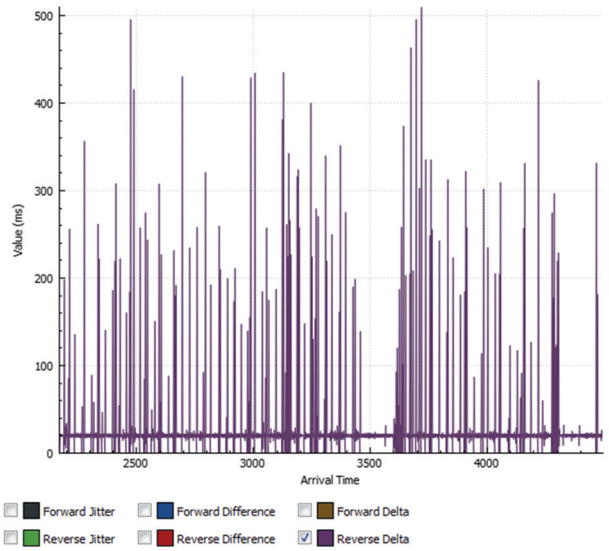

Fig. 16. Reversed delta for the whole stream

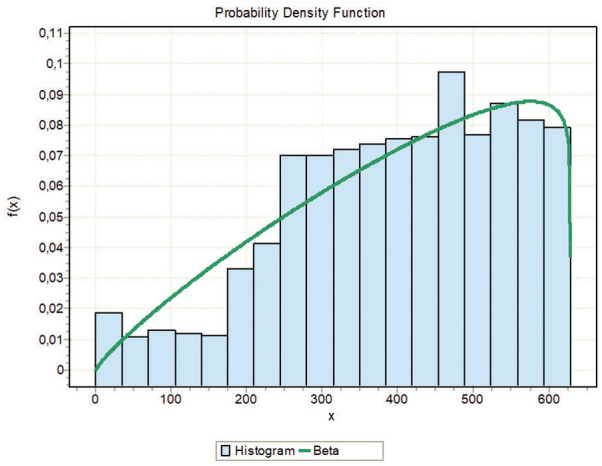

Fig. 17. Mathematical distribution for the real network

As it can be seen from the distribution for the experimental network, the delay between packets varies and it can be claimed to be constant at times, but not as it is on the virtual network, where MPLS is configured. This statement is further supported by the Beta approximation. It shows that the time delay is constantly increasing. Again, the use of the approximation makes it easier to read and understand the results of the distribution.

5. CONCLUSIONS

A virtual IP - based network has been created and it is configured to work with MPLS. A real experimental IP based network is also created. There is connectivity between the two networks. Both networks are connected to the Internet.

Monitoring programs for IP – based networks and mathematical distribution have been used to evaluate the performance of the two networks. Based on the results from the monitoring of the two networks, the following results were obtained: the mean and maximum values of the jitter in the virtual network in the forward direction are much smaller than the one in the experimental network.

The delta parameter in the virtual network in the forward direction is the lowest. In the reverse direction a significant improvement in the instantaneous values of the parameter are noted compared to the values of the parameter in the real network.

The instantaneous values of the jitter in the reversed direction are drastically improved too, compared to the values from the real network.

The deterioration of the flow parameters caused by the experimental network is partially compensated in the virtual network. This is due to the configured MPLS in the virtual network.

The mathematical distributions also confirm the results of the monitoring. The time delay on the network using MPLS is constant, unlike the experimental real

network. This statement is further confirmed by the two used approximations - Wekaby and Beta.

The obtained results from the monitoring and the mathematical distributions confirm that, in an IP - based network that uses MPLS, the performance (in terms of packet time delays) is much better than without using MPLS. The use of the MPLS technology in an IP - based network, in which real time traffic (VoIP traffic) will be transmitted, significantly improves network performance - the time delay between packets is constant. It is therefore advisable to use this technology in IP networks where the transmitted traffic is in real time.

The used methodology in this work - the use of monitoring programs and mathematical distributions, can be applied to evaluate the performance of other IP-based networks through which other types of real-time traffic is transmitted as video.

6. ACKNOWLEDGMENT

This paper is supported by the National Scientific Program "Information and Communication Technologies for a Single Digital Market in Science, Education and Security (ICTinSES)", financed by the Ministry of Education and Science

7. REFERENCES:

[1] F. Sapundzhi, M. Popstoilov, "C # implementation of the maximum flow problem", Proceedings of the 27th National Conference with International Participation TELECOM, Sofia, Bulgaria, 30-31 October 2019, pp. 62-65.

[2] M. Taruk, E. Budiman, M. Wati, Haviluddin, "OSPF Wireless Mesh with MPLS Traffic Engineering", Proceedings of the International Conference on Electrical, Electronics and Information Engineering, Denpasar, Bali, Indonesia, 3-4 October 2019, pp. 119-122.

[3] M. A. Ridwan, N. A. M. Radzi, W. S. H. M. Wan Ahmad, F. Abdullah, M. Z. Jamaludin, M. N. Zakaria, "Recent trends in MPLS networks: technologies, applications and challenges," IET Communications, Vol. 14, No. 2, 2020, pp. 177-185.

[4] O. Lemeshko, O. Yeremenko, "Linear optimization model of MPLS Traffic Engineering Fast ReRoute for link, node, and bandwidth protection", Proceedings of the 14th International Conference on Advanced Trends in Radioelecrtronics, Telecommunications and Computer Engineering, Lviv-Slavske, Ukraine, 20-24 February 2018, pp. 1009-1013.

[5] T. Chang, Y. Tang, Y. Chen, W. Hsu, M. Tsai, "Maximum Concurrent Flow Problem in MPLS-Based Software Defined Networks", Proceedings of the IEEE Global Communications Conference, Abu Dhabi, United Arab Emirates, 9-13 December 2018, pp. 1-7.

[6] E. N. Lallas, A. Xenakis, G. Stamoulis, J. Korinthios, "QoS and MPLS design issues in NoCs", Proceedings of the South-Eastern European Design Automation, Computer Engineering, Computer Networks and Society Media Conference, Kastoria, Greece, 22-24 September 2018, pp. 1-4.

[7] O. Nevzorova, O. Lemeshko, A. Mersni, A. M. Hailan, A. S. Ali, S. Harkusha, "Improved Two-Level Method of Multicast Routing in MPLS-TE Network", Proceedings of the 2nd Ukraine Conference on Electrical and Computer Engineering, Lviv, Ukraine, 2-6 July 2019, pp. 846-850.

[8] S. T. Mirtchev, "Investigation of Pareto/M/1/k Teletraffic System by Simulation", Proceedings of the 27th National Conference with International Participation TELECOM, Sofia, Bulgaria, 2019, 30-31 October 2019 pp. 70-73.

[9] M. Imran, M. A. Khan, M. Abdul Qadeer, "Design and Simulation of Traffic Engineering using MPLS in GNS3 Environment", Proceedings of the 2nd International Conference on Computing Methodologies and Communication, Erode, India, 15-16 February 2018, pp. 1026-1030.

[10] N. I. Sarkar, S. Gul, B. Anderton, "Gigabit Ethernet with Wireless Extension: OPNET Modelling and Performance Study", Proceedings of the International Conference on Information Networking, Kuala Lumpur, Malaysia, 9-11 January 2019, pp. 216-221.

[11] Cherneva G., H. Spiridonova, "Determination of the Impulse Response of a Communication Channel in the Process of Information Transmissions", Journal of the Technical University of Gabrovo, Vol.57, 2018, pp.103-106.

[12] S. T. Mirtchev, "Packet-Level Link Capacity Evaluation for IP Networks", Cybernetics and Information Technologies, Vol. 18, No. 1, 2018, pp. 30-40.

[13] F. I. Sapundzhi, M. S. Popstoilov, "Optimization Algorithms for Finding the Shortest Paths", Bulgar-

ian Chemical Communications, Vol. 50, No. Special Issue B, 2018, pp. 115-120.

[14] B. Korniyenko, L. Galata, L. Ladieva, "Research of Information Protection System of Corporate Network Based on GNS3", Proceedings of the International Conference on Advanced Trends in Information Theory, Kyiv, Ukraine, 18-20 December 2019, pp. 244-248.

[15] M. A. Barry, J. K. Tamgno, C. Lishou, M. B. Cissé, "QoS impact on multimedia traffic load (IPTV, RoIP, VoIP) in best effort mode", Proceedings of the 20th International Conference on Advanced Communication Technology, Chuncheon, South Korea, 11-14 February 2018, pp. 694-700.

[16] R. K. CV, H. Goyal, "IPv4 to IPv6 Migration and Performance Analysis using GNS3 and Wireshark", Proceedings of the International Conference on Vision Towards Emerging Trends in Communication and Networking, Vellore, India, 30-31 March 2019, pp. 1-6.

[17] A. Siswanto, A. Syukur, E. A. Kadir, Suratin, "Network Traffic Monitoring and Analysis Using Packet Sniffer", Proceedings of the International Conference on Advanced Communication Technologies and Networking, Rabat, Morocco, 12-14 April 2019, pp. 1-4.

[18] K. Sinchana, C. Sinchana, H. L. Gururaj, B. R. Sunil Kumar, "Performance Evaluation and Analysis of various Network Security tools", Proceedings of the International Conference on Communication and Electronics Systems, Coimbatore, India, 17-19 July 2019, pp. 644-650.

[19] P. Goyal, A. Goyal, "Comparative study of two most popular packet sniffing tools-Tcpdump and Wireshark", Proceedings of the 9th International Conference on Computational Intelligence and Communication Networks, Girne, Northern Cyprus, 16-17 September 2017, pp. 77-81.

[20] R. Das, G. Tuna, "Packet tracing and analysis of network cameras with Wireshark", Proceedings of the 5th International Symposium on Digital Forensic and Security, Tirgu Mures, Romania, 26-28 April 2017, pp. 1-6.

[21] P. Navabud, C. Chen, "Analyzing the Web Mail Using Wireshark", Proceedings of the 14th International Conference on Natural Computation, Fuzzy Systems and Knowledge Discovery, Huangshan, China, 28-30 July 2018, pp. 1237-1239.

[22] T. Szigeti, C. Hattingh, "End-to-End QoS Network Design: Quality of Service in LANs, WANs, and VPNs", Cisco Press. Part of the Networking Technology series, 2004

[23] Cisco - Understanding Delay in Packet Voice Networks, white paper, https://www.cisco.com/c/en/us/support/docs/voice/voice-quality/5125-delay-details.html (accessed: 2021)

[24] M. M. Alani, "Mathematical Approximation of Delay in Voice over IP", International Journal of Computer and Information Technology, Vol. 3, No. 1, 2014, pp. 78-82.

[25] K. Hammad, A. Moubayed, A. Shami, S. Primak, "Analytical Approximation of Packet Delay Jitter in Simple Queues", IEEE Wireless Communications Letters, Vol. 5, No. 6, pp. 564-567, 2016.

[26] R. Dehghan, M. Keyanpour, "A numerical approximation for delay fractional optimal control problems based on the method of moments", IMA Journal of Mathematical Control and Information, Vol. 34, No. 1, 2017, pp. 77-92.

Analyzing the Resilience of Convolutional Neural Networks Implemented on GPUs: Alexnet as a Case Study

Case study

Khalid Adam
University Malaysia Pahang,
College of Engineering, Department of Electrical Engineering
26300, Pahang, Malaysia
khalidwsn15@gmail.com

Izzeldin I. Mohd
University Malaysia Pahang,
College of Engineering, Department of Electrical Engineering
26300, Pahang, Malaysia
izzeldin@ump.edu.my

Younis Ibrahim
College of IoT Engineering,
Hohai University
Changzhou, Jiangsu 213022, China
Younis@hhu.edu.cn

Abstract *– There have been an extensive use of Convolutional Neural Networks (CNNs) in healthcare applications. Presently, GPUs are the most prominent and dominated DNN accelerators to increase the execution speed of CNN algorithms to improve their performance as well as the Latency. However, GPUs are prone to soft errors. These errors can impact the behaviors of the GPU dramatically. Thus, the generated fault may corrupt data values or logic operations and cause errors, such as Silent Data Corruption. unfortunately, soft errors propagate from the physical level (microarchitecture) to the application level (CNN model). This paper analyzes the reliability of the AlexNet model based on two metrics: (1) critical kernel vulnerability (CKV) used to identify the malfunction and light- malfunction errors in each kernel, and (2) critical layer vulnerability (CLV) used to track the malfunction and light-malfunction errors through layers. To achieve this, we injected the AlexNet which was popularly used in healthcare applications on NVIDIA's GPU, using the SASSIFI fault injector as the major evaluator tool. The experiments demonstrate through the average error percentage that caused malfunction of the models has been reduced from* **3.7***% to* **0.383***% by hardening only the vulnerable part with the overhead only 0.2923%. This is a high improvement in the model reliability for healthcare applications.*

Keywords *– Convolutional neural networks, Reliability, Soft errors, GPUs, healthcare applications*

1. INTRODUCTION

Convolutional Neural Networks (CNNs) are special type DNNs that have shown state-of-the-art results on many competitive benchmarks such as medical image classification [1], pathological brain detection [2], and disease detection [3] among many others. In fact, reports have revealed that CNNs is considered to be more effective, for they own the paradigms of more biologically inspired structures than other traditional networks [4]. This has led to the development of different CNNs including AlexNet [5], VGG [6], and DenseNet [7]. These CNNs derive their competence from being trained to a large database named ImageNet, Large-Scale Visual Recognition Challenge [8]. Hence, they occupy high positions of suitability in modern image classification. In fact, these machine learning networks have the ability to understand hierarchically classified data from lower to higher levels by developing a deep pattern of the input data. Based on these salient features and performance of CNNs, several researchers have exploited them to perform new tasks like the classification of medical images. Specifically, the knowledge acquired when these networks have been trained on millions of images are transferred into new tasks, thereby taking advantage of certain weights of their learned parameters (i.e., Transfer learning).

CNNs are applied to a wide variety of accelerators (i.e. FPGAs, GPUs, DSPs, etc.) each of which has its own elements, behaviour and execution flow. However, due to their computational power, graphics processing units (GPUs) are extensively used in CNNs to overcome the inherent computational challenges of healthcare applications [9] [10] [11] [12]. Notwithstanding, there are certain GPU units that if exposed to soft errors, can disrupt the reliability of the GPU operations; these units include memory elements such as register file and logic resources such as Arithmetic Logic Units (ALUs) [13]. Hence, when using GPUs to accelerate CNNs models in healthcare applications it is important to ensure that potential data corruption is avoided and failure rates must be reduced to the minimum and should not exceed 10 Failures in Time (FIT), which is defined as errors in10^9 hours of operations [14]. Thus, soft errors that occur in GPUs can eventually lead to misclassification of objects in CNNs, and the consequences would be disastrous. For instance, in [15] the authors have reported instances of the da Vinci robotic surgical system adverse events that included some kind of patient injuries and death, and reported as a "Malfunction", "unanticipated" and "unintended" errors. Food and Drug Administration (FDA), reported that 1078 of the adverse events (10.1%) were unintended errors (soft errors) happened, including 52 injuries and 2 deaths [16].

In this contribution, the reliability of the AlexNet model on a GPU was anayzed by conducting series of fault-injection campaigns, using NVIDIA's SASSIFI The first significant contribution of this study is the determination of soft errot resilience in AlexNet through comprehensive analysis, and ranking of vulnerable model parts from the perspective of kernel and layers. The second contribution is reduction of soft errors through a Selective Hardening approach. The subsequent sections of this paper are includes Section 2 related work. Section 3 which is brief background of AlexNet, Graphics Processing Units, and Soft Errors Propagation in GPUs. Section 4 desribes the Selective Hardening Strategy, and Section 5 contains the methodology while Section 6 presents the results generated from analysis of the Kernels and Layers. The experimental results and their analysis is presented in Section 7, whereas the Time Overhead Execution comparison is presented in Section 8 and the conclusion is in Section 9.

2. RELATED WORK

There are several studies in [17][18][19] [20][21] authors evaluated and analyzed the reliability of CNN models. Hence, it has been established that there are varieties of CNN architectures, with each having different bevavior and workflows. The different CNNs have been implemented on various accelerators including GPUs, ASICs, and TPU, through their peculiar execution flow based on their varying components. This makes it difficult to directly generalize the case of a particular CNN to other architectures [22]. Andru et al. [23] proposed a CNN architecture called EndoNet to automatically recognize the presence of surgical tools. The model trained on the Cholec80 dataset. But, the authors address the reliability of the proposed model in terms of temporal precision, which is different from our perspective. Amy et al. [24] introduce an approach to analyzing and tracking the movements of the surgical tool. They used the CNN model and m2cai16 dataset to train the model. However, the authors did not consider the reliability of the model. Grewal et al. [25] described an approach for automated brain hemorrhage detection from computed tomography. The study used DenseNet201 architecture as an emergency diagnosis tool, but the authors did not consider the reliability of such a model for the intended application, which is actually a safety-critical application, based on real-time CNN model detection.

In another study by Dunnmon et al. [26], three CNN models (Alexnet, ResNet, and DenseNet201) were used to classify chest radiographs into groups categorized as either normal or abnormal. This approach can help to prioritize abnormal chest radiographs automatically. In addition, the use of chest radiographs to predict multiclass thoracic diagnosis was reliably addressed in the study. Notwithstanding, the reliability of the models has not been considered. In another study, robot-assisted surgery was proposed by Wang and Fey [27]. Specifically, a deep analytical framework for learning and assessment of skills in surgical training was implemented. The individual skill levels in multivariate data with various time series were mapped to the motion kinematics using a deep CNN. Interestingly, instantaneous feedback can be obtained from personalized surgical training if the model is incorporated into the robot-assisted surgical systems pipeline. However, the reliability of the model to the intended application was not considered by the authors. Notably, several approaches have been developed to reduce the occurrence of the soft error in GPUs, through software solutions. This include Double Modular Redundancy (DMR) and Triple Modular Redundancy (TMR). However, the major drawback to the use of these solutions is the runtime overheads.

3. BACKGROUND

3.1. ALEXNET NEURAL NETWORK

AlexNet is a CNNs architecture, composed of eight layers with weights; the first five are convolutional layers and the remaining three are fully connected layers. The fully-connected layers generally consist of 4096-dimensional features [5]. AlexNet has been confirmed to be suitable for classifying medical images for diseases like lung diseases, heart challenges and, cancer. As presented in (Fig. 1), the input image in AlexNet should be augmented to an image size of 227 x 227 x 3. The window shape size applied to the first layer 96 convolution filter is 11 × 11, whereas it is 5×5 in the second

layer 256 convolution filter. Subsequently, 3×3 window size is applied to the remaining 384, 384, and 256 convolution filters, respectively. A maximum pooling layer of 3×3, with 2 strides is present in the network after the first, second, and last convolutional layers. Asides these five convolution layers, 4096 neuron outputs are present in the seven fully-connected layers following the fifth convolutional layer. Then, one fully connected output layer is situated at the end of the network which initially contains 7 output classes. Generally, an excellent performance of tasks involving computer visions can be achieved by using important keys like Dropout, ReLU, and preprocessing. The pre-trained AlexNet model with and weight configuration can be found on the Darknet framework.

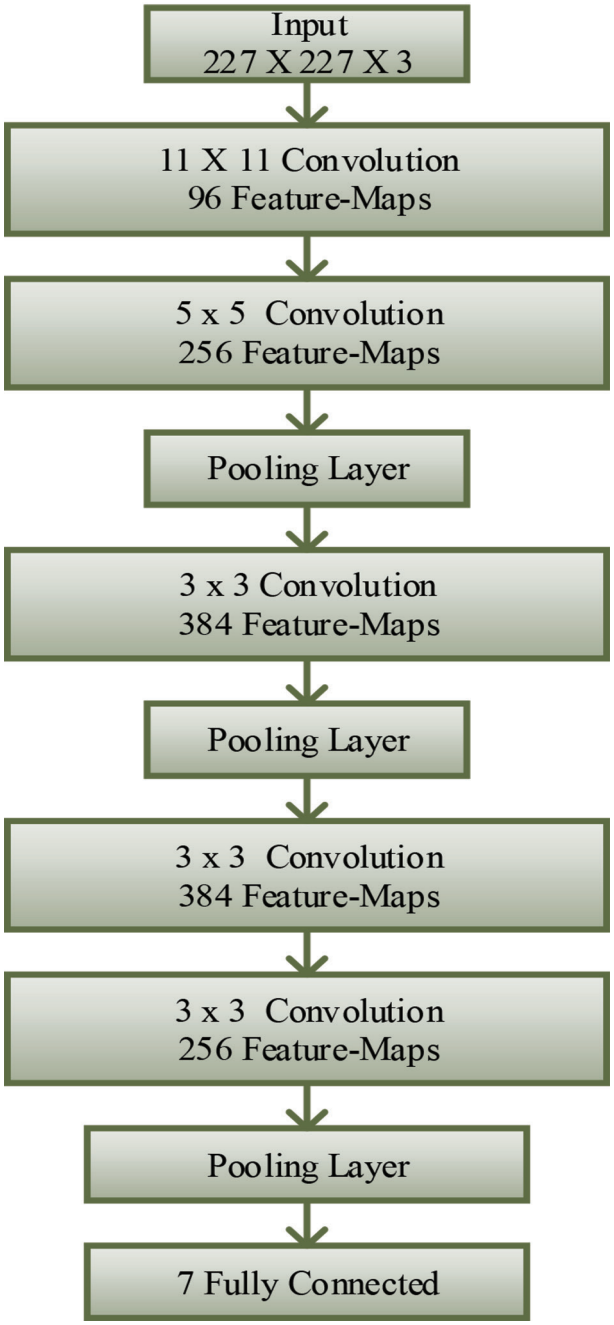

Fig. 1. AlexNet Architecture

3.2. GRAPHICS PROCESSING UNITS

The use of GPUs have recently extended beyond being used solely for graphics tasks to being used in more general-purpose devices. In fact, currently considered as the main DNN accelerators [28]. The increased interest in GPUs is mainly associated with its great computational power and massively parallel architecture. Based on these, they are more preferable in algorithms that require intense computing such as neural networks. It can be seen in (Fig. 2) that the basic GPUs architecture is based on generation of Compute Unified Device Architecture (CUDA) as the programming model. The basic building block unit in GPUs is known as Streaming Multiprocessor (SM). The SM is made up of several components such as streaming processors (SPs) that are used in arithmetic calculations, and special function units (SFUs) which function for sine, cosine, and square root operations. In addition, the SM comprises load/store (LD/ST) units used in memory operations, as well as many other registers for caches. SMs are the core idea of parallelism in GPUs. The basic structure of SMs in the GPU architecture is shown in Fig 2, each of which can only execute one thread in a clock cycle with dedicated registers from the register file. The warp scheduler to be executed next on the CUDA cores in a given SM selects a group of 32 threads (called a warp), and then instructions are dispatched by the instruction dispatch unit. The threads in each warp execute in a SIMT (single instruction, multiple threads) fashions. The global system memory of a GPU is located in the dynamic random-access memory and the global memory would normally be accessible to the SM. The L2 cache is a shared memory mainly shared by the SPs in the SMs.

Hence, read and write instructions can be executed at the L2 cache level by each SM. On the other hand, all the SPs in an SM can access the register file. The register file is basically mapped in the SMs to enhance computational performance through data caching for the running threads on each SM.

3.3. SOFT ERRORS PROPAGATION IN GPUS

The features of modern GPUs can be significantly affected by radiation strikes either in space or on earth and this can invariably result in computational failure or data corruption. Therefore, one of the notable unreliability sources in modern systems is soft errors. This is because electronic devices like GPUs would malfunction when they are struck by high-energy particles [29]. Usually, the tolerance to failure in safety-critical systems is restricted to 10 Failures in Time (FIT). Therefore, since soft errors in DNN accelerators (GPU inclusive) are more deleterious compared to other electronic devices, there is a need to pay deliberate attention to them for two main reasons.

Firstly, the complex memory hierarchy is used for improved latency. Secondly, the massively-parallel structure of the GPUs, that tends to disperse a single fault

to multiple faults. Usually, when memory elements of a GPU (indicated by the red sections in Fig. 3) are hit by particles, it can significantly affect all the threads that utilize such storage components. When functional components of the GPU such as ALU (INST) or Floating-point (FP) units are hit by a particle, it creates temporary-voltage pulses, Single Event Transients (SETs). The SET can then travel through the logic components of the GPU where it can be captured by a storage component. Specifically, a latch or flip-flop would trigger the flip of one or more bits from one value to another such as from 0 to 1 or from 1 to 0. However, this can be curtailed by applying a fault detection technique such as DMR, TMR, and ABFT. Generally, faults generated in GPUs in form of data values or logic operations often results in errors like Silent Data Corruption (SDC), system hang otherwise called Detected Unrecoverable Error (DUE), or outright crash of the application.

However, the errors might sometimes not result in an observable error in which case it is known as Masked errors. The propagation of errors could be via different processes, in this case, layers, until they arrive at the program output (AlexNet) where they will eventually lead to problems such as the misclassification of objects. Due to this, soft error in GPU is a very critical issue in safety-critical healthcare applications where high reliability is generally required. This is mainly due to the fact that even small errors might lead to serious injury or death as reported by the Food and Drug Administration (FDA) department [30].

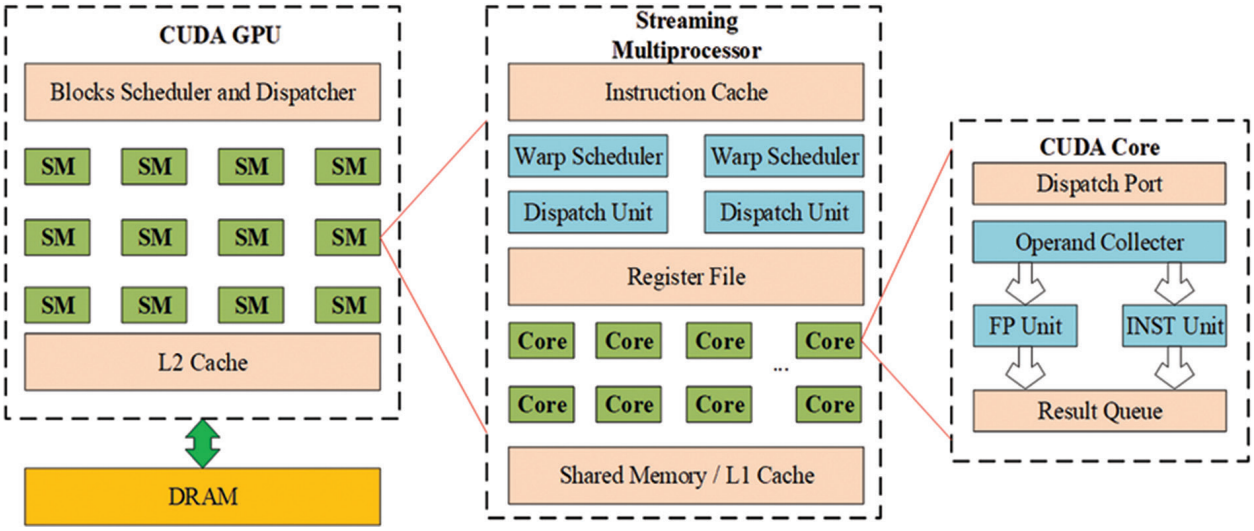

Fig. 2. GPU architecture and memory

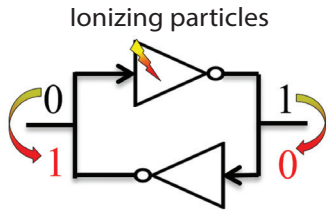

(a) Single Memory cell (bit)

1	0	0	1	1	0	0	1
1	0	0	0	1	0	0	1

(b) Memory Byte (8-bits)

Fig. 3. Memory-element strikes

4. SELECTIVE HARDENING STRATEGY

In this section, we developed Selective Hardening Strategy (SHS) by identifying the most vulnerable kernels for AlexNet, via fault injection (soft errors). In order to identify the most vulnerable kernels in the AlexNet model, we present a methodology (section 4). The key concept of SHS is that it is based on the well-known Triple Modular Redundancy (TMR), and it intertwines three copies of the instructions and adds majority voting. In short, this SHS mitigation consists of triple kernels, by means of majority voters. Based on this concept, our strategy is a selective solution that protects only the vulnerable kernels instead of duplicating the whole as in DMR and TMR, to reduce the overheads, and thereby offering more flexibility to designers.

5. METHODOLOGY

5.1. DATASET

The AlexNet model was trained and evaluated with a Cholec80 dataset. Eighty cholecystectomy videos which were recorded at the Strasbourg University Hospital (25 fps) are contained in the dataset [23]. In addition, tool presence annotation is present in the dataset at 1 fps. Seven different tools were utilized in the dataset including hook, clipper, irrigator, bipolar, grasper, specimen bag, and scissors. If at least half the tip of the tool appears in the scene, then it is considered a present tool. The AlexNet was trained with the first forty videos while the remaining videos were used for validation.

5.2. FAULT-INJECTION SETUP

A Maxwell architecture-based GPU GTX 750 Ti was used for this purpose [31], with a SASSIFI fault injector which was primarily used to assess the reliability of AlexNet model runs on GPUs. This was achieved through fault injection campaigns which made it easier to determine the possibility of a low-level corruption to propagate to the output. Notably, the AlexNet model was trained on the Cholec80 dataset for the surgical tool detection. With this tool, it was possible to carry out fault injection through three distinct modes. The first mode is the Register File (RF) mode which was used to determine the Architectural Vulnerability Factor (AVF) of the register file, as well as the response of our model (AlexNet), to errors present in the memory elements. The second mode is the Instruction Output Address (IOA) mode while the third mode is the Instruction Output Value (IOV) mode. The second and third modes (IOA and IOV) were used evaluate the Program Vulnerability Factor (PVF). In addition, they were used to investigate how a single error modifies the result of instruction and propagates to the program output (AlexNet).

A total of 1000 faults was injected for each of the three modes RF, IOA, and IOV. this number of injections was enough to guarantee that the worst-case statistical error bars at 95% confidence are at 1.96%. Notably, various bit-flip models can be obtained from SASSIFI including zero value, single bit-flip, a random value, and multiple bit-flip. Nevertheless, only the single bit-flip and random value models were selected for the three injection modes of this present study. These models were preferentially selected because single-bit flip is more suitable and realistic for memory errors. On the other hand, all the other three bit-flip models are represented by the random value. The AVF of the register file is measured when errors are injected with RF mode while the PVF of the algorithm is measured if the errors are injected with IOA and IOV.

As a consequence of fault injection and comparison of program output with the golden output (i.e., the pure outcome), three categories are expected, Masked, DUE, or SDC. It should be noted that SDC is the only error of interest to this study when studding the error propagation within the model. This is because crash and hand errors (DUEs) are not being propagated to a subsequent layer. Similarly, masked errors are instantaneously masked at the location of occurrence. The SDC errors and the mechanism of their propagation through layers were further grouped into three categories, for a better understanding of the concept. The first group is the Malfunction SDCs which represent errors that propagate, arrive at the program output, and alter the probabilities vector thereby impacting the object's rank via misclassification. The second groups are the Light-Malfunction SDCs. These are errors that propagate, arrive at the program output, and alters the probabilities without changing the object's rank. This situation is otherwise called tolerable SDC meaning object misclassification did not occur. The third groups are the No-Malfunction SDCs which are the error that propagates without reaching the final program output. This means the errors are masked in some layers but this group of SDCs are different from Masked errors which do not propagate at all.

6. KERNELS AND LAYERS FAULT INJECTION RESULTS AND ANALYSIS

The results generated from our fault-injection campaign, and their analysis are presented in this section. A detailed sensitivity analysis was conducted to assess the resilience of the AlexNet model. This was performed through the evaluation of two metrics. The first metric is the critical kernel vulnerability (CKV) which helps to recognize the presence of malfunction and light-malfunction errors in each kernel. The second metric is the critical layer vulnerability (CLV) which enables tracking of malfunction and light-malfunction errors within the layers.

6.1. CKV

As discussed in section 2.1, several layers are present in the Alexnet model. Implementation of these layers on a GPU would result in the generation of several kernels (special functions) for each layer. Notably, the kernel is a component of the source code that is implemented on a GPU, not a CPU and the kernels have distinctly peculiar computing characteristics. Therefore, all the static kernels required for a particular task is needed for an in-depth analysis of the vulnerability levels of the different kernels to malfunction and light-malfunction errors. This is also required to determine how they influence the final output of the model through object classification. Nevertheless, we only consider the kernels that are required for inference whereas the kernels used for training not incorporated as presented in Table 1. After fault injection, each kernel of the injected program is analyzed and the most vulnerable kernels of our AlexNet are determined. It is worth noting that in Fig. 4, Fig. 5, and Fig. 6, the probabilities of the whole graph sum up to 100% rather than the vertical bars of each kernel. This is because the AlexNet model program consists of all these kernels in Table 1. In other words, AlexNet programs are divided into small pieces of programs (kernels) that are executed in the GPU.

The kernels that produce a larger amount of errors can be easily identified by observing Fig. 4, Fig. 5, and Fig. 6. Likewise, the resilient kernels can be seen in the stated figures. Generally, Malfunction, Light-Malfunction, and DUEs in RF, IOA, and IOV are noticeable for all the kernels. However, the two kernels with the highest vulnerability in the AlexNet model are Im2col and Add_bias. In contrast, only a small number of DUEs, Malfunction and Light-Malfunction are noticeable in the other kernels which indicates that they are highly resilient to soft errors. Similarly, the Fill kernel

shows little small Malfunction and Light-Malfunction error which suggests that they are highly resilient to soft errors. It can also be observed that the building of one CNN layer such as Conv. Or activations layers can be obtained from the contributions of more than one kernel. Statistically, it is easier to identify the layers that are more susceptible to faults, thereby facilitating decision-making at the error mitigation step. It is evident in Fig. 4 that the kernels in the RF mode produce larger number of DUE errors, compared to Malfunction and Light-Malfunction errors. In contrast, Fig. 5 and Fig. 6 shows that the kernels in IOA and IOV modes tend to produce higher levels of Malfunction and Light-Malfunction errors compared to DUE errors. The reason for this behavior as reported by [32] is that RF injection is the lowest injection level whereas higher injection levels are performed at IOA and IOV sites because instructions are manipulated. Generally, the result discussed here indicates that different vulnerabilities are associated with the static kernels of the AlexNet model. These results make it easy to determine the kernels that need to be duplicated as a means of saving costs, rather than duplicating the entire, which is a very costly process.

Table 1. AlexNet inference kernels and their corresponding layers

Layer	Kernel	Kernel Task
Convolutional	Im2col_gpu, Add_bias, Fill_gpu	Operation to matrix-multiplication operation and add biases to the necessary parameters after the matrix multiplication
Max pooling	Forward_ maxpool	To reduce the spatial dimension of the input volume for next layers
Activation	Activation_array	Apply nonlinearity to the feature maps to reduce the input linearity for the next layer
Softmax	Softmax	To calculating the probabilities of each class

6.2. CLV

For a detailed understanding of the mechanism of error propagation through the layers of AlexNet to the output, the PVF was measured while the fault-injection mode is in the IOA and IOV. Fig. 7 to Fig. 9 presents the error propagation at each AlexNet layer, showing their different sensitivity to soft errors. Hence, the errors (Malfunction and No-Malfunction) that are propagated from the injected layers can be tracked to the last layer. The three SDC categories were investigated for each layer and the categories were calculated as discussed in section 4.1. The AVF and PVF values were measured for the given errors to determine the layers with a high probability to generate errors that can significantly alter the model prediction (object misclassification). The first observation is that the probability values of each layer do not sum up to 100%. The reason is that if a layer is injected, it produces three types of errors: DUE, Masked, and SDC. However, because in this subsection, we intend to analyze the propagation of errors, and only SDC errors propagate through layers. Therefore, we shall mainly focus on the three SDC types which are Malfunction SDCs, Light-Malfunction SDCs, and No-Malfunction SDCs. This is the reason why they do not sum up to 100%.

It is evident in Fig. 7 that in RF mode, the layers only tend to generate zero amounts of Malfunction. Layers 0 to 6 generates big amounts of Light-Malfunction on an average 12.57% AVF. On the other hand, the layers with No-Malfunction is on the average of 3.9%. This is an indication that RF injections present a less significant influence on the resilience of layers against Malfunction errors. However, different amount of DUE errors is produced by the layers, due to reasons earlier stated in Section 6.1. The injection of faults into the IOA and IOV generates SDC errors in different layers, and this influences their resilience. Therefore, these two modes are discussed and analyzed in further detail. However, a lesser percentage of DUE errors was generated by the IOA and IOV injections, compared to RF mode.

As can be seen in Figure 8, in the IOA mode, layers 0, 1, and 7 generate Malfunction errors of 0.2% and this value is considered too high in safety critical applications. However, they still generate Light-Malfunction with an approximate value of 18.6% due to the AlexNet structure. On the other hand, 67.9% of the injected faults represent No-Malfunction. Likewise, several percentages of DUE errors are produced by the layers on the average 1%. However, about half of the layers including layer 7, 8, 9, 10, 11, 12, and 13 are not significantly affected by DUE errors. As illustrated in Fig. 9 for the IOV mode, an average Malfunction value of 0.8% was generated by the layers. This significantly impacts the reliability of the model which suggests that the percentage is unacceptable. About 3.4% of the total Malfunction generated by the model was statistically contributed by layers 0 and 2. In addition, the largest percentage of Light-Malfunction and No-Malfunction were produced by these two layers which indicates that they are more vulnerable than other layers of the model. In SASSIFI, IOV mode is considered to be the highest injection level among the three modes and this is why layers injections performed through IOV mode is most unlikely to terminate the model execution. Generally, from the IOA and IOV model results presented in Fig. 8 and Fig. 9, layers 0 and 2 generate more Light-Malfunction errors and No-Malfunction compared to

other layers present in the network. In addition, the convolutional (11x11 and 5x5) of the AlexNet as described in Fig. 1 is represented by these layers. Based on the explanation in Section 2.1, linear function is the activation function within these layers, and this equates the output and input thereby retaining the initial size. This observation clearly describes the structure of the AlexNet model itself, whereby larger input sizes are possessed by these layers. The direct relationship between the execution time of each layer and the corresponding exposure time in soft errors is not surprising because longer layer exposure should expectedly produce higher rates of Malfunction errors. It is noticeable that relatively fewer errors are generated at the layers close to the output layer. This is probably due to the gradual reduction of the 227×227×3 matrix input size at the first layer as it propagates and reaches the output layer where the size is 13x13x256, before becoming a vector of 7 probabilities.

Most of the SDC errors (all categories) at the AlexNet output originate from faults that are related to the Conv. layers. Considering the size of input and filter numbers, it is evident that all the convolutional layers utilize the same kernels and possess the same AVF and PVF values. Nevertheless, Fig. 7, 8, and 9 shows that the possibility of an output model being impacted by injection is mainly dependent on the position of the layer in the network. This is particularly evident in layer 7 which is located just after convolutional layers. Herein, Softmax is observed to be the most reliable layer because no error is generated in this layer and most of the Malfunction and Light-Malfunction are masked. This can be attributed to two main reasons. Firstly, contrary to the case for other layers, Softmax is invoked just once and this significantly reduces its execution time thereby making it almost impossible for errors to generate in it. Secondly, the vector probability functionality of Softmax sums up to one. Therefore, even if SDC (Malfunction and Light-Malfunction) alters the input value of Softmax, there could still be retention of a probability percentage such that error will be No-Malfunction. The scores of a vast majority of the output-probability are zeros because the classified object should bear similarity with some of the remaining objects among the 7 classes needed for classification. This is a confirmation of the underlying feature of the ANNs, which is fault tolerance. This means that if the values are negative, they represent No-Malfunction.

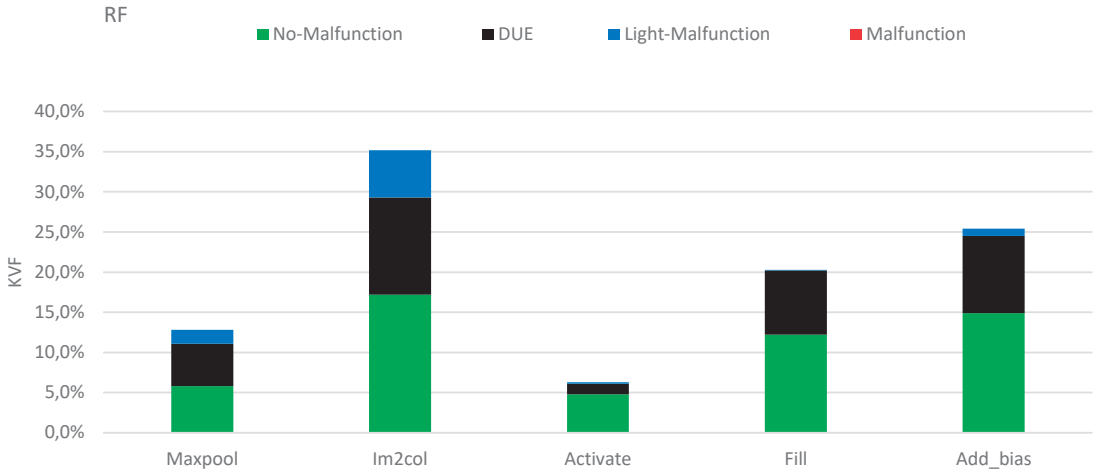

Fig. 4. Kernels vulnerability of AlexNet models for RF mode

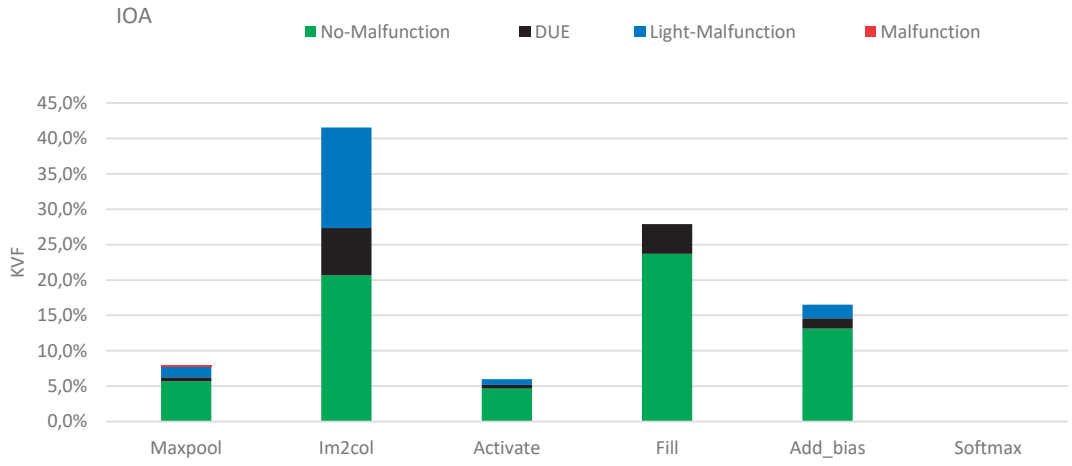

Fig. 5. Kernels vulnerability of AlexNet models for IOA mode

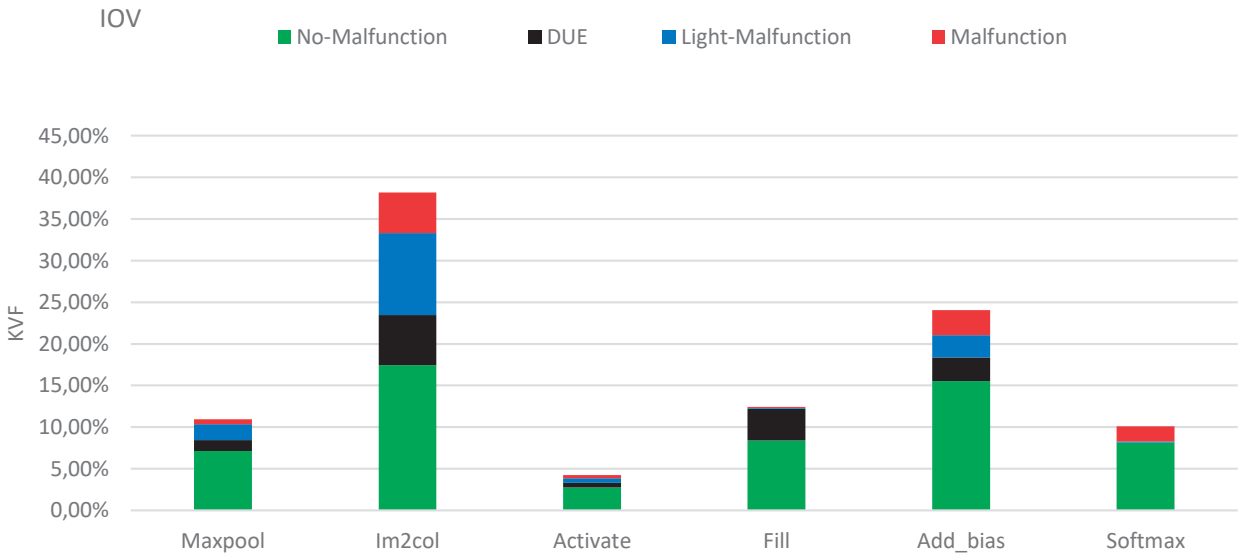

Fig. 6. Kernels vulnerability of AlexNet models for IOV mode

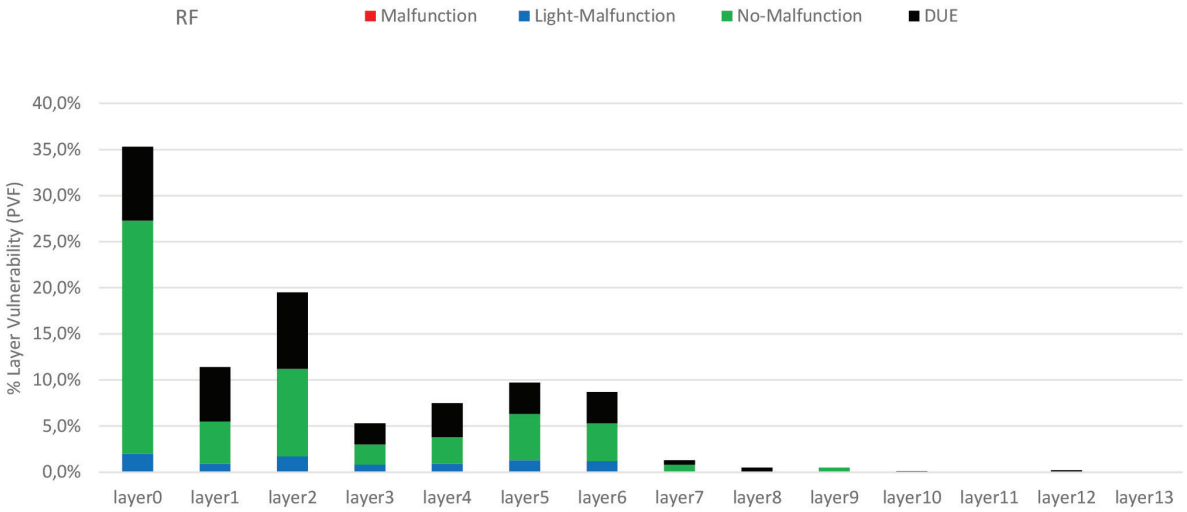

Fig. 7. AVF of RF Mode layer for Malfunction SDCs,
Light-Malfunction SDCs, No-Malfunction SDCs and DUE

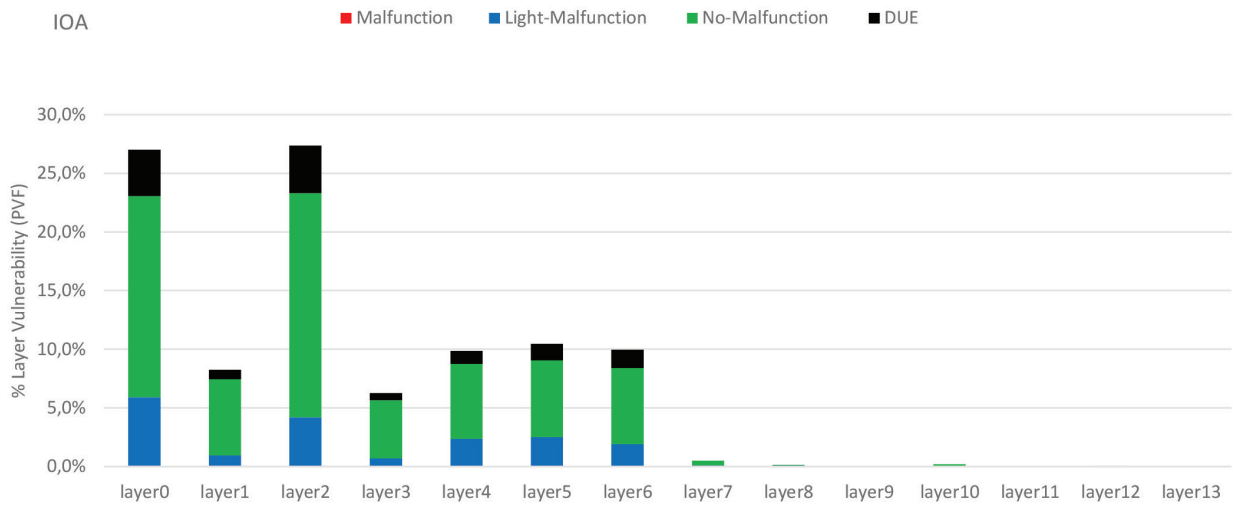

Fig. 8. PVF of IOA Mode layer for Malfunction SDCs,
Light-Malfunction SDCs, No-Malfunction SDCs and DUE AlexNet

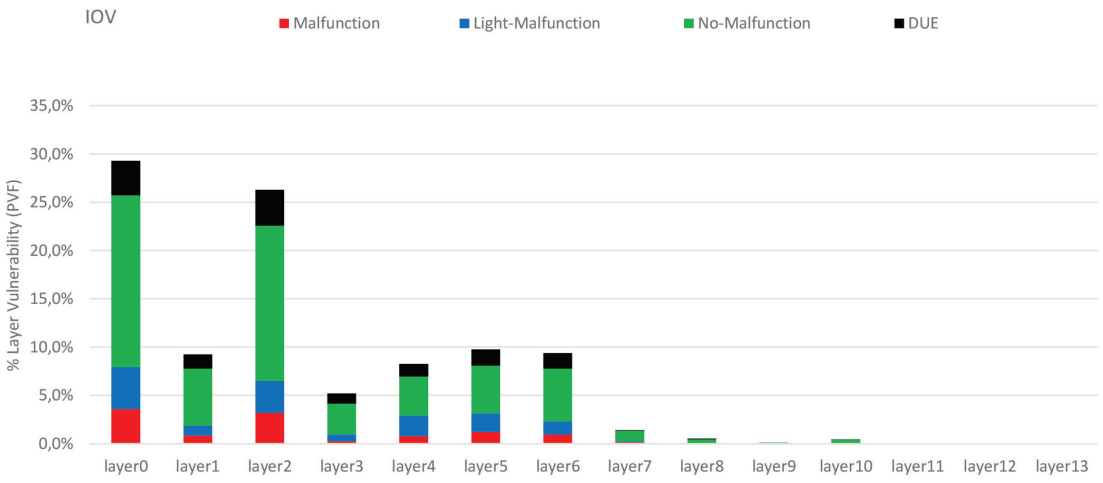

Fig. 9. PVF of IOV Mode layer for Malfunction SDCs, Light-Malfunction SDCs, No-Malfunction SDCs and DUE

7. EXPERIMENTAL RESULTS AND ANALYSIS WITH SHS

7.1. CKV ANALYSIS

In RF, IOA, and IOV kernels in Fig. 10, Fig. 11, and Figure 12 respectively, we evaluated the kernels by applying our SHS. Based on our analysis in section (5.1) the top-2 vulnerable kernels for AlexNet are Im2col and Add_bias in all three modes. All the Malfunction SDCs in these kernels become No-Malfunction. Our technique shows significant improvement in the AlexNet model, the errors in top-2 vulnerable kernels (Im2col and Add_bias). The errors in RF mode reduce from 5.90% to 0.00% Light-Malfunction in Im2col and from 0.90% to 0.00% Light-Malfunction in Add_bias, while there is not any modification on both kernels in Malfunction errors (still zero). Whereas, the errors in IOA mode reduce from 14.20% to 0.00% Im2col and 1.90% to 0.10% Add_bias in Light-Malfunction. Meanwhile, there is not any change in both kernels in Malfunction errors (still zero). They are also significantly improved in IOV mode, where errors are reduced from 9.82% to 0.78% in Im2col and 2.69% to 0.12 in Add bias in Light-Malfunction.

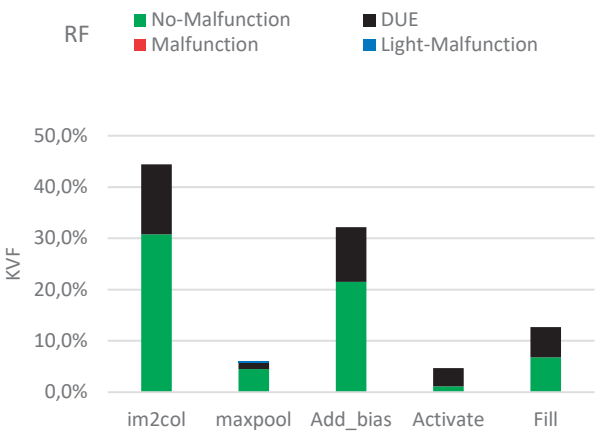

Fig. 10. Kernels vulnerability of AlexNet models for RF mode after applying our SHS

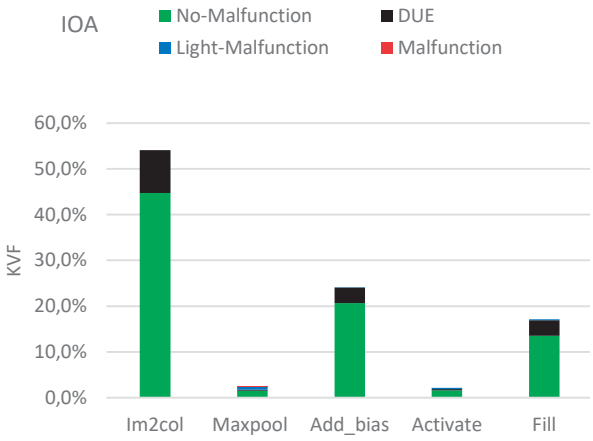

Fig. 11. Kernels vulnerability of AlexNet models for IOA mode after applying our SHS

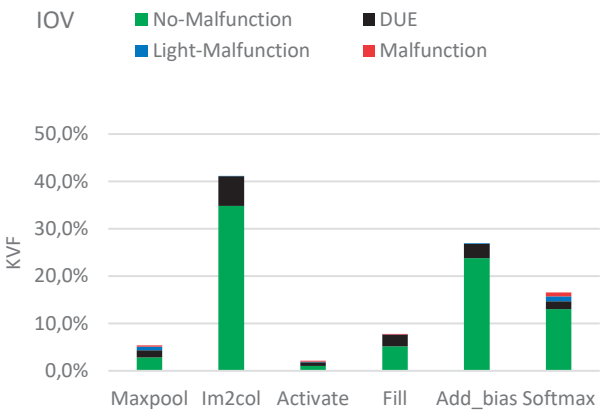

Fig. 12. Kernels vulnerability of AlexNet models for IOV model after applying our SHS

7.2 CLV ANALYSIS

In this subsection, the resilience of the AlexNet was reevaluated from a layer perspective through analysis of the resilience of the layer after applying our technique. As error propagates through layers is the main target in this phase, we measure all types of SDC errors including

Malfunction SDCs, Light-Malfunction SDCs, No-Malfunction SDCs, and DUEs. Fig. 13 shows the RF model after applying our mitigation technique, the experimental result shows only 0.00% and 0.30% errors of Malfunction and Light-Malfunction respectively. While it still produced a big amount of No-Malfunction SDCs in the percentage of 62.80 %. Despite the amount of the DUEs still high at 36.90%. On the anther hand, Fig. 14 and Fig. 15 show IOA and IOV, both of the modes produced less amount of the DUEs 16.55% and 15.6% respectively, compared to the RF mode, and the reason that IOA and IOV have a different level of injections. Therefore, in Fig. 14 IOA, produced Malfunction and Light-Malfunction on average 0.01% and 0.09% respectively, meanwhile most of the errors 82.10% No-Malfunction SDCs. On the anther hand, IOV in Fig. 15 produced less amount of the Malfunction and Light-Malfunction on average 0.08% and 0.19% respectively, where 80.76% of the errors No-Malfunction.

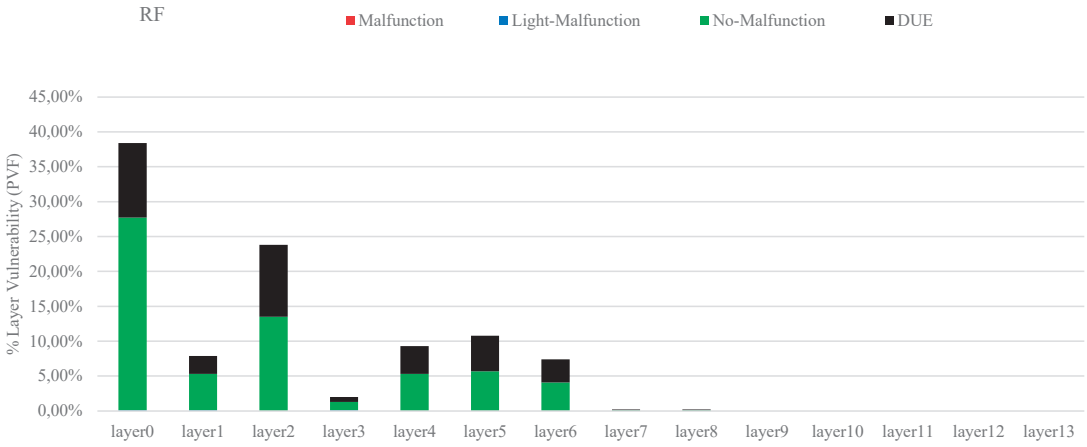

Fig. 13. AVF of each layer (after applying our SHS)

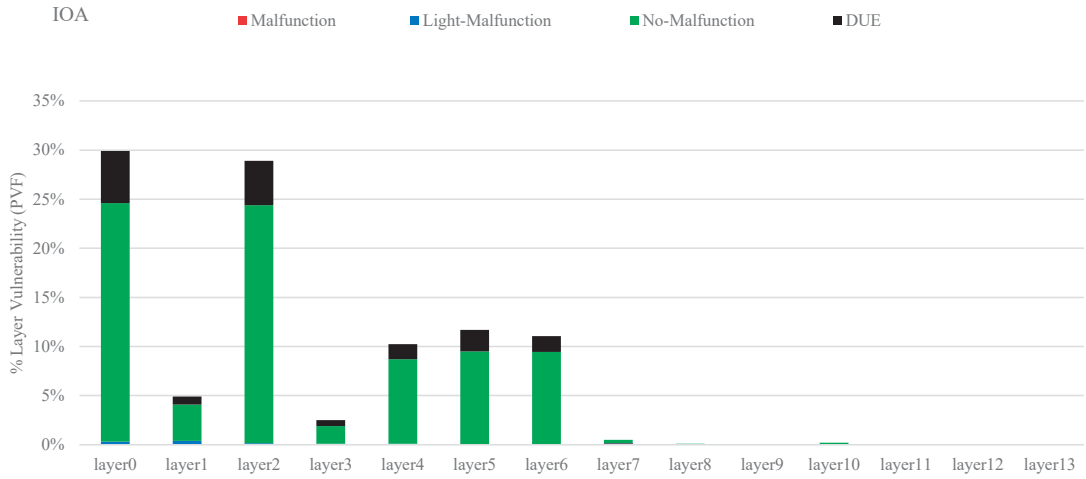

Fig. 14. PVF of each layer (after applying our SHS)

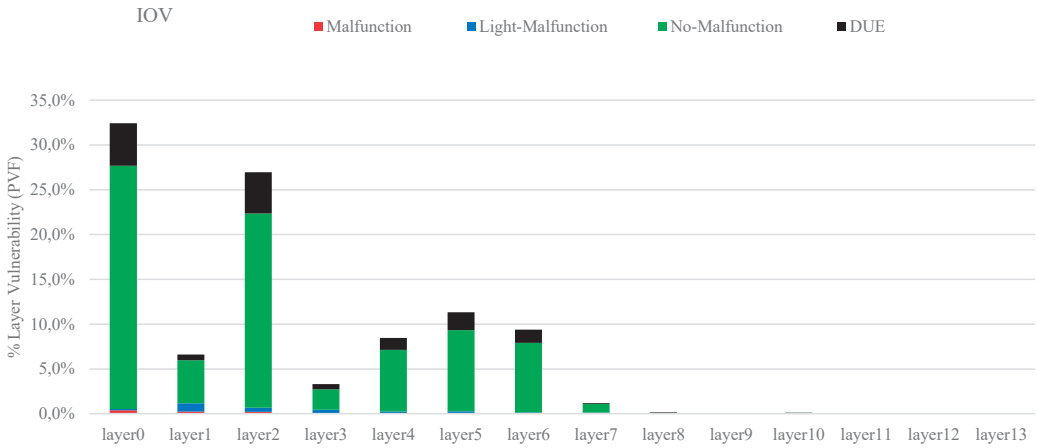

Fig. 15. PVF of each (after applying our SHS)

In this section, we evaluate our proposed solution by measured the performance overheads for whole models (AlexNet) and vulnerability kernels. By calculating the execution time (performance) for the whole model and the vulnerable kernels before and after implementing our technique. Table 2 shows the overheads of our technique, DMR, and TMR techniques summarizes the error injection, and each kernel after applying our mitigation strategy technique. As our technique to achieve a low-overhead with sufficient reliability, we selectively hardened only the vulnerability kernels. Consequently, the overhead can be reduced, by exploiting the SHS that is executed and overhead has only increased by 0.2923%, thus improved the reliability of models. Compared to the DMR and TMR whereas the overhead increased 97.461% and 200.881% respectively. Therefore, our technique shows highly significant error mitigation by only hardened selective kernels. And removed the unnecessary overhead especially in the safety-critical system (healthcare applications) that comes with strict deadlines, the overhead associated with duplication whole model is unacceptable.

Table 2. Comparison of overhead of Unhardened model, S-MTTM-R, DMR and TMR

Kernels (Time by MS)	Number of invocations	Unhardened	SHS	DMR	TMR
Im2col	5	0.0002303	0.0104156	0.0208312	0.0312468
Add_bias	5	0.000708	0.0035207	0.0070414	0.0105621
Maxpool	4	0.0237066	0.0237066	0.0474132	0.0711198
Activation	8	0.4267208	0.3935817	0.7871634	1.1807451
Fill	5	0.0948266	0.14224	0.2844858	0.4267258
Softmax	1	0.1201457	0.0948267	0.1896534	0.2844801
The whole model	1	0.666338	0.6682913	1.3157572	2.0048797

8. CONCLUSION

In this contribution, we analyzed and evaluated the Malfunction and Light-Malfunction SDCs of soft errors for the AlexNet model on the GPU. Our CKV and CLV identify the most vulnerable kernels and layers. Based on the analysis in Section 5 on the reliability of the model's bit sensitivity, the vulnerable bits can be selectively protected using SHS. Our result shows a high reduction rate of errors in the top vulnerable kernels such as Im2col and Add_bias. Besides, the model achieved a high reduction in No-Malfunction from 54.9%, 67.9%, and 59.4% to 62.80%, 82.10%, and 80.76% in the three modes such as RF, IOA, and IOV, respectively. Moreover, the performance overhead of our solution is compared with the well-known protection techniques such as Algorithm-Based Fault Tolerance (ABFT), Double Modular Redundancy (DMR), and Triple Modular Redundancy (TMR). The proposed solution shows the least overhead while correcting up to about 82.8% of the SDC errors in a CNN, thereby remarkably improving the healthcare domain's model reliability.

9. ACKNOWLEDGEMENT

This research was supported by Universiti Malaysia Pahang, through the UMP internal grant (PGRS190325)

10. REFERENCES

[1] R. M. Haralick, I. Dinstein, K. Shanmugam, "Textural Features for Image Classification", IEEE Transactions on Systems, Man and Cybernetics, Vol. SMC-3, No. 6, 1973, pp. 610–621.

[2] S. Lu, Z. Lu, Y. Zhang, "Pathological brain detection based on AlexNet and transfer learning", Journal of Computational Science, Vol. 30, 2019, pp. 41–47.

[3] F. Demir, A. Şengür, V. Bajaj, K. Polat, "Towards the classification of heart sounds based on convolutional deep neural network"", Health Information Science and Systems, Vol. 7, No. 1, 2019, pp. 1–9.

[4] W. Rawat, Z. Wang, "Deep convolutional neural networks for image classification: A comprehensive review", Neural computation, Vol. 29, No. 9, 2017, pp. 2352–2449.

[5] A. Krizhevsky, I. Sutskever, G. E. Hinton, "ImageNet classification with deep convolutional neural networks", Communications of the ACM, Vol. 60, No. 6, 2017, pp. 84–90.

[6] A. Vedaldi, A. Zisserman, "Vgg convolutional neural networks practical", Department of Engineering Science, University of Oxford, 2016, p. 66.

[7] G. Huang, Z. Liu, G. Pleiss, L. Van Der Maaten, K. Weinberger, "Convolutional Networks with Dense Connectivity", IEEE Transactions on Pattern Analysis and Machine Intelligence, 2019, pp. 1–1. (in Press)

[8] O. Russakovsky et al., "Imagenet large scale visual recognition challenge", International journal of computer vision, Vol. 115, No. 3, 2015, pp. 211–252.

[9] T. Kalaiselvi, P. Sriramakrishnan, K. Somasundaram, "Survey of using GPU CUDA programming

model in medical image analysis", Informatics in Medicine Unlocked, Vol. 9, 2017, pp. 133–144.

[10] A. A. Shvets, A. Rakhlin, A. A. Kalinin, V. I. Iglovikov, "Automatic instrument segmentation in robot-assisted surgery using deep learning", Proceedings of the 17th IEEE International Conference on Machine Learning and Applications, Orlando, FL, USA, 17-20 December 2018, pp. 624–628.

[11] E. Kuznetsov, V. Stegailov, "Porting CUDA-Based Molecular Dynamics Algorithms to AMD ROCm Platform Using HIP Framework: Performance Analysis", Proceedings of the Russian Supercomputing Days, Moscow, Russia, 23-24 September 2019, pp. 121–130.

[12] Tsinghua Univesity, Beijing innovation center for future chips, "White Paper on AI Chip Technologies", 2018. (Online: https://www.080910t.com/downloads/AI%20Chip%202018%20EN.pdf).

[13] D. A. G. De Oliveira, L. L. Pilla, T. Santini, P. Rech, "Evaluation and mitigation of radiation-induced soft errors in graphics processing units", IEEE Transactions on Computers, Vol. 65, No. 3, 2016, pp. 791–804.

[14] D. A. G. Oliveira, S. Member, L. L. Pilla, T. Santini, S. Member, P. Rech, "Evaluation and Mitigation of Radiation-Induced Soft Errors in Graphics Processing Units", Vol. 9340, No. C, 2015, pp. 1–14.

[15] H. Alemzadeh, J. Raman, N. Leveson, Z. Kalbarczyk, R. K. Iyer, "Adverse events in robotic surgery: A retrospective study of 14 years of fda data", PLoS ONE, Vol. 11, No. 4, 2016, pp. 1–20.

[16] H. Alemzadeh, J. Raman, N. Leveson, Z. Kalbarczyk, R. K. Iyer, "Adverse events in robotic surgery: A retrospective study of 14 years of fda data", PLoS ONE, Vol. 11, No. 4, 2016, pp. 1–20, 2016.

[17] F. F. dos Santos et al., "Analyzing and Increasing the Reliability of Convolutional Neural Networks on GPUs", IEEE Transactions on Reliability, Vol. 68, No. 2, 2018, pp. 663–677.

[18] G. Li et al., "Understanding error propagation in Deep Learning Neural Network (DNN) accelerators and applications", Proceedings of the International Conference for High Performance Computing, Networking, Storage and Analysis, Denver, CO, USA, 12-17 November 2017, p. 8-19.

[19] L. Weigel, F. Fernandes, P. Navaux, P. Rech, "Kernel vulnerability factor and efficient hardening for histogram of oriented gradients", Proceedings of the IEEE International Symposium on Defect and Fault Tolerance in VLSI and Nanotechnology Systems, Cambridge, UK, 23-25 October 2017, pp. 1–6.

[20] C. Lunardi, F. Previlon, D. Kaeli, P. Rech, "On the Efficacy of ECC and the Benefits of FinFET Transistor Layout for GPU Reliability", IEEE Transactions on Nuclear Science, Vol. 65, No. 8, 2018, pp. 1843–1850.

[21] F. F. dos Santos, L. Draghetti, L. Weigel, L. Carro, P. Navaux, P. Rech, "Evaluation and mitigation of soft-errors in neural network-based object detection in three gpu architectures", Proceedings of the 47th Annual IEEE/IFIP International Conference on Dependable Systems and Networks Workshops, Denver, CO, USA, 26-29 June 2017, pp. 169–176.

[22] Y. Ibrahim et al., "Soft Error Resilience of Deep Residual Networks for Object Recognition", IEEE Access, Vol. 8, 2020, pp. 19490–19503.

[23] A. P. Twinanda, S. Shehata, D. Mutter, J. Marescaux, M. De Mathelin, N. Padoy, "EndoNet: A Deep Architecture for Recognition Tasks on Laparoscopic Videos", IEEE Transactions on Medical Imaging, Vol. 36, No. 1, 2017, pp. 86–97, 2017.

[24] A. Jin et al., "Tool detection and operative skill assessment in surgical videos using region-based convolutional neural networks", Proceedings of the IEEE Winter Conference on Applications of Computer Vision, Lake Tahoe, NV, USA, 12-15 March 2018, pp. 691–699.

[25] M. Grewal, M. M. Srivastava, P. Kumar, S. Varadarajan, "RADnet: Radiologist level accuracy using deep learning for hemorrhage detection in CT scans", Proceedings of the International Symposium on Biomedical Imaging, Washington, DC, USA, 4-7 April 2018, pp. 281–284.

[26] J. A. Dunnmon, D. Yi, C. P. Langlotz, C. Ré, D. L. Rubin, M. P. Lungren, "Assessment of convolutional neural networks for automated classification of chest radiographs", Radiology, Vol. 290, No. 3, 2019, pp. 537–544.

[27] Z. Wang, A. M. Fey, "Deep learning with convolu-

tional neural network for objective skill evaluation in robot-assisted surgery", International Journal of Computer Assisted Radiology and Surgery, Vol. 13, No. 12, 2018, pp. 1959–1970.

[28] J. H. Ko, B. Mudassar, T. Na, S. Mukhopadhyay, "Design of an Energy-Efficient Accelerator for Training of Convolutional Neural Networks using Frequency-Domain Computation", Proceedings of the Design Automation Conference, Austin, TX, USA, 18-22 June 2017.

[29] A. Azizimazreah, Y. Gu, X. Gu, L. Chen, "Tolerating Soft Errors in Deep Learning Accelerators with Reliable On-Chip Memory Designs", Proceedings of the IEEE International Conference on Networking, Architecture and Storage, Chongqing, China, 11-14 October 2018, pp. 1–10.

[30] H. Alemzadeh, J. Raman, N. Leveson, Z. Kalbarczyk, R. K. Iyer, "Adverse events in robotic surgery: A retrospective study of 14 years of fda data", PLoS ONE, Vol. 11, No. 4, 2016, pp. 1–20, 2016.

[31] Nvidia, "750 Ti White Paper", 2014. (Online: http://international. download. nvidia. com/geforce-com/international/pdfs/GeForce-GTX-750-Ti-Whitepaper. Pdf).

[32] R. C. Baumann, "Radiation-induced soft errors in advanced semiconductor technologies", IEEE Transactions on Device and materials reliability, Vol. 5, No. 3, 2005, pp. 305–316.

Performance Investigation of Digital Lowpass IIR Filter Based on Different Platforms

Case Study

Raaed Faleh Hassan
Middle Technical University, College of Electrical Engineering Technology,
Department of control and automation eng. Techniques, Iraq
drraaed_alanbaki@mtu.edu.iq

Abstract *– The work presented in this paper illuminates the design and simulation of a recursive or Infinite Impulse Response (IIR) filter. The proposed design algorithm employs the Genetic Algorithm to determine the filter coefficients to satisfy the required performance. The effectiveness of different platforms on filter design and performance has been studied in this paper. Three different platforms are considered to implement and verify the designed filter's work through simulation. The first platform is the MATLAB/ SIMULINK software package used to implement the Biquad form filter. This technique is the basis for the software implementation of the designed IIR filter. The HDL – Cosimulation technique is considered the second one; it inspired to take advantage of the existing tools in SIMULINK to convert the designed filter algorithm to the Very high-speed integrated circuit Hardware Description Language (VHDL) format. The System Generator is employed as the third technique, in which the designed filter is implemented as a hardware structure based on basic unit blocks provided by Xilinx System Generator. This technique facilitates the implementation of the designed filter in the FPGA target device. Simulation results show that the performance of the designed filter is remarkably reliable even with severe noise levels.*

Keywords *– Low pass IIR Filter, Genetic Algorithm, Biquad form, HDL-co simulation, XSG*

1. INTRODUCTION

Digital filters have become essential for removing unwanted signals in recently outspread communication and control systems [1]. Digital filters are categorized into two classes according to their impulse response [2]. The first category is the Finite Impulse Response (FIR), while the Infinite Impulse Response (IIR) is the second one [2]. As its name, the FIR filter possesses a finite impulse response due to the absence of the feedback loop, and it is also known as a non – recursive filter. On the other hand, the IIR filter has a feedback loop; therefore, it works recursively. The digital filter design aims to achieve high attenuation at the stopband with a steep roll-off. An IIR filter satisfies these requirements and significantly reduces the computational process compared with the FIR filter [3]. In Very Large Scale Integrated (VLSI) realization, it is preferable to adopt an IIR filter rather than an FIR filter. The IIR filter's drawback is the weakness of instability problems that can overcome by using advanced techniques [4] – [7]. A word length arises as a significant situation that influences the filter behavior in implementing the digital filters. Therefore, a finite – word – size becomes a crucial parameter in the digital filter design issue. The principal idea beyond this approach is to engage a proper filter structure for each application [8]. The IIR filter design can be achieved based on two directions: the transformation and optimization methods [9]. The transformation method performed by transforming the designed analog filter to the digital filter at some given specifications is the bilinear process which is the most widely used transformation method. This method's developed digital filter mostly suffers from poor behavior due to a multimodal error surface and instability [10]. These problems can be avoided when the design parameters are bounded in some criteria allocated using optimization methods [10] – [19]. The most prevalent optimization method is the Genetic Algorithm (GA) which can search versatile spaces and optimizes challenging functions that are very complicated to investigate [1], [8]. Employing GA for the digital filter design is preferable because it can construct the filter in any form with the lowest order [8]. Recently, the most interesting parallel processing hardware devices for implementing digital filter algorithms are the field-programmable gate array (FPGA) [2], [3], [19] – [22]. FPGA is a VLSI logic chip that can configure for realizing widespread logic functions [23]. No matter how the logic function is involved, the FPGA structure's nature facilitates the function's implementation in parallel, leading to very high-speed computation. However, the hardware implementation of digital systems using FPGA is somewhat tricky and needs the training to deal with Hardware Description Language (HDL). Therefore, a virtual environment for de-

signing, implementing, and testing the digital systems using FPGA is needed [24].

Recently, Matlab/Simulink provides this virtual environment utilizing co-simulation with ModelSim and implementing a digital system using the Xilinx system generator. Employing co-simulation with Modelsim permits the verification of an HDL module of the system against its Simulink model. In this case, the Simulink environment will act as a test bench that stimulates an HDL module [25]. The most realistic visualization of digital system performance can be achieved using Xilinx System Generator (XSG). Adopting this platform enables designing a digital system in the Simulink environment using Xilinx-specific blocks in the Simulink library. XSG design can easily be placed on the FPGA target device as a bit file with the possibility of obtaining the HDL code for further optimization and integration with other projects within the Xilinx environment. This paper explores these platforms' features to implement and analyze the performance of the digital low pass IIR filter.

2. DIGITAL IIR FILTER:

According to its name, this type of filter has an infinite impulse response, as indicated in the following difference equation:

$$y_n = \sum_{k=0}^{M} b_k x_{n-k} + \sum_{k=1}^{N} a_k y_{n-k} \qquad N \geq M \quad (1)$$

Where y_n is the current sample of the filter output, y_{n-k} are the k^{th} previous samples of the output, x_{n-k} are the k^{th} previous samples, including the current sample of the input signal, a_k and b_k are the filter coefficients, M is the numerator's order, and N is the denominator's order [1], [2]. From eq. (1), it can be seen that the filter output y_n is determined recursively; in other words, it is a function of the current and previous samples of the input signal and the output signal's previous samples. Taking the z – transform for eq. (1) leads to the following system function:

$$H(z) = \frac{B(z)}{A(z)} = \frac{\sum_{k=0}^{M} b_k z^{-k}}{1+\sum_{k=1}^{N} a_k z^{-k}} \quad (2)$$

2.1 IIR FILTER REALIZATION:

Several practical realization architectures that implement the digital IIR filter were outlined in the literature; these are:

DFI: The digital IIR filter can be realized in the direct form I according to eq. (1) which comprises a non – recursive part and recursive part. The implementation of the digital IIR filter in this form is shown in Figure (1); for each output sample, it requires ($N + M$) delays, (N+M+1) multiplications, and (N+M) additions.

DFII: In the direct form II structure, shared delay elements between the recursive and non – recursive parts of the digital IIR filter are employed, as shown in Figure (2). The determination process of each output sample requires max (N or M) delays, (N+M) additions, and (N+M+1) multiplications [2].

The benefit of DFII is its more economical utilization of the delay units. However, both separate the poles sections from the zero sections, DFII can share the delay units between them. Therefore, a significant reduction in the number of delay units can be achieved when adopting DFII. The drawback of the DFII is that the pole units precede the zero units and imposes an unfeasible dynamic range on the delay units' intersection at some frequencies. As a result, DFII suffers from overflow, while DFI has immune from this effect [2]. The transposed structure of the DFII, shown in Figure (3), precedes the zero sections and shares the delay units between zeros and poles. Therefore, this structure has the advantage of DFII with more robust behavior [23].

Cascade Structure:

For the higher-order IIR filters (higher than 2) with transfer function given by eq. (2) with $N \geq M$, the transfer function can be factorized into a cascaded second-order subsystem as expressed below:

$$H(z) = \prod_{k=1}^{\frac{N+1}{2}} H_k(z) \quad (3)$$

Where $$H_k(z) = \frac{b_{k0}+b_{k1}z^{-1}+b_{k2}z^{-2}}{1+a_{k1}z^{-1}+a_{k2}z^{-2}} \quad (4)$$

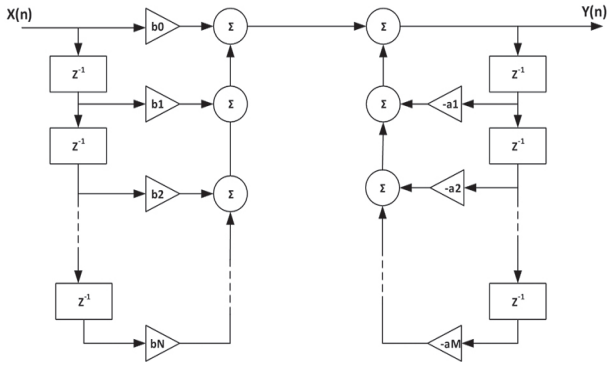

Fig. 1. DFI structure

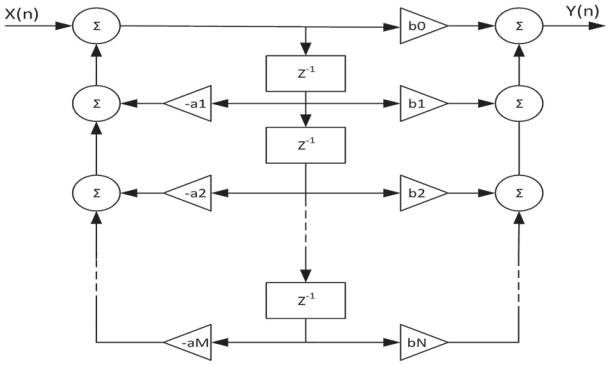

Fig. 2. DFII structure

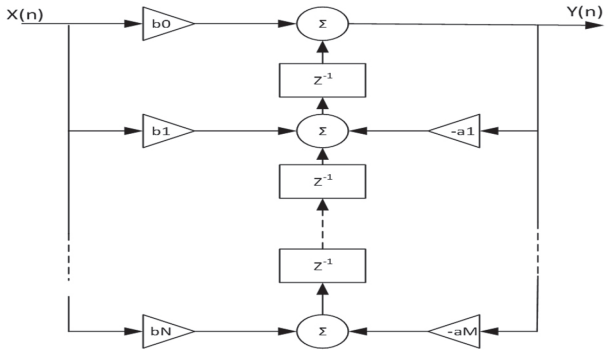

Fig. 3. Transposed DFII Structure

The coefficients $\{a_{ki}\}$and $\{b_{ki}\}$ in eq. (4) are real, which implies that any pair of real or complex conjugate poles or zeros are grouped in second-order or quadratic form. This structure reduces the effects of using finite word length representation of the filter coefficients [20]. The cascade structure can be implemented by a series-connected of first-order and/or second-order structures, as shown in Figure (4). Each of the 2nd order subsystems in eq. (3) can be implemented as DFI or DFII or transposed DFII.

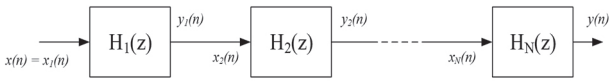

Fig. 4. Cascade Structure

A parallel structure of an IIR filter can be synthesized based on a partial fraction expansion performed on H(z) in eq. (2). When $N \geq M$ in eq. (2). Moreover, the poles are distinct, the partial – fraction expansion of H(z) produces the following results:

$$H(z) = C + \sum_{k=1}^{N} \frac{A_k}{1-P_k z^{-1}} \quad (5)$$

Where: P_k are the poles, A_k are coefficients, and $C=b_N/a_N$.

Figure (5) shows the block diagram representation of eq. (5). Generally, H(z) may contain some complex-valued poles. In this case, the produced coefficients Ak are also complex-valued. The avoidance of multiplication by complex numbers can be achieved by combining pairs of complex conjugate poles to form a 2nd order subsystem. Each of these subsystems has the form:

$$H_k(z) = \frac{b_{k0}+b_{k1}z^{-1}}{1+a_{k1}z^{-1}+a_{k2}z^{-2}} \quad (6)$$

Where $\{a_{ki}\}$ and $\{b_{ki}\}$ coefficients are real-valued system parameters. The modified transfer function can now be expressed as

$$H(z) = C + \sum_{k=1}^{\frac{N+1}{2}} H_k(z) \quad (7)$$

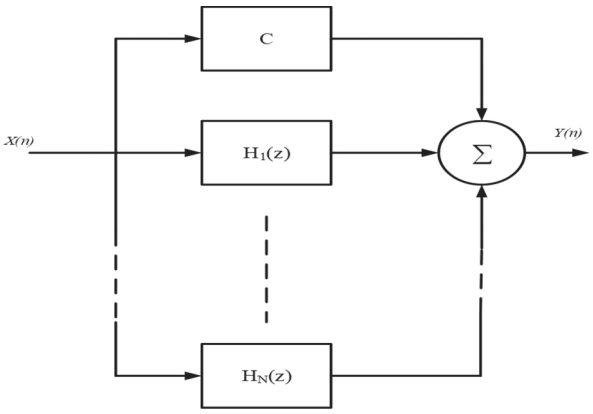

Fig. 5. Parallel Structure

Proposed Structure:

The design process's main task is to determine the filter coefficients (a_k & b_k) to perform the desired performance while ensuring stability [8]. The most popular realization structure of the digital IIR filter is to stack some 1st order and (or) second-order in cascade. Therefore, Eq. (3) can be modified into the stacked of the cascaded second-order form (assuming $M = N$):

$$H(z) = \prod_{k=1}^{N/2} G_k \frac{1+c_{1k}z^{-1}+c_{2k}z^{-2}}{1+d_{1k}z^{-1}+d_{2k}z^{-2}} \quad (8)$$

Let $z = e^{j\Omega}$, Eq. 8 becomes:

$$H(e^{j\Omega}) = \prod_{k=1}^{N/2} G_k \frac{1+c_{1k}e^{-j\Omega}+c_{2k}e^{-2j\Omega}}{1+d_{1k}e^{-j\Omega}+d_{2k}e^{-2j\Omega}} \quad (9)$$

The magnitude frequency response of the filter is determined as follows:

$$\left|H(e^{j\Omega})\right| = \left|\prod_{k=1}^{N/2} G_k \frac{1+c_{1k}e^{-j\Omega}+c_{2k}e^{-2j\Omega}}{1+d_{1k}e^{-j\Omega}+d_{2k}e^{-2j\Omega}}\right| \quad (10)$$

Furthermore, the phase-frequency response is determined as follows:

$$\angle H(e^{j\Omega}) = tan^{-1}\left(\frac{Img(H(j\Omega))}{Re(H(j\Omega))}\right) \quad (11)$$

3. GENETIC ALGORITHM BASED IIR FILTER DESIGN:

Genetic Algorithm (GA) can be considered as the most popular and robust search algorithm in recent years [8] - [14]. It is established according to the theories of social evolution or natural selection. In these theories, natural selection can be regarded as an exploration procedure to evaluate the optimum DNA that maximizes a species' persist possibility to procreate, thereby spread the species. The optimum DNA was obtained during the DNA crossover through sexual reproduction with unqualified offspring's depletion due to low accommodation with the surroundings [22]. GA utilizes natural selection principles to accomplish the

task of evaluating the optimum solution of the prescribed problem. Initially, the population parameters are selected randomly to confirm that the exploration space is widely and evenly sampled. The fitness function is used to determine and choose the members of a population with reasonable solutions sufficient to produce the next generation. Similar to natural selection, the crossover process is adopted to perform the swapping between the sections of the randomly designated pairs. GA may be stuck in the suboptimal region, and the mutation is considered to permit the GA to skip outside this region. From many types of mutation, a swap mutation is employed in this work, in which two genes are selected randomly and interchange their positions. With predefined filter order, the objective of the IIR filter design is to determine its coefficients. When the GA is considered the filter design tool, the filter coefficients act as chromosomes that constitute the population. The fitness function can be derived from comparing the magnitude response given in Eq. (10) with the desired magnitude response.

For the low pass filter design issue, the chosen magnitude response is:

$$\left|H_d\left(e^{j\Omega}\right)\right| = \begin{cases} 1-\delta_p & \Omega \le \Omega_p \\ \delta_s & \Omega \ge \Omega_s \end{cases} \quad (12)$$

Where:

$H_d(e^{j\Omega})$: The desired magnitude response.

Ω_p, Ω_s : The passband and stopband frequencies, respectively.

δ_p, δ_s : The passband and stopband allowed ripples, respectively.

The error of the magnitude response is defined as follows:

$$E_p(\Omega) = \left|H_d\left(e^{j\Omega}\right)\right| - \left|H\left(e^{j\Omega}\right)\right| \quad (13)$$

The fitness function to be minimized is:

$$J_{min} = \sum_{\Omega}\left|E_p(\Omega)\right|^2 \quad (14)$$

The digital IIR filter considered in this paper will be a fourth-order low – pass filter, which has the following system function in cascade form:

$$H(z) = \prod_{k=1}^{2} G_k \frac{1+c_{1k}z^{-1}+c_{2k}z^{-2}}{1+d_{1k}z^{-1}+d_{2k}z^{-2}} \quad (15)$$

Therefore, the population contains ten individuals; these are: $[G_1\ c_{11}\ c_{21}\ d_{11}\ d_{21}\ G_2\ c_{12}\ c_{22}\ d_{12}\ d_{22}]$. It must now be clear that to achieve IIR filter design, the GA is utilized to minimizes the fitness function. The minimization process results in evaluating the best values of the individuals. Figure 6 shows the flow chart of the GA-based fourth-order low pass IIR filter design.

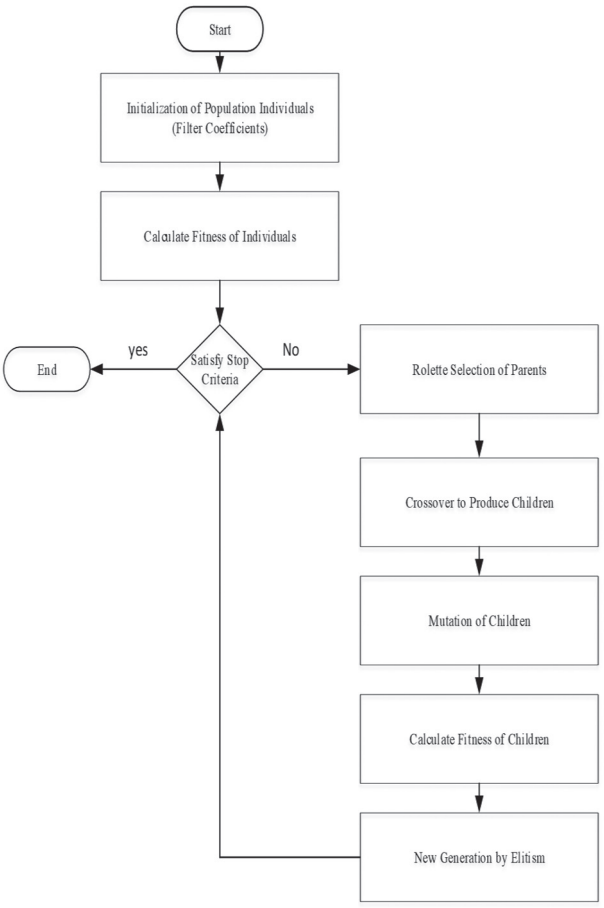

Fig. 6. GA flow chart

The GA optimization issue was performed using (optimtool) in the MATLAB software package. Table 1 shows the GA parameters setting

Table 1. GA parameters

Genetic Algorithm Parameters	
No. of variables	10
Maximum δp and δs	0.1
Generation	2000
Population size	200
Crossover Function	Two Point
Crossover	0.8
Elite Count	10
Mutation Function	Gaussian
Selection Function	Roulette
Stall Generation	50
Function Tolerance	0.001

From the genetic Algorithm, the resulting iir filter coefficients are indicated in Table 2:

These filter coefficients have been exported to fdatool in Matlab to examine the frequency, phase responses, and the poles/zeros of the designed filter, as shown in Figure 7.

Table 2. Filter coefficients

First stage		Secon stage	
Filter coefficient	value	Filter coefficient	value
G_1	2.44×10^{-4}	G_2	2.3976×10^{-4}
C_{11}	2	C_{12}	2
C_{21}	1	C_{22}	1
d_{11}	-1.9753	d_{12}	-1.942638
d_{21}	0.97624	d_{22}	0.94359

4. SOFTWARE IMPLEMENTATION:

This section demonstrates the implementation of the designed IIR filter based on different implementation technologies, as shown in Figure 8. The first one is the algorithm implementation of the designed filter based on the biquadratic technique. This technique is provided by the MATLAB software package and implements the higher-order IIR filter as a cascade of second-order sections. This technique aims to verify the effectiveness of the design algorithm, which has been considered. The second approach is to employ the HDL- Cosimulation, which accomplishes the interfacing between MATLAB and the Modelsim environments. An IIR filter based on VHDL code is generated and incorporated in Modelsim, then it is called and executes from the MATLAB environment. This technique can be considered as a software implementation of the designed filter. This technique's key feature is to employ MATLAB or Simulink to stimulate the design and analyze its response based on HDL simulation. System Generator is considered as the 3rd approach for implementing the designed filter. It is mixed with the assistance of a rich verification environment provided by Simulink to quickly create a production-quality filter implementation compared to conventional RTL approaches. The detailed implementation of the designed filter based on the system generator approach is shown in Figure 9. Fig.9(a) shows the 4th order IIR low pass filter block diagram using system generator, which consists of a cascaded two stages 2nd order sections. The detailed implementation of each stage of the designed filter is shown in Fig.9(b).

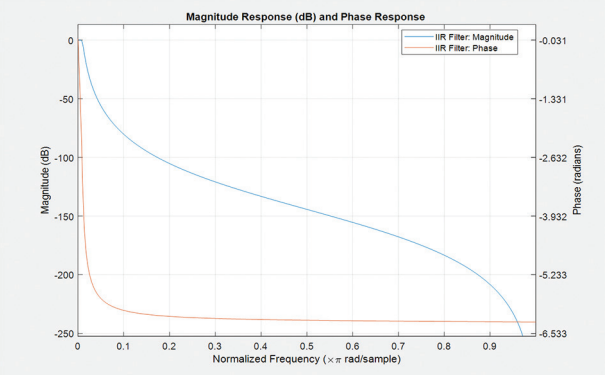

(a)

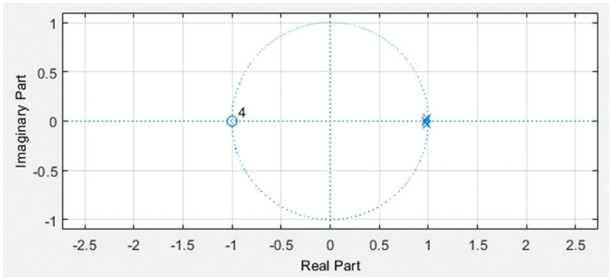

(b)

Fig. 7. (a) Frequency & Phase response **(b)** Poles/Zeros

5. SIMULATION RESULTS:

For comparison, the simulation process has been performed on the proposed three approaches parallelly, as shown in Figure 8. The considered original signal is a sine wave of the amplitude of 1 and a frequency of 500 Hz corrupted by white Gaussian noise of 0.5 variances, as shown in Figure 10. There is significant convergence in the resulting frequency responses from the three methods, as indicated in Figure 11.

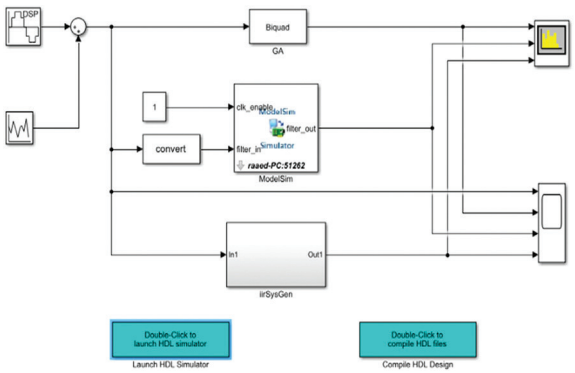

Fig. 8. Implementation of designed IIR filter.

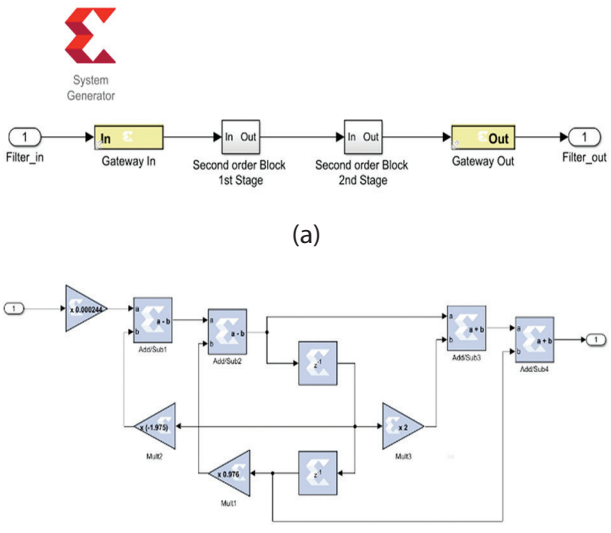

(a)

(b)

Fig. 9. System Generator Based fourth-order IIR filter: **(a)** Block diagram **(b)** implementation of the 2nd order stage.

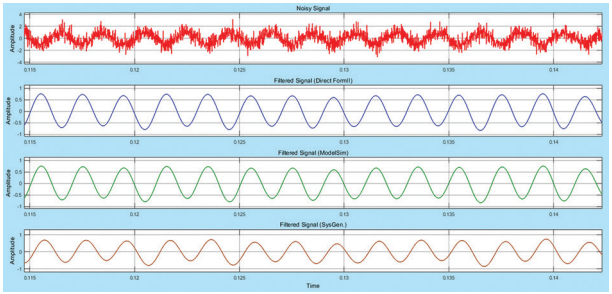

Fig. 10. Simulation of the filtering process based on three approaches

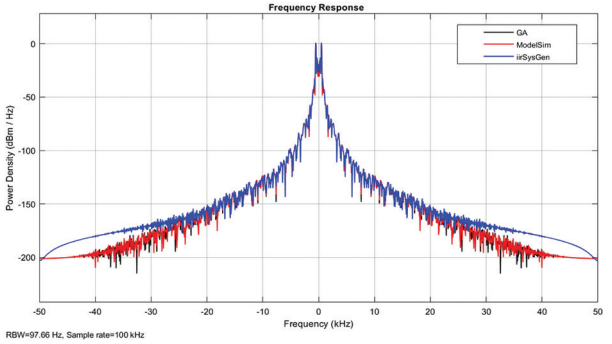

Fig. 11. The frequency response of the IIR

Figure 12 shows the simulation results of the IIR filter performed in the Modelsim package. Table III shows the design implementation and utilization summary of the target FPGA device (**7k325tffg900-2**) that implements the designed IIR filter based on the System Generator.

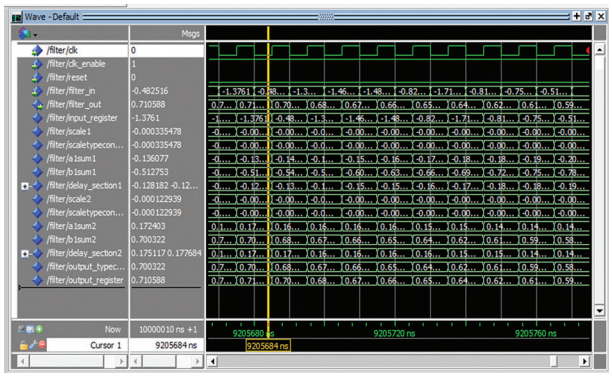

Fig. 12. simulation of the IIR filter in Modelsim

Table 3. Utilization Summary.

Site Type	Used	Fixed	Available	Util%
Slice LUTs*	896	0	203800	0.44
LUT as Logic	0	0	203800	0.00
LUT as Memory	896	0	64000	1.4
Slice Registers	896	0	407600	0.22
Register as Flip Flop	896	0	407600	0.22
Register as Latch	0	0	407600	0.00
F7 Muxes	0	0	101900	0.00
F8 Muxes	0	0	50950	0.00

6. CONCLUSIONS

In this paper, an Infinite Impulse Response (IIR) low pass filter is constructed based on a Genetic Algorithm (GA). The implementation of the designed filter has been performed using three implementation techniques. The first two techniques were Biquad, and HDL simulation represents the software implementation techniques. The third implementation technique is the System Generator (SG) which facilitates the designed filter's hardware implementation based on Field Programmable Gate Array (FPGA). Implementation of the designed filter in the FPGA target device indicates a small size utilization. The frequency response through the three mentioned techniques shows that the designed filter behaves as planned. An intense, noisy signal was applied to the filter input, and the simulation results showed that the signals were filtered out perfectly.

7. REFERENCES

[1] S. T. Pan, "Evolutionary Computation on Programmable Robust IIR Filter Pole-Placement Design", IEEE Transactions on Instrumentation and Measurement, Vol. 60, No. 4, 2011, pp. 1469-1479.

[2] P. Bujjibabu, N. Sravani, "Architecture-based performance evaluation of IIR digital filters for DSP", Proceedings of the International Conference on Big Data Analytics And Computational Intelligence, Chirala, India, 23-25 March 2017.

[3] S. Saman, X. Yao, C. Charayaphan, "Design of Optimal and Narrow-Band Laguerre Filters for Sigma-Delta Demodulators", IEEE Transactions on Circuits and Systems II: Analog and Digital Signal Processing, Vol. 50, No. 7, 2003, pp. 368-375.

[4] L. Yin, K. P. Keshab, "Architectures for Recursive Digital Filters using Stochastic Computing", IEEE Transactions on Signal Processing, Vol. 64, No. 14, 2016, pp. 3705-3718.

[5] L. Yin, K. P. Keshab, "Lattice FIR Digital Filter Architectures Using Stochastic Computing", Proceedings of the IEEE International Conference on Acoustics, Speech, and Signal Processing, Brisbane, QLD, Australia, 19-24 April 2015.

[6] C. Yun-Nan, K. P. Keshab, "Architectures for digital filters using stochastic computing", Proceedings of the IEEE International Conference on Acoustics, Speech and Signal Processing, Vancouver, BC, Canada, 26-31 May 2013.

[7] T. Jinn-Tsong, C. Jyh-Horng, T.-K. Liu, "Optimal Design of Digital IIR Filters by Using Hybrid Taguchi Genetic Algorithm", IEEE Transactions on Industrial Electronics, Vol. 53, No. 3, 2006, pp. 867-879.

[8] N. Karaboga, A. Kalinli, D. Karaboga, "Designing digital IIR filters using ant colony optimization algorithm", Engineering Applications of Artificial Intelligence, Vol. 17, No. 3, 2004, pp. 301-309.

[9] K. Adem, K. Nurhan, "Artificial immune algorithm for IIR filter design", Engineering Applications of Artificial Intelligence, Vol. 18, No. 8, 2005, pp. 919-929.

[10] K. Adem, K. Nurhan, "A new method for adaptive IIR filter design based on tabu search algorithm", International Journal of Electronics and Communications, Vol. 59, No. 2, 2005, pp. 111-117.

[11] Y. Yang, X. Yu, "Cooperative Coevolutionary Genetic Algorithm for Digital IIR Filter Design", IEEE Transactions on Industrial Electronics, Vol. 54, No. 3, 2007, pp. 1311-1318.

[12] D. Chaohua, C. Weirong, Y. Zhu, "Seeker Optimization Algorithm for Digital IIR Filter Design", IEEE Transactions on Industrial Electronics, Vol. 57, No. 5, 2010, pp. 1710-1718.

[13] W. Qiusheng, S. Jialing, Y. Haiwen, "Digital Multiple Notch Filter Design Based on Genetic Algorithm", Proceedings of the Fourth International Conference on Instrumentation and Measurement, Computer, Communication and Control, Harbin, China, 18-20 September 2014.

[14] D. Cesar, B. Kenneth, G. Keith, "Design of IIR Multi-Notch Filters Based on Polynomially-Represented Squared Frequency Response", IEEE Transactions on Signal Processing, Vol. 64, No. 10, 2016, pp. 2613- 2623.

[15] C. L. Mathias, "Least-Squares Design of IIR Filters with Prescribed Magnitude and Phase Responses and a Pole Radius Constraint", IEEE Transactions on Signal Processing, Vol. 48, No. 11, 2000, pp. 3109-3121.

[16] T. T. Engin, M. Aktas, "LSE and MSE Optimum Partition-Based FIR-IIR Deconvolution Filters With Best Delay", IEEE Transactions on Signal Processing, Vol. 53, No. 10, 2005, pp. 3780-3790.

[17] P. Lorenzo, K. Izzet, "Adaptive IIR Filter Initialization via Hybrid FIR/IIR Adaptive Filter Combination", IEEE Transactions on Instrumentation and Measurement, Vol. 50, No. 6, 2001, pp. 1830-1835.

[18] S. Trini et al., "FFT Spectrum Analyzer Project for Teaching Digital Signal Processing With FPGA Devices", IEEE Transactions on Education, Vol. 50, No. 3, 2007, pp. 229-235.

[19] S. Vaishali et al., "High-throughput and compact reconfigurable architectures for recursive filters", IET Communications, Vol. 12, No. 13, 2018, pp. 1616-1623.

[20] C. V. G. Edilberto, M. R. P. Diego, J. G. Edwar, "Implementation and simulation of IIR digital filters in FPGA using MatLab system generator", Proceedings of the IEEE 5th Colombian Workshop on Circuits and Systems, Bogota, Colombia, 16-17 October 2014.

[21] S. M. R. Islam, R. Sarker, S. Saha, A. F. M. N. Uddin, "Design of a programmable digital IIR filter based on FPGA", Proceedings of the International Conference on Informatics, Electronics & Vision, Dhaka, Bangladesh, 18-19 May 2012.

[22] Z. Zhao, G. Li, "Comparative study of the generalized DFIIt structure and its equivalent state-space realization", Proceedings of the IEEE International Conference on Acoustics, Speech, and Signal Processing, Hong Kong, China, 6-10 April 2003.

[23] A. Bhattacharyya, P. Sharma, N. Murali, S. S. Murty, "Development of FPGA based IIR Filter implementation of 2-degree of Freedom PID controller", Proceedings of the Annual IEEE India Conference, Hyderabad, India, 16-18 December 2011.

[24] V. K. Singh, R. N. Tripathi, T. Hanamoto, "HIL Co-Simulation of Finite Set-Model Predictive Control Using FPGA for a Three-Phase VSI System", Energies, Vol. 11, No. 4, 2018, pp. 1-15.

[25] Y.-S. Kung et al., "Simulink/Modelsim Co-Simulation and FPGA Realization of Speed Control IC for PMSM Drive", Procedia Engineering, Vol. 23, 2011, pp. 718-727.

A Proposed Model for Predicting Employee Turnover of Information Technology Specialists Using Data Mining Techniques

Review paper

Ahmed Hosny Ghazi
Helwan University,
Faculty of Commerce & Business Administration,
Department of Business information systems,
Cairo, Egypt
hosnyghazi@gmail.com

Samir Ismail Elsayed
Helwan University,
Faculty of Commerce & Business Administration,
Accounting Department,
Cairo, Egypt
drsamironline@gmail.com

Ayman Elsayed Khedr
University of Jeddah, College of Computing and
Information Technology at Khulais,
Department of Information Systems,
Jeddah, Saudi Arabia
aeelsayed@uj.edu.sa

Abstract *– This article proposes a data mining framework to predict the significant explanations of employee turn-over problems. Using Support vector machine, decision tree, deep learning, random forest, and other classification algorithms, the authors propose features prediction framework to determine the influencing factors of employee turn-over problem. The proposed framework categorizes a set of historical behavior such as years at company, over time, performance rating, years since last promotion, and total working years. The proposed framework also classifies demographics features such as Age, Monthly Income, and Distance from Home, Marital Status, Education, and Gender. It also uses attitudinal employee characteristics to determine the reasons for employee turnover in the information technology sector. It has been found that the monthly rate, overtime, and employee age are the most significant factors which cause employee turnover.*

Keywords *– Data Mining Techniques, Prediction, Classification, Employees satisfactions and turnover*

1. INTRODUCTION

Despite the efforts made by the organization to develop and improve investments, employee turnover will remain one of the most hazardous challenges facing the organization's return on investments. A lot is spent on employees by the organizations in which they work in terms of orientation, training, development, and maintenance in their organizations. Therefore, managers should at any cost reduce staff turnover [1]. Although there is no specific approach for addressing the Employee attrition problem as a whole, a wide variety of variables have been found to be effective in describing employee turnover. The turnover problem requires more investigating and understanding of causes why employees leave their working organization. The factors that influence employee performance, the consequences, and methods can be placed in place by managers to reduce employee turnover. Organizations must continue to develop tangible products and provide services based on the strategies staff have developed [2].

In any organization, decision-makers should find out the significant factors that might lead to employee turnover in favor of organization sustainability. To find out these factors, managers used different methodologies and techniques. Some managers use interviews and another use questionnaire to determine turn over causes.

On other hand, some managers use mathematical or statistical models to find out why skillful employees may leave work. Also, decision-makers use some advanced machine learning and classification techniques. The last two approaches are preferable for some decision-makers because they are not biased to human interference. In this research, we will propose a classification model that helps decision-makers to illustrate the most significant factors affecting employee turnover [3].

As the employee turnover problem has not one direct and obvious reason, data mining has been considered a promising approach for information and knowledge discovery [4]. This discovered knowledge can be extracted and accessed through a large amount of data using well define mining algorithms [5]. The data mining approach comprises a set of techniques that can be used to extract relevant information and interesting knowledge from data which might provide a solution to any business problem.

Data mining explores and analyses large blocks of information to glean significant patterns and trends. It can be used in a variety of ways, such as database marketing, credit risk management, fraud detection, spam Email filtering, or even to discern the sentiment or opinion of users. Data mining includes different data analysis techniques such as classification, forecasting, prediction, and clustering [6], [7].

Classification is a supervised learning technique to find hidden patterns using learning by example approach.

Clustering is the process of grouping the data using unsupervised learning techniques such as k-mean, nearest neighbour algorithm and other. On other hand, classification is supervised learning techniques that classify the data element to known labels using different algorithms such as decision tree. Despite the mining technique the main aim is to find the most interested pattern which solve problem [8].

This research paper has been divided into parts. The second part illustrates a set of previous studies that focused on employee turnover reasons prediction using data mining techniques. The third part discusses the proposed model and data pre-processing, experiments, and results that have been achieved. The research summary and conclusions have been presented in the last part.

2. LITERATURE REVIEW

A lot of Researchers have been tried to find users' satisfaction reasons in many perspectives such as in [9], [10] and [11]. The following section discussed a number of published articles that illustrate some benefits of datamining techniques in the employee turnover problems briefly.

Classification technique has been used to predict employee performance rates [12],[13]. Their proposed model monitors employee performance, by knowing the most influential attributes, and through the application of classification algorithms. As a conclusion of that research, they found that job title, type, and relatively little impact. The Age attribute showed no obvious effect during the social status. In some of the performed experiments, gender attributes showed some effect on employee performance prediction. Also, Job satisfaction, salary, number of years of experience, and previous companies for each of these attributes have a degree of predictability of performance. In the end, the authors recommended that the model can be used to forecast new employee performance and help make the necessary decisions when hiring new employees to avoid recruiting a poor-performing employee.

Adaptation is one of the key elements in employee satisfaction which has been confirmed in many types of research such as in [14].The classification technique has been used to predict employee attrition rates. The researchers proposed employee attrition models which analyzing employee data to reduce the organization's future losses. The focus of their research was to provide a friendly graphical user interface to facilitate the work of a department of Human resources. They concluded that working experience, age, and technical skills, have the most significant impact on employee turnover. Different methods of data mining have been compared based on their precision, calculation time, and Ease of use [15].

Automated learning algorithms have been used to predict employee turnover factors. The main challenge in their study was noise-filled data from (Human Resource Information System (HRIS) [16]. The authors compared the results of their classifier against six other classifiers. Their proposed classifier has been achieved excellent results in terms of accuracy, time consumption, and memory allocation for predicting attrition. The proposed classifier confirmed that it was effective in solving the problem of data noise than HRIS than other classifiers. In the end, the article concluded that human resource management (HRM) has been overcome this challenge.

Classification methods has been used to estimate the turnover of employees and evaluating the number of attritions [17]. They took three mining algorithms Naïve Bayes, J48 (C4.5), and Random Tree, respectively. The authors analyzed the Employees attrition rate by classifying the data into two labels "Yes" and "No". the "Yes" label clarified the employees who leave the organization and the" No" label illustrated the employee's continuity in the organization. The research concluded that the percentage of employees leaving companies is 20.70% by Naïve Bayes, 31% by J48, and 100% by Random Tree. The retention ratio is 79.3% by Naïve Bayes, 69% by J48, and 0% by random tree. According to their assumption, the Naïve region performs better rather than two other algorithms.

As in [18],[19] the researchers proposed a classification model to find out the factor affecting employee

turnover. A predictive decision tree has been used. Their model has been used R language Environment to build the model. The proposed model used the c5.0 algorithm, decision tree algorithm, and Rap algorithm to determine these factors. This proposed model proofed that continuous communications between the employee and their managers might reduce the turnover problem. Table 1 illustrates a summary of related data mining algorithms which has been used in this paper's literature review.

Table 1. A summary of the datamining algorithms used in the previously related work

RESEARCH	DATA MINING TECHNIQUE	ALGORITHMS
[1]	Classification	Decision Tree and Naïve Bayes
[2]	Classification	Naive Bayes, decision trees and SVM.
[3]	Classification	Neural network
[4]	Classification	Random tree, naive Bayes, J48.
[5]	Classification	Random forest, decision tree

3. PROPOSED METHODOLOGY

The proposed framework can be divided into three phases input, processing and output, respectively . The Specification of the framework is as follows:

- Phase1: Input

At first, the IT department collects the dataset which provides behavioral, demographic and attitudinal to help you predict Employee turnover according to HR department guidelines. Organization is concerned about the number of workers leaving their company for their rivals. The data are then put into another level which is the preprocessing where data is transformed and cleaned in such a way as that enables it to be used.

- Phase2: Processing

In this phase Data Mining algorithms will be tested to find out the optimal algorithm for prediction. Using these algorithms, the prediction model discovers hidden features from the collected datasets. Finally, the proposed model performs a comparison between the discovered features and determines which one affects the process of employee turnover.

- Phase3: Output

The output from the framework can be viewed as the way the result can be visualized to the decision- makers who are the practitioners in a form of, Reports and allows them to make the right decision at the right time. (Fig.1)shows the proposed framework.

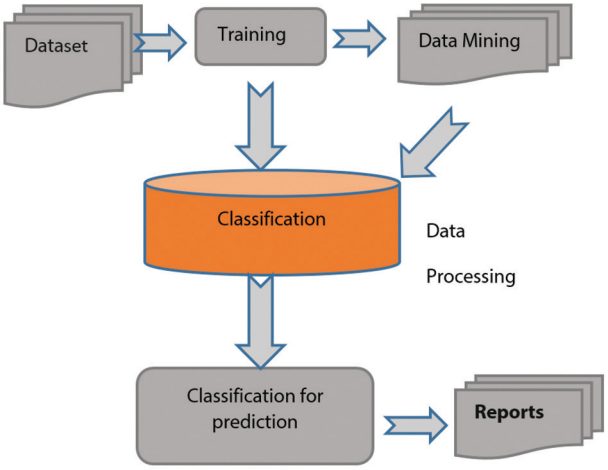

Fig. 1. The proposed framework

4. CASE STUDY

This study aims to create a model for predicting the turnover of employees using data mining techniques, in pursuit of a strong solution that can help and support decision-makers in organizations, so that they can make the right decisions when necessary, which helps to reduce the turnover rate and reduce it. Recognizing the turnover before making the necessary precautions and decisions to retain employees contributes effectively to increasing the organization's profit rate.

- Data selection and pre-processing

The first step in this model is data selection and cleaning.

In this step, we utilize to predict employee attrition by using the HR Employee Attrition dataset provided by IBM. Table 2 illustrates a brief summary of the dataset features. The dataset contains employee information, the factors on which the Employee turnover depends upon are: Behavioral such as:

- Years at Company
- Over Time
- Performance Rating
- Years since Last Promotion
- Total Working Years

Demographics such as:

- Age
- Monthly Income
- Distance from Home
- Marital Status
- Education
- Gender

Attitudinal such as:

- Environment Satisfaction
- Job Satisfaction
- Work-Life Balance
- Number of Companies Worked

Table 2. The dataset features description

Attribute	Values
Age	18 To 60
Daily Rate	102 To 1499
Distance from Home	1 To 29
Hourly Rate	30 To 100
Monthly Income	1009 To 19973
Monthly Rate	2044 To 26999
Number of Companies Worked	0 To 9
Percent Salary Hike	11 To 25
Total Working Years	0 To 40
Training Times Last Year	0 To 6
Years at Company	0 To 36
Years in Current Role	0 To 17
Years since Last Promotion	0 To 15
Years with Current Manager	0 To 17
Department	H.R, Research &Development, Sales, IT
Education	1 To 5
Gender	Male , Female
Environment Satisfaction	1To 4
Job Involvement	1 To 4
Job Level	1 To 5
Job Role	Manager, Sales Executive, Laboratory Technician, Research Director, Human Recourses, Healthcare Representative, Manufacturing Director.
Job Satisfaction	1 To 4
Marital Status	Single, Married, Divorced
Over Time	Yes, No
Performance Rating	3, 4
Work Life Balance	1 To 4
Relationship Satisfaction	1 To 4

- **Classification**

It is the task of data analysis, that is, the process of finding the model that represents and characterizes layers and concepts of the data [6]. Classification is the question of defining each class category based on the data set of training that includes notes and determines class membership.

Classification depends on machine learning, where each entity is categorized into one of a predefined set of categories or groups within a collection of data The system is built in such a way that data classification data elements into groups. The classification, for example, can be extended to records of workers who have left the firm, In this case, the employee records are divided into two categories called "leave" and "the rest," and then the Data Mining techniques will identify the employees into those two predefined classes. Various algorithms were used to test the data. The Generalized Linear Model, Deep learning, Logistic Regression, logistic slope, and support vector machine. In this research, the test was carried out by applying a set of classification algorithms such as logistic regression, random forest, Fast Large Margin, Gradient Boosted Trees. These algorithms were implemented through data mining software (Rapid Miner).

- **Prediction**

Prediction or expectation of Data Mining techniques that expose the relationship between independent and non-independent variables; In other words, if we want to use sales forecasting approaches to estimate future earnings, if we find revenue to be an independent variable, then that may be a dependent variable. Prediction is similar to classification, except that we are trying to predict the value of a numerical variable (e.g., amount of purchase) rather than a class (e.g. Purchaser or no purchaser). Of course, in classification, we seek to forecast a class, but the term prediction refers to forecast the value of a continuous variable [7].

5. RESULTS

In this part, we have used classification algorithms to know the most suitable algorithms in the process of predicting employee turnover, and the most influential algorithms have been monitored that have achieved the highest percentage of accuracy such as:

Generalized Linear Model Achieved accuracy by 87.9%, Deep learning Achieved accuracy by 86.2%, Logistic Regression Achieved accuracy by 85.5%, Naive Bayes Achieved accuracy by 85.2%, Gradient Boosted Trees Achieved accuracy by 85%, Random Forest Achieved accuracy by 83.1%, Support Vector Machine Achieved accuracy by 83.1%%, Fast Large Margin Achieved accuracy by 83.1%. The results have been summarized in figure 2 for all the algorithms used and from the application and the results are summarized. The most appropriate classification algorithms have been known in the prediction process.

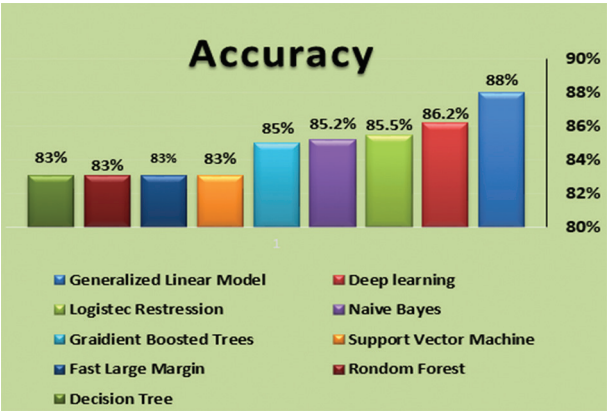

Fig. 2. The classification algorithms accuracy summary

- **Detailed Accuracy**

The accuracy of the details for each algorithm includes precision and Recall and F-measure. Table 3 shows the Detailed Accuracy.

Table 3. Classification algorithms accuracy, precision, recall and F-Measure

Algorithm	Accuracy	Precision	Recall	F-Measure
Generalized Linear Model	87.9%	88.4%	98.3%	93.1%
Deep learning	86.2%	85.9%	99.7%	92.3%
Logistic Regression	85.5%	85.6%	99.5%	92.0%
Naive Bayes	85.2%	85.1%	99.7%	91.8%
Gradient Boosted Trees	85%	84.9%	99.7%	91.7%
Support Vector Machine	83.1%	83.1	100%	90.8%
Fast Large Margin	83.1%	83.1	100%	90.8%
Random Forest	83.1%	83.1	100%	90.8%
Decision Tree	83.1%	83.4%	99.4%	90.7%

- **Important factors by weights**

This section contains the most important factors affecting the employee turnover process for each algorithm by weight. They are in the order of age, Over Time, Monthly Income, Total Working years, Years At a company as shown in Table 4, Training Time last year, Department, Job Satisfaction, Job involvement, Environment Satisfaction as shown in Table 5 and Stock Option Level, Hourly Rate, Daily Rate, Job Role, Job Level as shown in Table 6.

Table 4. Significant features with weights

Algorithm / Attribute	Weights				
	Age	Over Time	Monthly Income	Total Working year	Year At company
Generalized Linear Model	0.152	0.619	0.073	0.038	0.003
Deep learning	0.078	0.480	0.058	0.079	0.020
Logistic Regression	0.136	0.287	0.027	0.120	0.024
Naive Bayes	0.199	0.371	0.232	0.217	0.165
Gradient Boosted Trees	0.077	0.515	0.247	0.042	0.025
Support Vector Machine	0.014	0.015	0.011	0.013	0.012
Fast Large Margin	0.091	0.001	0.777	0.090	0.157
Random Forest	0.150	0.085	0.288	0.039	0.145
Decision Tree	0.094	0.018	0.067	0.011	0.021

- **Age**

As shown in table 4 the age is one of the most important factors affecting employee turnover, where the average age of employees is 37 years as shown in the figure., and the higher the employee's age than this average, the less likely the employee will leave work. (Fig.3) illustrates the significant employee age for employee turnover.

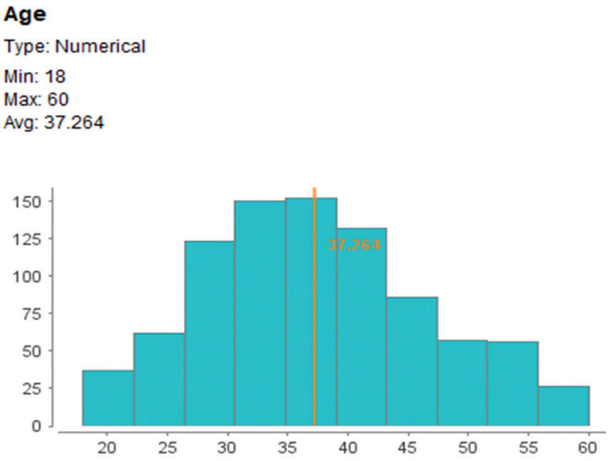

Fig. 3. the significant age for employee turnover

- **Overtime**

The more overtime is calculated and added to the employee, the less likely the employee will be left to work. The overtime description is shown in the (Fig.4).

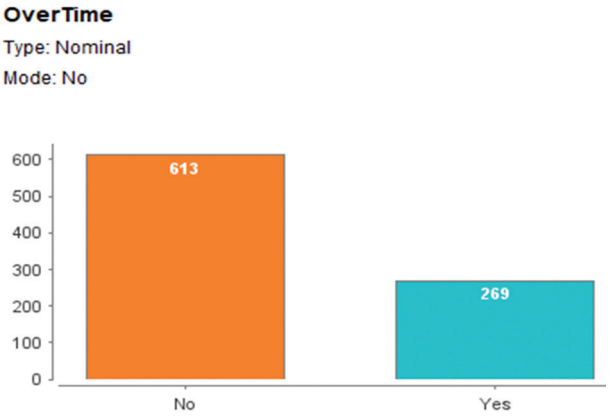

Fig. 4. Overtime impacts in the employee turnover

- **Monthly Income**

One of the most important factors affecting employee turnover is the monthly income of an employee. The higher the employee's monthly income, the more likely he will be left to work. Describe the monthly income as shown in the (Fig.5).

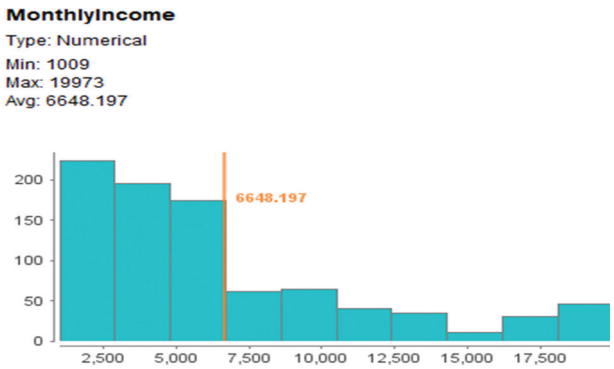

Fig. 5. Monthly Income description

- **Total Working year**

Working years is one of the most important factors affecting employee turnover. The more years an employee has worked in the organization, the less likely he will leave. Description of working years as shown in (Fig.6).

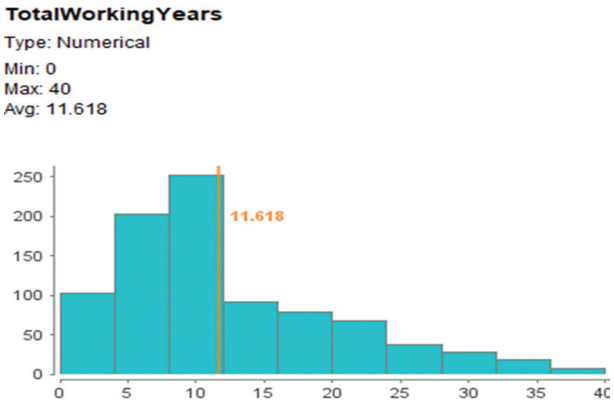

Fig. 6. working years significant value in employee turning over

- **Years at a company**

The years in a company are one of the most important factors that affect employee turnover. The average number of years in a company is about 7 years, and the longer the number of years exceeds the expected, the less likely the employee will leave the organization and the description of work years as shown in (Fig.7).

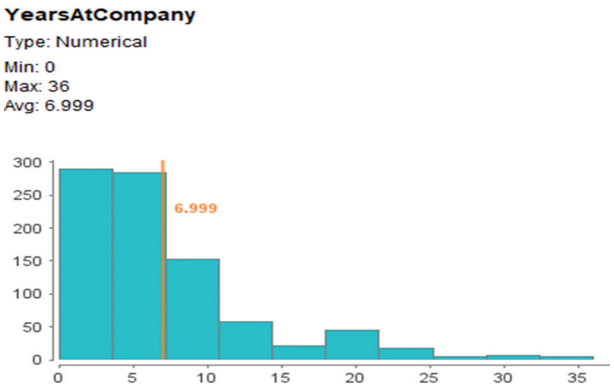

Fig.7. the significant working years at the same company value

Table 5. Significant features with weights

Algorithm \ Attribute	Training Time last year	Department	Job Satisfaction	Job involvement	Environment Satisfaction
	Weights				
Generalized Linear Model	0.161	0.105	0.135	0.101	0.146
Deep learning	0.104	0.070	0.139	0.040	0.083
Logistic Regression	0.073	0.010	0.145	0.007	0.029
Naive Bayes	0.051	0.056	0.030	0.038	0.013
Gradient Boosted Trees	0.053	0.036	0.033	0.043	0.061
Support Vector Machine	0.010	0.013	0.009	0.015	0.008
Fast Large Margin	0.011	0.026	0.122	0.119	0.004
Random Forest	0.036	0.025	0.034	0.054	0.014
Decision Tree	0.068	0.040	0.013	0.015	0.013

- **Training time last year**

Continuous employee training increases his skills and efficiency, and therefore, the higher the employee's training, the less likely they are to leave the job. Describe the training times as shown (Fig.8).

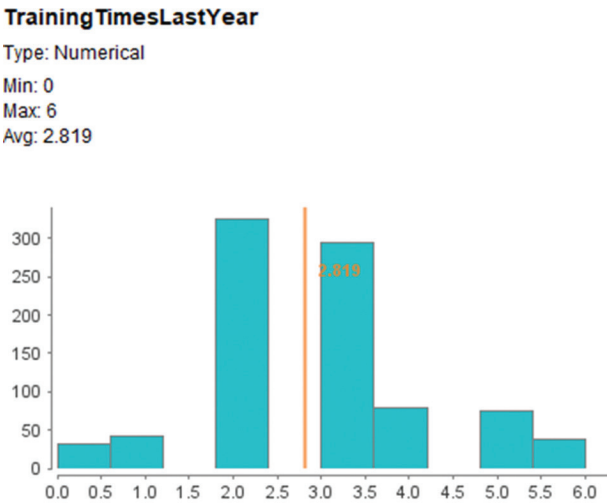

Fig.8. the significant training time last year value

- **Departments**

Regarding the departments, the Research and Development Department has the largest number of employees, as shown in the (Fig.9).

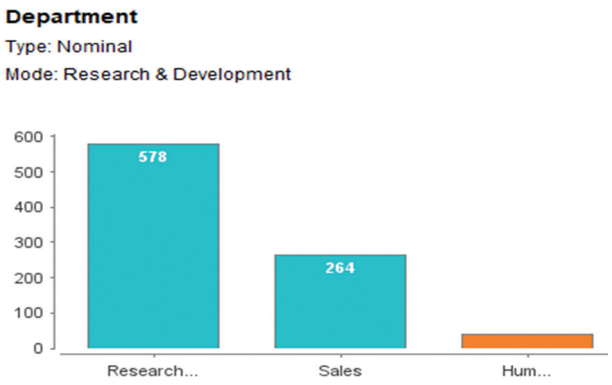

Fig.9. Departments Description

- **Job Satisfaction**

Undoubtedly, job satisfaction is one of the most important factors for employees and its job performance. The higher the job satisfaction rate for an employee, the more related to the institution and not leaving it to work. The job Satisfaction description is shown in the (Fig.10).

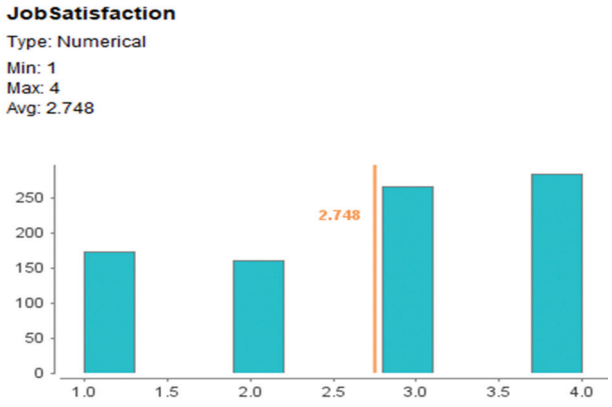

Fig.10. Job Satisfaction significant turnover value

- **Job involvement**

Job involvement is one of the most important factors that affect employee turnover, so the higher the employee's job participation rate, the less likely he will leave the job. Job involvement description as shown in the (Fig.11).

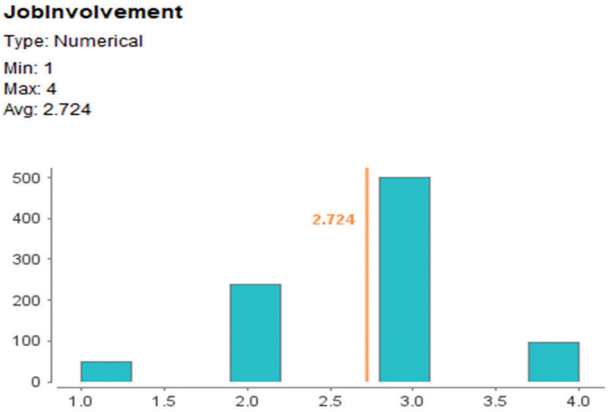

Fig.11. Job involvement significant employee turnover value

- **Environment Satisfaction**

The higher the degree of satisfaction with the work environment in terms of capabilities and workplace, the more employee is attached to the organization and a difficult legacy of work. Add satisfaction to the environment shown in (Fig.12).

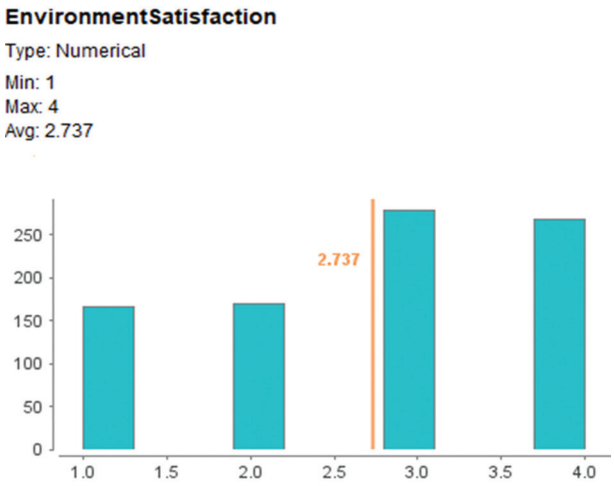

Fig.12. Environmental Satisfaction histogram

Table 6. Significant features with weights

Algorithm / Attribute	Weights: Stock Option Level	Hourly Rate	Daily Rate	Job Role	Job Level
Generalized Linear Model	0.169	0.117	0.058	0.045	0.074
Deep learning	0.104	0.077	0.043	0.050	0.059
Logistic Regression	0.087	0.051	0.002	0.069	0.022
Naive Bayes	0.119	0.053	0.034	0.069	0.102
Gradient Boosted Trees	0.123	0.052	0.009	0.059	0.055
Support Vector Machine	0.013	0.010	0.012	0.012	0.015
Fast Large Margin	0.004	0.180	0.001	0.002	0.011
Random Forest	0.057	0.035	0.102	0.039	0.040
Decision Tree	0.032	0.070	0.056	0.025	0.019

- **Stock Option Level**

The stock option level contains values 1 to 3, on average 0.755.As shown in the (Fig.13).

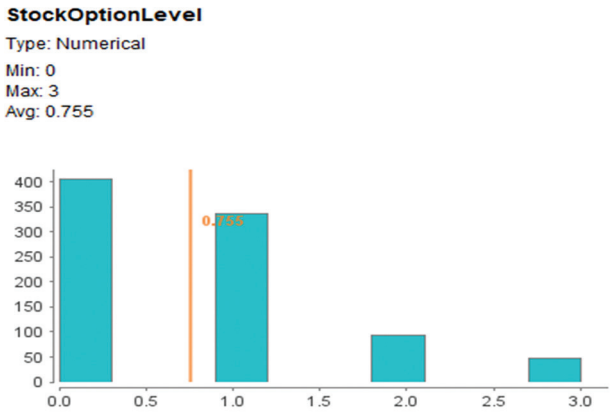

Fig.13. Stock option level significant value for employee turnover

- **Hourly Rate**

The Hourly rate contains values 30 to 100, on average 65.5. As shown in (Fig.14).

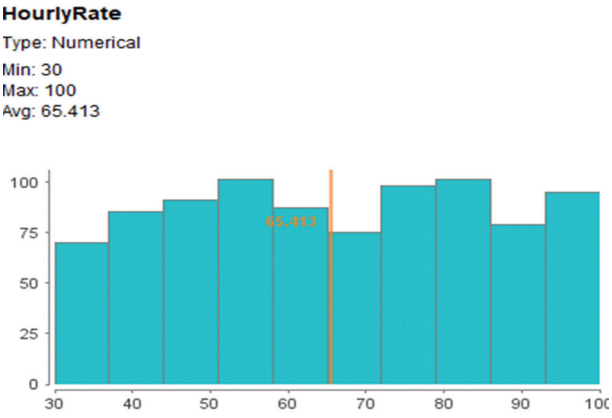

Fig.14. Hourly Rate histogram

- **Daily Rate**

The Daily rate contains values 102 to 1499, on average 799. As shown in (Fig.15).

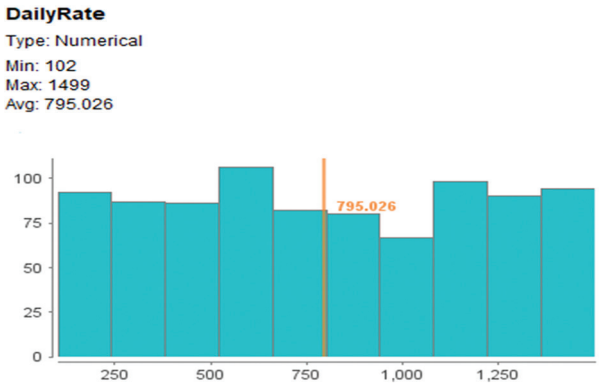

Fig.15. daily rate histogram

- **Job Role**

Job roles contain a range of roles such as Sales Director, Laboratory Technician Research Director (Fig.16) illustrates a description of the job roles.

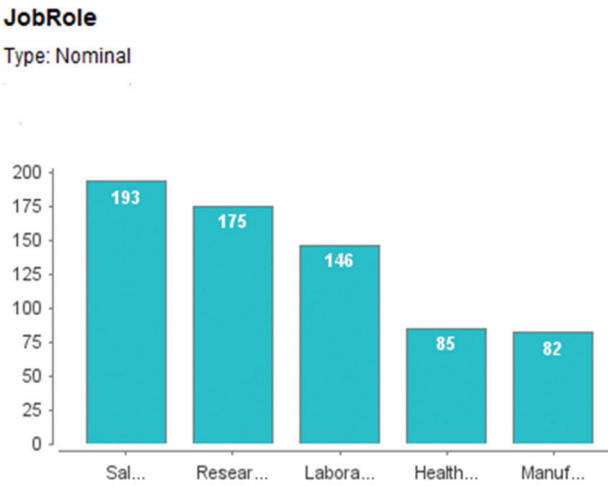

Fig.16. Job role histogram

- **Job Level**

The job level contains values 1 to 5, on average 2.09. As shown in the (Fig.17).The higher the employee's career level, the less likely the employee is to leave work.

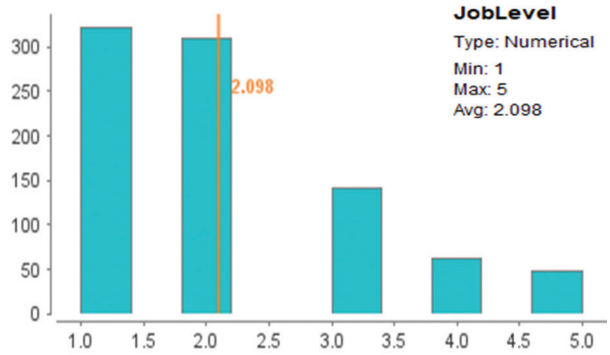

Fig.17. Job level histogram

6. CONCLUSION

This paper proposes a case study for predicting employee turnover features using data mining techniques that have effectively contributed to the accuracy of expected employee turnover. The proposed model performs classification using some of the well-known benchmark algorithms such as support vector machine, decision tree, linear regression, random forest, and deep learning with an average accuracy rate of 88%. Also, the model defines the most important factors affecting employee turnover according to its significant weights. Demographic features such as Age, Monthly Income and behavioral features such as Over Time, Years at Company, Total Working Years and attitudinal factors such as Environment Satisfaction, Job Satisfaction have been found as the most significant factors affecting employee turnover.

7. REFERENCES

[1] Q. A. Al-Radaideh, E. Al Nagi, "Using data mining techniques to build a classification model for predicting employee's performance", International Journal of Advanced Computer Science and Applications, Vol. 3, No. 2, 2015, pp. 144-151.

[2] A. Sikaroudi, S. Rouzbehghousi, A. Esmaieelisikaroudi, "A Data Mining Approach To Employee Turnover Prediction (Case Study: Arak Automotive Parts Manufacturing)", Journal Of Industrial And Systems Engineering, Vol. 8, No. 4, 2016, pp. 106-121.

[3] R. Punnoose, P. Ajit, "Prediction Of Employee Turnover In Organizations Using Machine Learning Algorithms", International Journal Of Advanced Research In Artificial Intelligence, Vol. 5, No. 9, 2016, pp. 20-27.

[4] P. S. Devi, B. Umadevi, "A Novel Approach to Control the Employee's Attrition Rate of an Organization", International Journal of Computer Science and Mobile Applications, Vol. 6, No. 7, 2018, pp.43-52.

[5] L. Girmanova, Z. Gašparová, "Analysis of Data on Staff Turnover Using Association Rules and Predictive Techniques", Quality Innovation Prosperity, Vol. 22, No. 2, 2018, pp. 82-99.

[6] Y. Helmy, A. E. Khedr, S. Kolief, E. Haggag, "An Enhanced Business Intelligence Approach for Increasing Customer Satisfaction Using Mining Techniques", International Journal of Computer Science and Information Security, Vol. 17, No. 4, 2019, pp. 159-176.

[7] A. E. Khedr, J. N. Kok, "Adopting Knowledge Discovery In Databases for Customer Relationship Management in Egyptian Public Banks", Proceedings of the International Conference on Professional Practice in Artificial Intelligence, Santiago, Chile, 21-24 August 2006, pp. 201-208.

[8] A. M. Mostafa, A. E. Khedr, A Abdo, "Advising Approach to Enhance Students' Performance Level in Higher Education Environments", Journal of Computer Science, Vol. 13, No. 5, 2017, pp. 130-139.

[9] K. K. Tsiptsis, A. Chorianopoulos, ''Data mining techniques in CRM: inside customer segmentation", John Wiley & Sons, 2011.

[10] C. A. Al Mamun, M. N. Hasan, "Factors affecting employee turnover and sound retention strategies in business organization: a conceptual view", Problems and Perspectives in Management, Vol. 15, No. 1, 2017, pp. 63-71.

[11] R. Mendes, J. P. Vilela, "Privacy-preserving data mining: methods, metrics, and applications," IEEE Access, Vol. 5, 2017, pp. 10562-10582.

[12] R. B. Palepu, R. R. Muley, "Analysis of agriculture data using data mining techniques: application of big data", Journal of Big Data, Vol. 4, No. 20, 2017.

[13] M. M. Nazier, A. E. Khedr, M. Haggag, "Business Intelligence and its role to Enhance Corporate Performance Management", International Journal of Management & Information Technology, Vol. 3, No. 3, 2013, pp. 8-15.

[14] G. Shmueli, G. Shmueli, P. C. Bruce, I. Yahav, N. R. Patel, K. Lichtendahl Jr, "Data mining for business analytics: concepts, techniques, and applications in R", John Wiley & Sons, 2017.

[15] A. E. Khedr, A. M. Idrees, "Adapting Load Balancing Techniques for Improving the Performance of e-Learning Educational Process", Journal of Computers, Vol. 12, No. 3, 2017, pp. 250-257.

[16] S. Rajendran, W. Meert, D. Giustiniano, V. Lenders, S. Polin, "Deep learning models for wireless signal classification with distributed low-cost spectrum sensors", IEEE Transactions on Cognitive Communications and Networking, Vol. 4, No. 3, 2018 pp. 433-445.

[17] A. Khedr, S. Kholeif, F. Saad, "An Integrated Business Intelligence Framework for Healthcare Analytics", International Journal of Advanced Research in Computer Science and Software Engineering, Vol. 7, No. 5, 2017, pp. 263-270.

[18] S. Rajeswari, K. Suthendran. "C5.0: Advanced Decision Tree (ADT) classification model for agricultural data analysis on cloud", Computers and Electronics in Agriculture, Vol. 156, 2019, pp. 530-539.

[19] N Sultan, A. E. Khedr, A Idrees, S Kholeif, "Data Mining Approach for Detecting Key Performance Indicators", Journal of Artificial Intelligence, Vol. 10, No. 2, 2017, pp. 59-65.

INTERNATIONAL JOURNAL OF ELECTRICAL AND COMPUTER ENGINEERING SYSTEMS

Published by Faculty of Electrical Engineering, Computer Science and Information Technology Osijek,
Josip Juraj Strossmayer University of Osijek, Croatia.

About this Journal

The International Journal of Electrical and Computer Engineering Systems publishes original research in the form of full papers, case studies, reviews and surveys. It covers theory and application of electrical and computer engineering, synergy of computer systems and computational methods with electrical and electronic systems, as well as interdisciplinary research.

Topics of interest include, but are not limited to:

- Power systems
- Renewable electricity production
- Power electronics
- Electrical drives
- Industrial electronics
- Communication systems
- Advanced modulation techniques
- RFID devices and systems
- Signal and data processing
- Image processing
- Multimedia systems
- Microelectronics
- Instrumentation and measurement
- Control systems
- Robotics
- Modeling and simulation
- Modern computer architectures
- Computer networks
- Embedded systems
- High-performance computing
- Parallel and distributed computer systems
- Human-computer systems
- Intelligent systems
- Multi-agent and holonic systems
- Real-time systems
- Software engineering
- Internet and web applications and systems
- Applications of computer systems in engineering and related disciplines
- Mathematical models of engineering systems
- Engineering management
- Engineering education

Paper Submission

Authors are invited to submit original, unpublished research papers that are not being considered by another journal or any other publisher. Manuscripts must be submitted in doc, docx, rtf or pdf format, and limited to 30 one-column double-spaced pages. All figures and tables must be cited and placed in the body of the paper. Provide contact information of all authors and designate the corresponding author who should submit the manuscript to https://ijeces.ferit.hr. The corresponding author is responsible for ensuring that the article's publication has been approved by all coauthors and by the institutions of the authors if required. All enquiries concerning the publication of accepted papers should be sent to ijeces@ferit.hr.

The following information should be included in the submission:

- paper title;
- full name of each author;
- full institutional mailing addresses;
- e-mail addresses of each author;
- abstract (should be self-contained and not exceed 150 words). Introduction should have no subheadings;
- manuscript should contain one to five alphabetically ordered keywords;
- all abbreviations used in the manuscript should be explained by first appearance;
- all acknowledgments should be included at the end of the paper:
- authors are responsible for ensuring that the information in each reference is complete and accurate. All references must be numbered consecutively and citations of references in text should be identified using numbers in square brackets. All references should be cited within the text;
- each figure should be integrated in the text and cited in a consecutive order. Upon acceptance of the paper, each figure should be of high quality in one of the following formats: EPS, WMF, BMP and TIFF;
- corrected proofs must be returned to the publisher within 7 days of receipt.

Peer Review

All manuscripts are subject to peer review and must meet academic standards. Submissions will be first considered by an editor-in-chief and if not rejected right away, then they will be reviewed by anonymous reviewers. The submitting author will be asked to provide the names of 5 proposed reviewers including their e-mail addresses. The proposed reviewers should be in the research field of the manuscript. They should not be affiliated to the same institution of the manuscript author(s) and should not have had any collaboration with any of the authors during the last 3 years.

Author Benefits

The corresponding author will be provided with a .pdf file of the article or alternatively one hardcopy of the journal free of charge.

Units of Measurement

Units of measurement should be presented simply and concisely using System International (SI) units.

Bibliographic Information

Commenced in 2010.
ISSN: 1847-6996
e-ISSN: 1847-7003

Published: semiannually

Copyright

Subscription Information

The annual subscription rate is 50€ for individuals, 25€ for students and 150€ for libraries.

Postal Address

Faculty of Electrical Engineering,
Computer Science and Information Technology Osijek,
Josip Juraj Strossmayer University of Osijek, Croatia
Kneza Trpimira 2b
31000 Osijek, Croatia

IJECES Copyright Transfer Form

(Please, read this carefully)

This form is intended for all accepted material submitted to the IJECES journal and must accompany any such material before publication.

TITLE OF ARTICLE (hereinafter referred to as "the Work"):

COMPLETE LIST OF AUTHORS:

The undersigned hereby assigns to the IJECES all rights under copyright that may exist in and to the above Work, and any revised or expanded works submitted to the IJECES by the undersigned based on the Work. The undersigned hereby warrants that the Work is original and that he/she is the author of the complete Work and all incorporated parts of the Work. Otherwise he/she warrants that necessary permissions have been obtained for those parts of works originating from other authors or publishers.

Authors retain all proprietary rights in any process or procedure described in the Work. Authors may reproduce or authorize others to reproduce the Work or derivative works for the author's personal use or for company use, provided that the source and the IJECES copyright notice are indicated, the copies are not used in any way that implies IJECES endorsement of a product or service of any author, and the copies themselves are not offered for sale. In the case of a Work performed under a special government contract or grant, the IJECES recognizes that the government has royalty-free permission to reproduce all or portions of the Work, and to authorize others to do so, for official government purposes only, if the contract/grant so requires. For all uses not covered previously, authors must ask for permission from the IJECES to reproduce or authorize the reproduction of the Work or material extracted from the Work. Although authors are permitted to re-use all or portions of the Work in other works, this excludes granting third-party requests for reprinting, republishing, or other types of re-use. The IJECES must handle all such third-party requests. The IJECES distributes its publication by various means and media. It also abstracts and may translate its publications, and articles contained therein, for inclusion in various collections, databases and other publications. The IJECES publisher requires that the consent of the first-named author be sought as a condition to granting reprint or republication rights to others or for permitting use of a Work for promotion or marketing purposes. If you are employed and prepared the Work on a subject within the scope of your employment, the copyright in the Work belongs to your employer as a work-for-hire. In that case, the IJECES publisher assumes that when you sign this Form, you are authorized to do so by your employer and that your employer has consented to the transfer of copyright, to the representation and warranty of publication rights, and to all other terms and conditions of this Form. If such authorization and consent has not been given to you, an authorized representative of your employer should sign this Form as the Author.

Authors of IJECES journal articles and other material must ensure that their Work meets originality, authorship, author responsibilities and author misconduct requirements. It is the responsibility of the authors, not the IJECES publisher, to determine whether disclosure of their material requires the prior consent of other parties and, if so, to obtain it.

- The undersigned represents that he/she has the authority to make and execute this assignment.
- For jointly authored Works, all joint authors should sign, or one of the authors should sign as authorized agent for the others.
- The undersigned agrees to indemnify and hold harmless the IJECES publisher from any damage or expense that may arise in the event of a breach of any of the warranties set forth above.

_____ _____

Author/Authorized Agent **Date**

CONTACT
International Journal of Electrical and Computer Engineering Systems (IJECES)
Faculty of Electrical Engineering, Computer Science and Information Technology Osijek
Josip Juraj Strossmayer University of Osijek
Kneza Trpimira 2b
31000 Osijek, Croatia
Phone: +38531224600,
Fax: +38531224605,
e-mail: ijeces@ferit.hr